DEPARTMENT OF THE AIR FORCE

AIR UNIVERSITY

AIR FORCE INSTITUTE OF TECHNOLOGY

Wright-Patterson Air Force Base, Ohio

AFIT/GAE/AA/88D-13

COMPRESSIVE PROPERTIES OF HIGH PERFORMANCE POLYMERIC FIBERS

THESIS

Scott A. Fawaz
2nd Lieutenant, USAF

AFIT/GAE/AA/88D-13

Approved for public release; distribution unlimited

AFIT/GAE/AA/88D-13

COMPRESSIVE PROPERTIES OF HIGH PERFORMANCE POLYMERIC FIBERS

THESIS

Presented to the Faculty of the School of Engineering

of the Air Force Instititute of Technology

Air University

In Partial Fulfillment of the

Requirements for the Degree of

Master of Science in Aeronautical Engineering

Scott A. Fawaz

2[nd] Lieutenant, USAF

December 1988

ACKNOWLEDGEMENTS

I would like to express my sincere gratitude to my thesis advisor, Dr. Anthony N. Palazotto, for his expert advise and guidance throughout the study. Also, the support given by the Air Force Materials Laboratories, who sponsored this study, was essential to successfully completing the project. A special thanks to Dr. Chyi-Shan Wang of the University of Dayton Research Institute, UDRI, for his patience, guidance, and expertise while introducing me to the world of experimental research.

Sincere thanks is given to the AFWAL/MLBP division for the use of their facility and cooperation amongst their people. Specifically, I would like to thank Kenneth Lindsey, of UDRI, whose extensive knowledge of the micro-tensile testing machine made the study possible. Also, the continual support of Bill Click, Jacque Henes, and Lisa Denny for laboratory and computer resource support.

Finally, I would like to thank my wonderful wife [redacted] for her patience, tolerance, and support throughout my academic pursuits.

Scott A. Fawaz

TABLE OF CONTENTS

LIST OF FIGURES

LIST OF TABLES

ABSTRACT

In directing the research effort for improving the compressive properties of rigid rod polymeric composite fibers, a reliable testing technique for determining compressive properties is needed. The technique developed used the Tecam Micro-Tensile Testing Machine, MTM-8 and allowed direct tension and compression testing of composite fibers of extremely short gage length. The measured data was analyzed for corrections in machine compliance and possible errors in gage length misreading, fiber slippage, glue deformation, fiber misalignment, and non-uniform stress distribution. A non polymeric fiber was tested to determine if any fiber material dependence existed. The data was compared to the compressive properties obtained from the elastica loop, bending beam, recoil, and composite tests. This was the only known research of high performance polymer fibers in direct tension and compression testing which allowed the construction of a complete stress strain curve.

In developing the technique, the gage length and load cycle had to be determined as well as mounting the fiber without damage. The gage length used had to limit the possibilities of Euler Buckling and a non-uniform stress distribution across the cross-section of the fiber.

The stress strain relationships covering both tension and compression were constructed for poly(p-phenylene benzobisoxazole), PBO, Kevlar 29™, Kevlar 49™, and an experimental carbon fiber. Compressive strengths were determined for the first three fibers, however, the compressive strength of the carbon fiber was out of the range of the machine. The apparent tensile and compressive moduli were gage length dependent, as the gage length decreased; the moduli decreased. The corrected tensile and compressive moduli were obtained from machine compliance curves. Quantitative results for the effect of misreading the gage length and fiber slippage were inconclusive.

INTRODUCTION

Rigid rod aromatic heterocyclic polymers have shown superior thermal and thermal/oxidative stability compared to current metal systems (1:135;20). They can be processed into fibers with nearly perfect uniaxial orientation resulting in excellent tensile properties compared to the state-of-the-art. These fibers are titled high performance fibers because their axial tensile properties are an order of magnitude larger than common textile fibers (15:1). Due to their excellent tensile properties, these fibers are promising candidates for structural applications when used in composites. Their relatively low density elicits potential applications in ultra-light weight structures such as a space station. This new class of electrically nonconductive fibers will have the greatest impact on military weapon systems such as the cruise missile and stealth aircraft. Presently, carbon fibers are the most widely used, but as the tensile properties of the rigid rod polymers approach those of the carbon based fibers; the above mentioned benefits will promote widespread use of the rigid rod polymeric fibers. Carbon fibers, which are 99% or more carbon, are not polymeric fibers even though they are synthesized from a polymeric precursor. The polymeric fibers have one significant deficiency; their compressive properties are an order of magnitude lower than required for operational use.

An extensive research effort has been directed toward improving fiber compressive strength (1;10;10;12;20;21). To precisely characterize the fiber compressive properties and provide direction for the research effort, a reliable testing technique must be developed. Manufacturing fiber embedded composites from the experimental fibers provides the most reliable data. However, in many cases sufficient quantities of the experimental fiber aren't available to manufacture enough test specimens to completely characterize the composite. Many attempts have been made to test a single fiber; such as the loop, bending beam, and recoil tests. Unfortunately none of the above three tests yield results consistent with the

composite data (see Background).

The inability of the loop, bending beam, and recoil tests to adequately determine the compressive strength and modulus have motivated the search for a more reliable testing technique. In this study, the fiber axial compressive properties are determined by directly compressing a single fiber. The Tecam Micro-Tensile Testing Machine was originally designed to test specimens in tension; however, with a slight modification, the ability to measure compressive strength, percent strain, and modulus from direct compression seemed promising. Results were compared with those from the other three test methods mentioned.

BACKGROUND

The loop test loads the fiber by bending as shown in Figure 1 (2:104). The stress field is both tensile and compressive depending upon which side of the neutral plane is the point of interest. The stress field through the cross-section of the fiber is purely compressive only on the concave side of the loop. The stress-strain data does not yield the true compressive strength and modulus because the fiber is loaded in tension and compression. Analogously, the tensile strength could be determined by this same approach, however this is usually not common practice; the validity of the elastica loop test is questionable.

The bending beam test, shown in Figure 2, used a fiber mounted to a beam with an aspect ratio over one hundred times as large as the fiber. The stress was applied by clamping one end of the fiber/beam combination and forcing a roller inward from the opposite end causing the beam to deflect vertically (13:15). The test was based on determining the distance from the clamped end to where the first internal or external kinkband was formed; therefore, only transparent fibers could be tested (20; 13:15). The compressive strain could be calculated, but the magnitude of the applied load was unknown; therefore, the compressive strength was determined by assuming the tensile and compressive moduli were the same. Using one dimensional Hooke's Law;

$$\sigma_c = E_t \varepsilon_c. \tag{1}$$

the compressive strength was determined. However, the fiber most likely behaved nonlinearly before failure, thus Hooke's Law no longer applied.

The recoil test dynamically loaded the fiber in compression; thus a linear stress-strain behavior was forced (3:853). A monofilament fiber is loaded in tension to a predetermined load then cut with an electric arc at the midpoint of the fiber. The fiber recoils as the stress wave propagates from the cut to the sample holders. The fiber

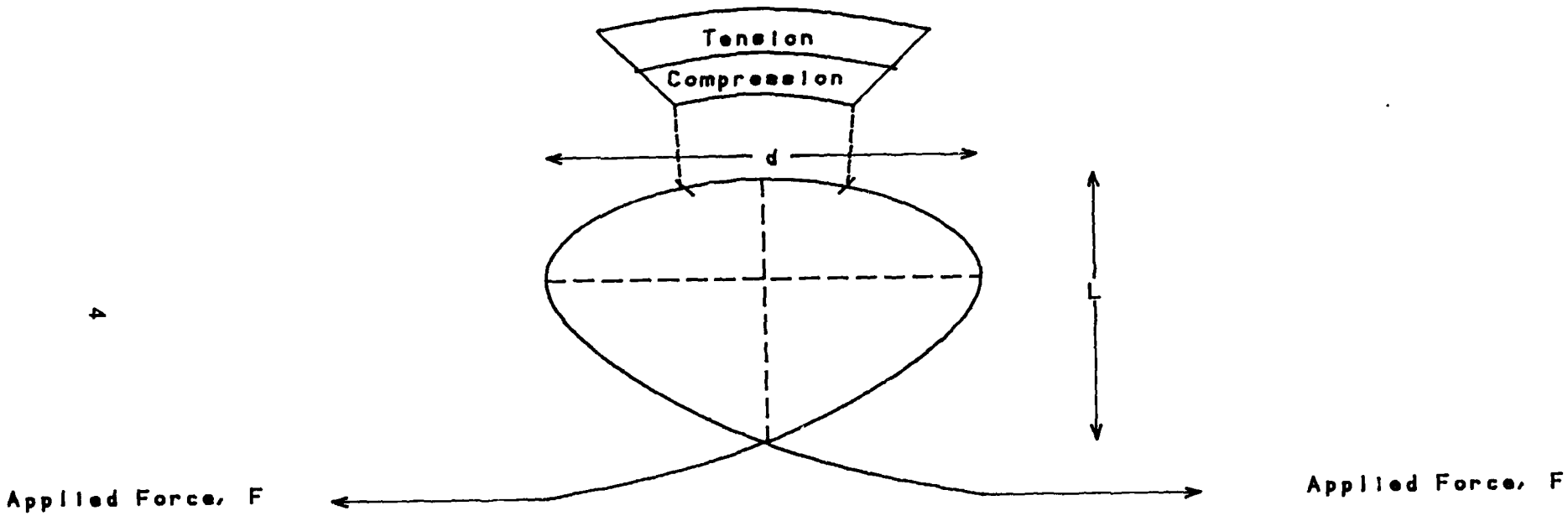

Figure 1. ELASTICA LOOP TEST

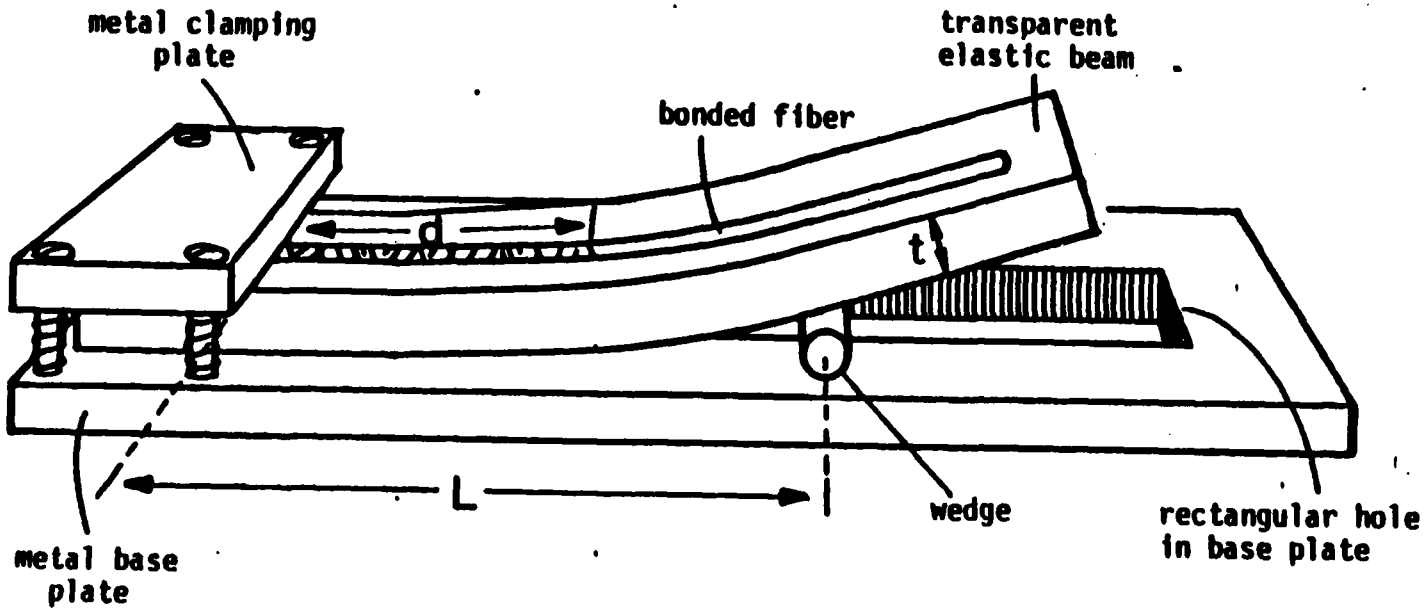

Figure 2. BENDING BEAM TEST

continues to recoil until it reaches the clamped end. Because the clamped end forms a rigid boundary, the kinetic energy of the fiber is transformed back into strain energy andthe compressive stress propagates back down the length of the fiber. The magnitude of the stress wave in compression and tension are equal but opposite in direction; therefore, compressive failure will occur first in a fiber whose compressive strength is lower than its tensile. By selectively controlling the tensile failure stress, a threshold stress for observation of recoil compressive damage could be determined; thus, a measure for fiber compressive strength obtained (3:855). The stress-strain behavior was forced to be linear due to the high stress wave velocity causing an extremely high strain rate. In addition, the fiber was assumed to recoil longitudinally only forcing the stress wave to propagate similarly. Since the recoil occurs so rapidly, the nature of the wave propagation can't be determined. The fiber may recoil longitudinally, laterally, or some combination of both; therefore, the derivations used to determine the compressive strength must account for this lateral motion which they do not. The compressive strength could be determined, but the compressive modulus could not since the material strain was unknown.

Using the MTM-8, the fiber was tested in direct compression eliminating the problems inherent in the above three tests. The main advantage of direct compression testing was the entire stress-strain curve was obtained from zero load to fracture. Specifically, fiber behavior during the linear and non-linear regions was illustrated; thus, the compressive modulus and fracture point were determined. The technique was based on loading a one-dimensional bar with a clamped/simple support boundary condition. The only assumption made was one-dimensional Hooke's Law applied. The possibility of a three dimensional stress field due to the anisotropy of the fiber is discussed later. The fibers are highly anisotropic, but exhibit linear behavior in the elastic region of the stress-strain curve in tension tests; therefore, were expected to behave similarly in compression.

The compressive modulus and strength are of prime concern since no testing has been accomplished which reliably determined these two quantities. Failure of the specimen

is characterized by kinkband formation in the fiber. Kinkbands are produced when the fiber experiences compressive stress. The formation of kinkbands was not dependent on the load condition, whether direct compression or combined loading, but formed as a result of compressive deformation as seen by Allen and DeTeresa (2:853, 13:8).

On the macroscopic level, if the specimen was loaded in direct compression the problem was much simpler since the only concern was to reduce the chance of Euler Buckling and the effects of a non-uniform stress distribution (4:1-4). Euler Buckling was derived for a linear elastic prismatic column which followed Hooke's Law. Polymeric fibers are extremely anisotropic, but in studying the buckling phenomenon the effects of the anisotropy were neglected in order to obtain a rough estimate of when Euler Buckling might occur. Euler Buckling, assuming a linear elastic prismatic column, occurred when the fiber became unstable due to an increase in its total potential energy. Increasing the compressive load drove the fiber towards its bifurcation point, a point which marked the intersection of two energy equilibrium paths. Prior to the bifurcation point, there was only one equilibrium path, the primary path; after the bifurcation point there was a secondary path, the adjacent or alternate equilibrium paths. The secondary path was simply a state where the fiber was just as inclined to exist as the primary path. With the possibility of being on either paths, the primary or adjacent, the instability of the fiber was created. When the fiber became unstable, the displacements become non-linear and the stress-strain curves showed this nonlinearity. Therefore, the avoidance of the instability, Euler Buckling, was advantageous to restrict the complexity of the problem. The most accurate method of determining the compressive strength was to load the fiber in direct compression; thus, forcing one dimensional constitutive relations. The one dimensionality of the problem was desired to reduce the complexity of the constitutive relations; the difference was having one stress resultant to characterize as opposed to three. At present, no method is available to deal with the out of plane stress components of the three dimensional problem using the current test equipment. The formation of kinkbands didn't depend

on the type of loading; however, if a combined loading technique were used, the complexity increases manyfold due to the three dimensionality, and was avoided. As a general rule, Euler Buckling could be avoided if an aspect ratio of 10 or less was maintained since the critical buckling load, the load at which the instability was reached, was a function of the geometry of the fiber by the follow equation (6:22);

$$P_{cr} = 4\pi \ EI/L \qquad (2)$$

where

E = Tensile Modulus of Elasticity
I = Area Moment of Inertia for a Linear Material
L = Fiber Gage Length

This is the general Euler Buckling equation for an isotropic material with a clamped simply supported boundary condition. If Euler Buckling occurred, kinkbands were created at the buckling point; however, the source of creation whether buckling or direct compression was difficult to discern. Kinkbands caused by buckling were of no concern here since the critical load that caused buckling was not necessarily the compressive strength of the fiber. The stress distribution across the cross-section of the fiber was effected by how the fiber was mounted in the testing machine. St. Venant's Principle for isotropic, perfect cylinders states that:

> the strains that are produced in a body by the application to a small part of its surface of a system of forces statically equivalent to zero force and zero couple are of negligible magnitude at distances which are large compared with the linear dimensions of the part. (4:495)

In practice, an aspect ratio larger than ten yielded negligible end effects. However for an anisotropic material this was not the case. However, based on Horgan's results for tensile loading of anisotropic ultra high modulus polyethylene, he showed for anisotropic materials the aspect ratio was determined by the following relationship:

$$l/d = (E/G) \qquad (3)$$

where l_f = fiber gage length, d = fiber diameter, E_t = tensile modulus, G = shear modulus (4:496,497;14).

The Euler Buckling gage lengths were the upper bound; whereas, the gage lengths from the stress distribution effects were the lower bound. In this study, Eq (2) and (3) serve as guidelines for selecting the appropriate gage length.

EXPERIMENTAL

The MTM-8 is a completely mechanical and optical system; thus the errors associated with electronic equipment were not present; i.e. electronic drift, noise, and environmental interference. Displacements were read on the one hundred Angstrom level having a possible error of 0.1% (19:1). A complete description of the MTM-8 is located in Appendix A. The ability to load a fiber in direct compression did not depend on the fiber geometric or material properties. Since the machine compliance was constant, fiber independence was quantitatively proven by comparing the machine compliance of various fibers? If the machine was fiber dependent, the machine compliance would have to be determined for every fiber tested; definitely a labor intensive task that may be prohibitive if a large quantity of fibers are tested.

Four fibers were thoroughly tested. Poly(p-phenylene benzobisoxazole), PBO, fibers obtained from Dow Chemical Company were dry jet/wet spun and heat treated at 600°C (21). Two other fibers were Kevlar 29™ and Kevlar 49™ which were commercial fibers from E. I. duPont de Nemours and Company, Incorporated. The fourth fiber tested was an experimental vapor grown carbon fiber courtesy of Applied Sciences Federated.

The MTM-8, top view shown in Figure 3, uses a series of micrometers, torsion bars, and levers to load the fiber in either direct tension or compression. Load is applied to the fiber by rotating the load micrometer, 18, which applied a moment to the torque rod system, 26, via a lever, 25. Rotation of the torque rod caused the right anvil, 13, to translate either inward or outward for direct compression or tension, respectively. When looking through the telescope, movement of the right anvil moved the left mirror, 27, forcing the mirror reflections to split. The image splitting is used to measure displacement, realigning the images via the displacement micrometer, 4, yielded fiber displacement in hundreds Angstroms. The MTM-8 allowed both the load and displacement to be recorded during testing. Details of machine operation can also be found in Appendix A.

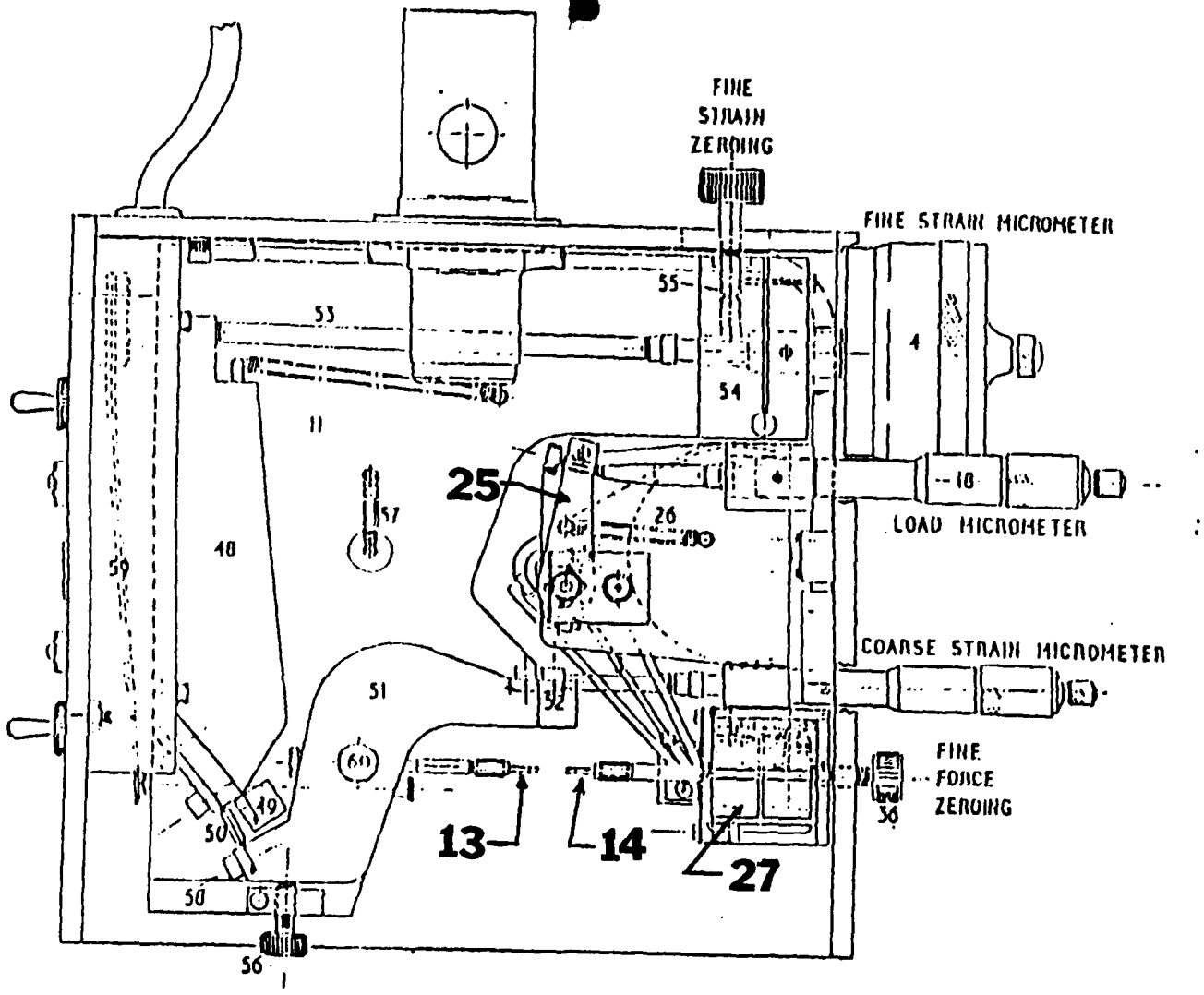

Figure 3. Top View of Tecam Micro-Tensile Testing Machine with Top Face Plate and Travelling Microscope Removed

The fiber was glued to the left then the right anvil, sample holder, using 1,5 diphenylcarbohydrazide, a thermoplastic polymer. In the current application, the behavior of the thermoplastic was not changed by melting it in its powdered form then letting it solidify, which was necessary when mounting the fiber (5:455). However, since the fiber was glued to the anvils, the possibility of fiber slippage and glue deformation must also be investigated. If the fiber was not aligned properly the glue could be remelted and fiber realigned since the left anvil had three-dimensional transnational freedom. When mounting the fiber the alignment was very critical, as the repositioning iterations increased the accuracy of the results decreases. Due to the frailty of the fiber, the fiber could be easily damaged during repositioning. The details of mounting the fiber in the MTM-8 are included in Appendix A.

Euler Buckling during a test would signal the test was a failure, and none of the data could be used because the stress-strain curve would be nonlinear in the region which was usually expected to be linear. The non-linearity would occur due to the large displacements present when the potential energy of the fiber moved from the primary to secondary equilibrium paths. If buckling did occur much was learned about how the fiber was mounted. If the fiber ends mounted in the anvils were parallel, which was checked with the traveling microscope, the buckling must have been caused by a misalignment of the anvils themselves, either laterally or vertically. If a lateral misalignment exists, a moment was produced due to the eccentricity of the load in relation to the longitudinal axes of the fiber. If a vertical misalignment was present, a transverse shear force was created. Having the moment or transverse shear force present resulted in a combined loading condition and a three dimensional problem. Furthermore, the combined loading drove the critical buckling load down forcing the fiber to fail prematurely.

Since the compressive strength was one of the quantities of interest, the fiber should not buckle before the compressive strength was determined. The range of compressive strength was predicted not to exceed 40 - 100 ksi for PBO 8A, based on results from Dow

Chemical Company, and corresponding critical lengths were calculated using Eq (2). Given E_t = 35.0 Mpsi, I = 4.60 x 10^{-8} for a diameter of 17.5μm yields the following critical lengths. The compressive strength range given in Table I was only an expected range based on the elastica loop, bending beam, recoil, and composite test data when available. Since the first three tests listed overestimate the compressive strength, using these values was a conservative premise.

Table I. Minimum Gage Length to Avoid Euler Buckling

Fiber	Compressive Strength Range (ksi)	Critical Gage Length (mm)
PBO 8A	40	0.813
	60	0.664
	80	0.575
	100	0.514
Kevlar 29™	40	0.354
	60	0.289
	80	0.250
	100	0.224
Kevlar 49™	40	0.390
	60	0.319
	80	0.276
	100	0.247
Carbon	100	0.975
	120	0.890
	140	0.824
	160	0.771

The gage length range was calculated based on the estimated compressive strengths; for example, if PBO 8A had a compressive strength of 40ksi the gage length would have to be less than 0.813mm in order to load the fiber to failure without causing Euler Buckiing.

The minimum gage lengths from Eq (2) and (3) gave an operating range for the gage length and are listed in Table II. The gage lengths used, determined by Eq (2) and (3),

varied from approximately 0.2 - 10.0mm even though the Tecam operations manual stated the error percentage increased for gage lengths less than 0.5mm (19:1). The cause of this

Table II. Gage Length Operating Range

Fiber	Eq (2) (mm)	Eq (3) (mm)
PBO 8A	0.529	0.514-0.813
Kevlar 29™	*	0.224-0.354
Kevlar 49™	0.185	0.247-0.390
Carbon	0.32	0.771-0.975

* Unknown Shear Modulus prohibited calculation.

error increase was not reported. However, tensile tests were run in the past yielding accurate results for gage lengths less than the 0.5mm minimum (19). The upper and lower bounds of the gage length range used at this stage were the largest and smallest lengths that could be consistently mounted in the anvils. The gage length was the length of fiber between the two anvils.

The load increment used was based on the extent of image splitting seen through the telescope. The load was incremented to generate many points on the load-deflection and stress-strain curves. The more points plotted, the higher the confidence was in determining the behavior of the fiber. The load was proportional to the displacement; therefore, larger loads caused larger displacements resulting in a wider image split. The wider the split, the easier the realignment of the images. If a small load increment was used, the split was indistinguishably small, resulting in improperly realigning the images causing a misreading of the displacement. The images are not very distinct, when viewed separately they become even more blurred. When realigning the images, the image created by the right

mirror can be realigned on the left, center, or right side of the image created by the left mirror. The difference between realigning at one of the three locations was indistinguishable when viewing the images, but could create a difference in measured displacements up to 200Å. The error could be decreased to range from zero to twenty angstroms by consistently realigning the images at one of the three positions for the entire test, thus promoting repeatability. All of the tests in this study had image realignment at the left position. If misalignment was present, it was not noticeable using the relatively low power microscope and magnifying glass. With the diameters of the fibers ranging from 12.0 - 35.3μm misalignment of the same order of magnitude as the diameters could be present and go undetected. The load increment used varied from 0.01 - 1.0g depending on the fiber being tested and adequate image splitting.

The first objective was to determining if the compressive modulus was the same as the tensile. The configuration of the MTM-8 had to be changed to allow for testing in both compression and tension. This was done by changing the zero of the load micrometer from zero to seven; thus, from zero to seven grams was compressive and seven to fifteen grams was tensile loading. As many as ten tests were completed, cycling the load to obtain many values of the moduli for one fiber. As long as the onset of plastic deformation was not reached, one fiber could go through many load cycles. Plastic deformation was not prevented in any way; however, the onset of plastic deformation was avoided by first finding the load which initiated plastic behavior. This load was determined by running one load cycle per fiber and gradually increasing the load increment for every fiber tested until the stress-strain relation became nonlinear. Since the number of load cycles for any one fiber was less than ten, no fatigue behavior was considered. The fiber was loaded in either tension or compression, unloaded to zero, loaded in the opposite direction, then unloaded again to zero. The load increment used for tension was generally larger than those for compression since in compression Euler Buckling had to be avoided.

The second objective was to determine compressive failure behavior, and was accomplished by loading the fiber from zero load to failure. Fiber failure was identified

when the mirror images could no longer be realigned due to excessive deformation. Excessive deformation could result from Euler Buckling or massive kinkband formation. If the cause was Euler Buckling, the test results were discarded; kinkband formation was the failure mechanism of interest, not Euler Buckling. Once the load causing compressive yield was determined for a given fiber, other fibers of the same type were tested numerous times without significant error in the moduli as long as the compressive yield point was not exceeded. Due to the time consuming mounting procedure, each fiber was tested as many times as possible to generate the most data possible.

As illustrated in Table III below, forty PBO fibers were tested in compression to determine repeatability of compressive strength and modulus and machine compliance. Another thirty-six tests were run in tension to determine repeatability of the tensile modulus, machine compliance, and the possibility of error due to misreading the gage length. An experimental vapor grown carbon based fiber developed by Applied Sciences Federated was tested twenty times in compression and fifty-two in tension. Kevlar 29™ and Kevlar 49™ were tested 24 and 52, and 43 and 50 in compression and tension; respectively.

Table III Number of Tension and Compression Tests.

Fiber	Compression	Tension
PBO 8A	40	36
Kevlar 29™	24	52
Kevlar 49™	43	50
Carbon	20	52

The number of tests completed depended on how quickly the general trend of the data appeared and how high was level of confidence of the results. The tensile tests were used to develop this confidence level since the MTM-8 had proven to work in tension; therefore, if any errors in the modulus were present, they could possibly be correlated to misreading the gage length, fiber slippage, glue deformation, and/or machine compliance (18). If the compression tests were used and an error was present, the cause could be something other than those listed, therefore no correlation could be made. For this reason, tension tests were used to determine possible errors.

The success or failure of the tests could not be determined until the raw data was reduced. Other than the two possibilities of error mentioned above, error could be induced by damaging the fiber before final mount, non-one dimensional boundary conditions, non-uniform strain rate, over correcting on the displacement micrometer, or jarring the machine. The sources of error are numerous, however if the errors existed, they were seen in the test results. The error was manifested by non-linearities in the assumed elastic range of the stress strain curve.

RESULTS

PBO 8A

The tensile modulus was the only tensile property of interest for all the fibers tested and was used for comparison to the compressive modulus. In the tension stress-strain curves, the last data point of each curve was not the tensile strength, but only the last load increment used to determine the tensile modulus. The repeatiblity of measuring the tensile modulus is illustrated in Figure 4 which showed negligible variation of modulus during the successive load cycles. If the tensile modulus was determined by the slope between two consecutive data points on the stress-strain curve, the accuracy of the tensile modulus decreased. The tensile modulus determined between any two consecutive points may vary considerably, but if it was determined from the entire data set it did not vary outside the limits of an experimental error of 5%. The average apparent tensile modulus for all the PBO 8A fibers are listed in Table IV. The measured stress-strain data was used to determine the average apparent tensile modulus and was not corrected for any possible errors at this stage. Figure 5 illustrated typical stress-strain relationships measured for PBO fibers with gage lengths between 0.3 - 7.68mm. The apparent tensile modulus was found to increase, as seen by the increasing slope, with the gage length. The modulus of elasticity being a material property should not vary with the geometry of the specimen; however, these moduli were not corrected for the compliance of the machine, thus the variation. The method used to determine the machine compliance was derived from the one dimensional Hooke's Law as follows:

$$\sigma_t = E\varepsilon \tag{4}$$

where σ_t is stress (force/unit area), E is modulus of elasticity (force/unit area), and ε is strain (length/length). Now substituting the strain-displacement relation:

$$\varepsilon = \Delta l_t / l_t \tag{4a}$$

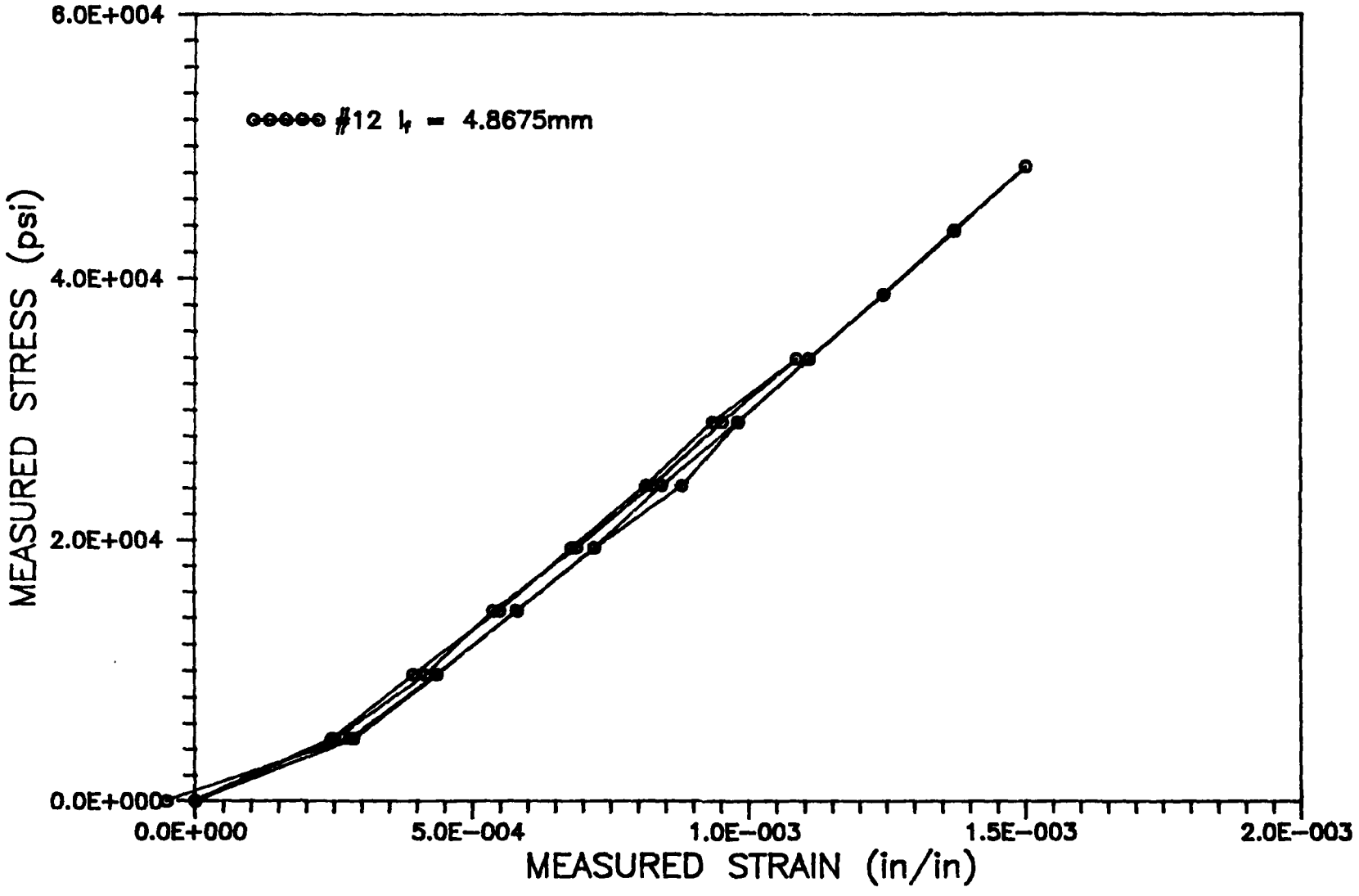

Figure 4. PBO 8A TENISON TEST

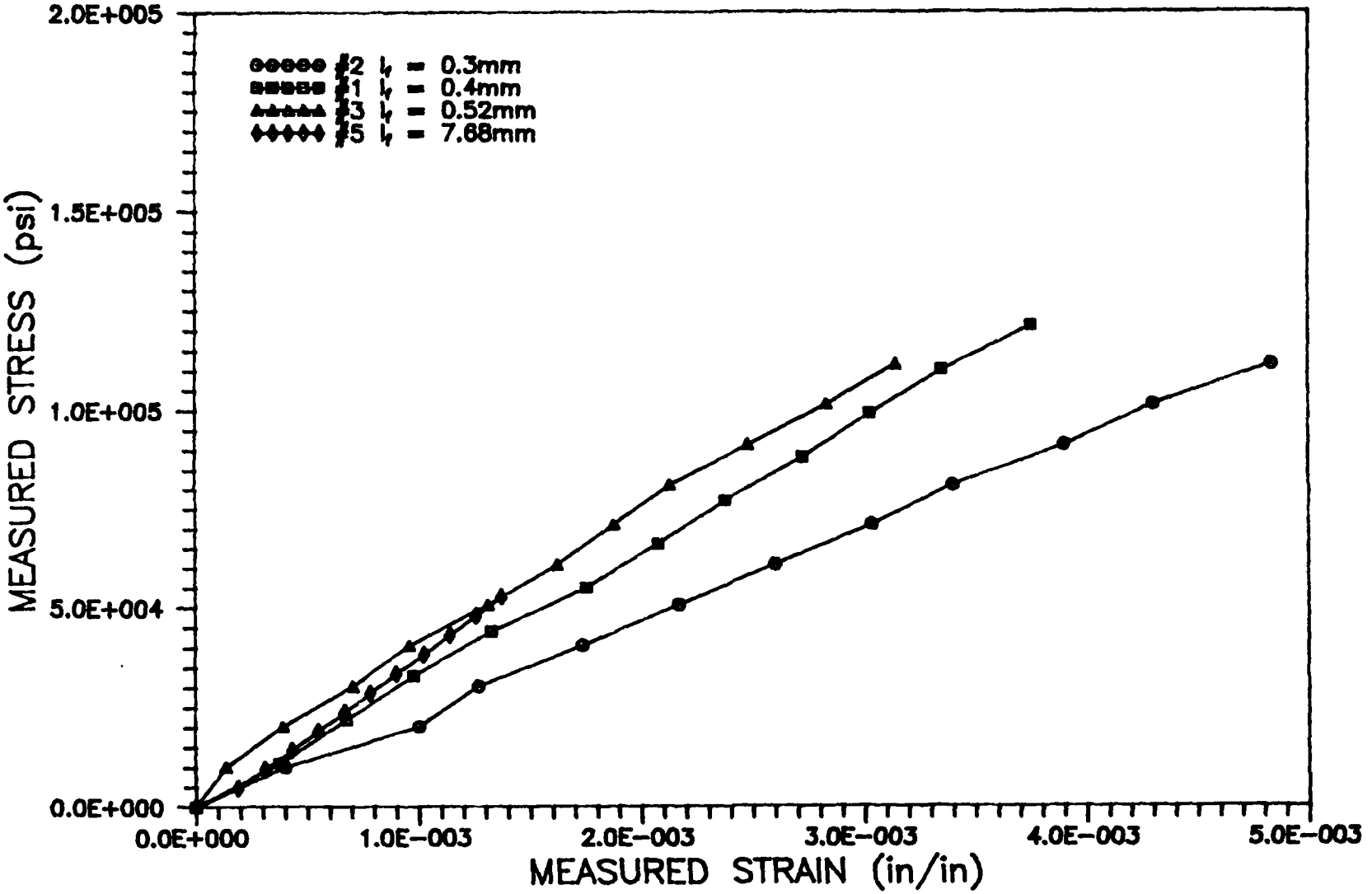

Figure 5. PBO 8A TENISON TESTS

Table IV Tensile Modulus Variation with Gage Length for PBO 8A

Fiber #	Diameter (μm)	Gage Length (mm)	Tensile Modulus (Mpsi)
5	17.5	0.4	15.4
11	17.8	0.35	15.9
17	17.8	0.49	18.4
24	17.3	0.55	18.6
23	17.3	0.7	19.9
4	17.5	0.5	20.4
10	17.8	0.75	20.6
8A	17.8	0.7	20.9
22	17.3	0.81	21.4
9	17.8	1.0	23.5
21	17.3	1.14	27.8
8	17.8	1.5	29.1
14	17.8	3.0	38.0
13	17.8	4.0	38.5
15	17.8	2.0	38.9

$$\sigma_t = E(\Delta l_f/l_f) \tag{4b}$$

where Δl_f is the fiber deformation and l_f is the gage length. Even though the strain was assumed to be caused by the deformation of the fiber, the displacement of the machine, Δl_m, cannot be neglected.

$$\sigma_t = E(\Delta l_f + \Delta l_m)/l_f \tag{4c}$$

Solving for 1/E to have the form y = mx + b,

$$1/E = (1/\sigma_t)\Delta l_f/l_f + (1/\sigma_t)\Delta l_m/l_f \tag{4d}$$

$$1/E = 1/E_o + \Delta l_m/\sigma_t(1/l_f) \tag{5}$$

where

E = measured (apparent) modulus of elasticity (force/unit area)
E_o = corrected modulus of elasticity
Δl_m = machine displacement (length)

The compliance curve was obtained by testing fibers of varying gage length to determine the measured modulus then plotting the inverse of the modulus versus inverse of the gage length. The corrected modulus was the y-intercept of the curve and was extrapolated. The number of data points needed was determined by how readily the trend of the curve was visible. Examining Eq (5) showed that as the stress level was increased the machine displacement, Δl_m must also increase to maintain a constant slope. Therefore, the machine displacement was not a constant, but varied with the load which insured the machine compliance, $\Delta l_f/\sigma$, was constant throughout the load cycle for a given fiber. Based on Eq (5), no dependence on any fiber material properties was present. The machine

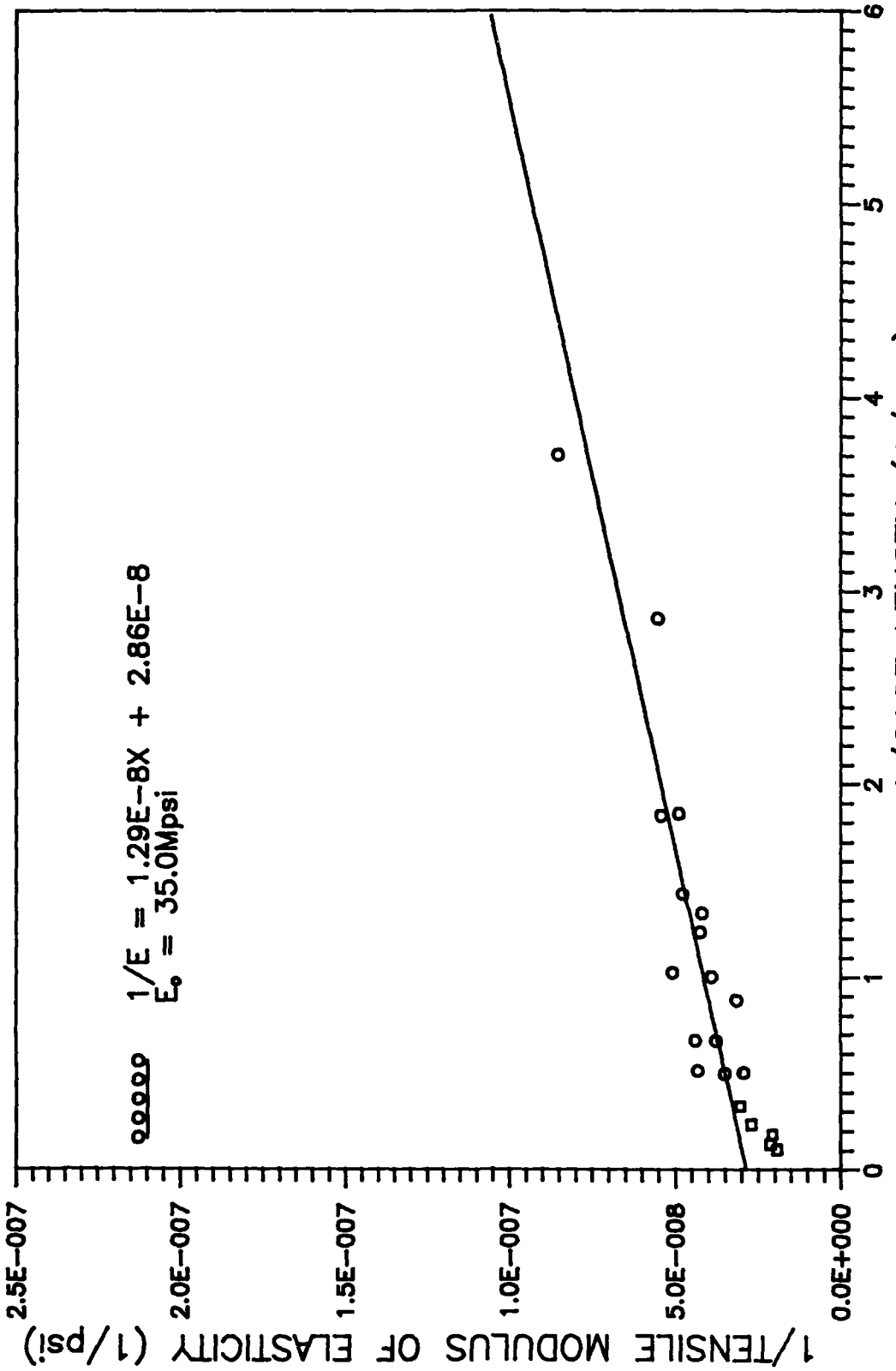

Figure 6. MACHINE COMPLIANCE CURVE for PBO 8A
TENSION TEST

compliance for the tension tests was plotted using linear regression and shown in Figure 6.The corrected modulus for PBO 8A was 35.0Mpsi and the machine compliance, $\Delta l_m/\sigma$ was 1.29 x 10^{-4}mm•in²/lb or 5.09 x 10^{-10}in²/lb. The moduli for PBO 8A with short gage lengths tended to scatter even for moduli with relatively equal gage lengths. From Figure 7 and 8, the apparent modulus increased with the gage length; therefore, the corresponding moduli were omitted in determining the linear regression curve for the machine compliance. The modulus approached an asymptote at approximately 2.0mm shown in Figure 8 indicating no dependence on the gage length. The asymptotic modulus was approximately 38.0Mpsi which was comparable to the 35.0Mpsi determined using the Instron at much larger gage lengths (20). The initial strong dependence of modulus on the gage length might be attributed to the machine compliance. The wide range of the moduli was due to varying the gage length which was the independent variable in determining the machine compliance. The apparent asymptotic modulus measured at the larger gage lengths was the actual modulus of the fiber and did not need to be corrected for the machine compliance. Specifically, the machine compliance did not significantly effect the modulus for these gage lengths.

Figure 8 depicts the variation of the apparent modulus for the range of gage lengths used. Correcting the apparent modulus for the machine compliance using Eq (5) and solving for E_o yielded no variation of the modulus with the gage length as shown in Figure 9. The mean corrected modulus was 35.0Mpsi with a standard deviation of 4.0 Mpsi.

What was labelled the machine compliance might also included the effects of the glue modulus. If the glue modulus was lower than that of the fiber, the glue might possibly yield; thus, the apparent modulus would be comprised of the modulus of the fiber, modulus of the glue, and true machine compliance. Furthermore, from the above derivation of "machine compliance", the individual contributions of the the true machine compliance and glue modulus could not be separated. As a result, the "machine compliance" contained the true machine compliance in addition to the possible but indeterminable effects of the

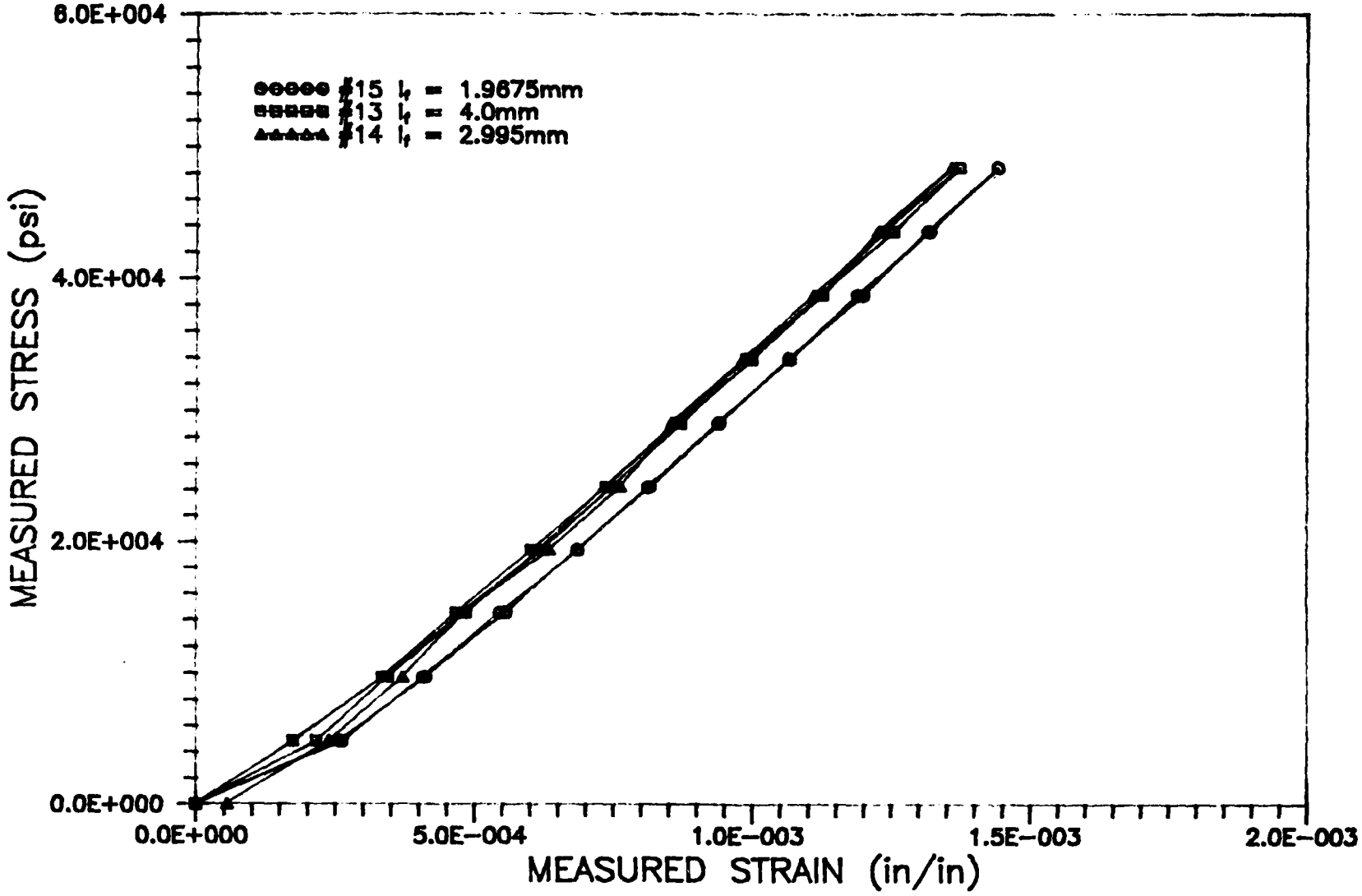

Figure 7. PBO 8A TENISON TESTS

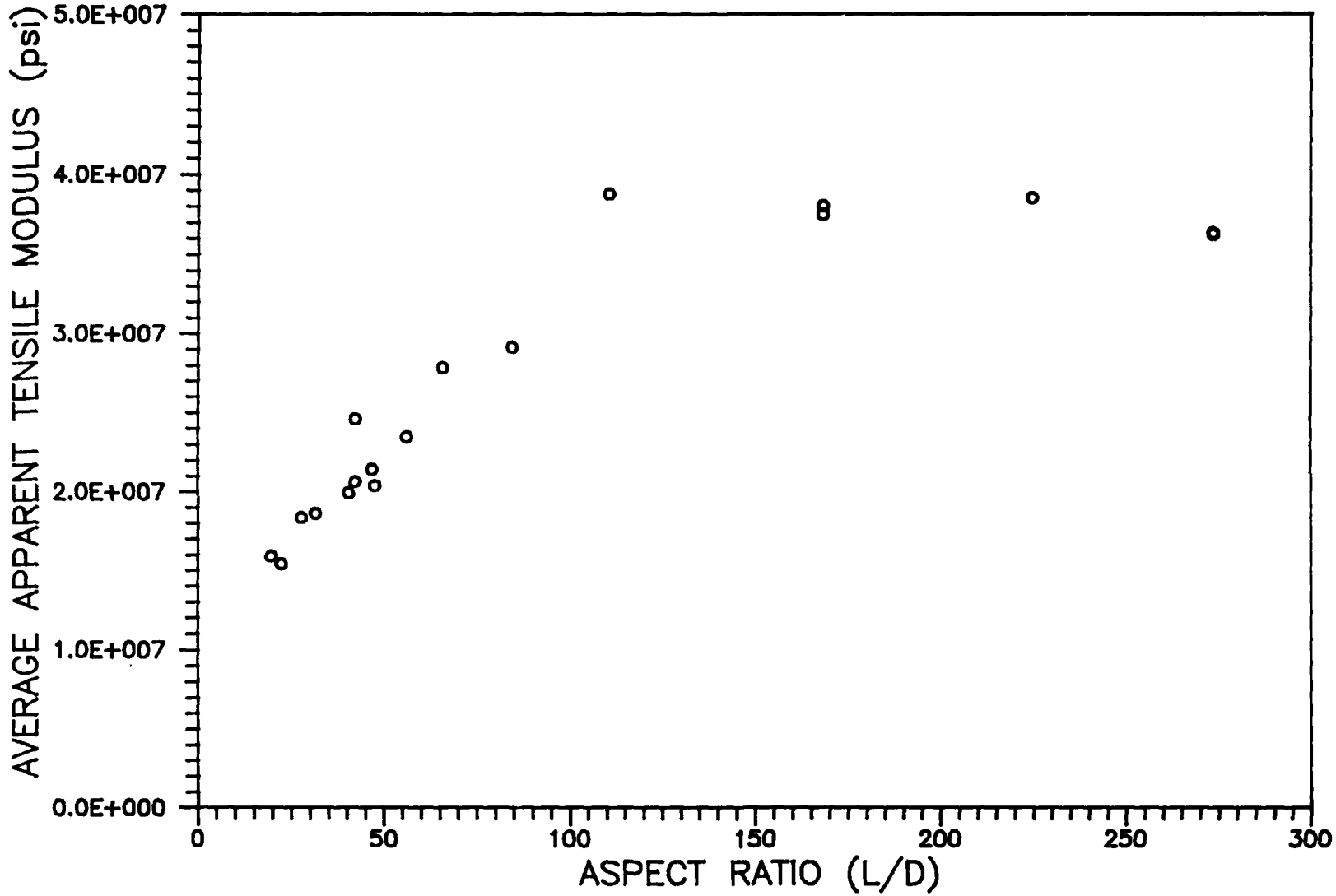

Figure 8. VARIATION of AVERAGE APPARENT TENSILE MODULUS with ASPECT RATIO for PBO 8A

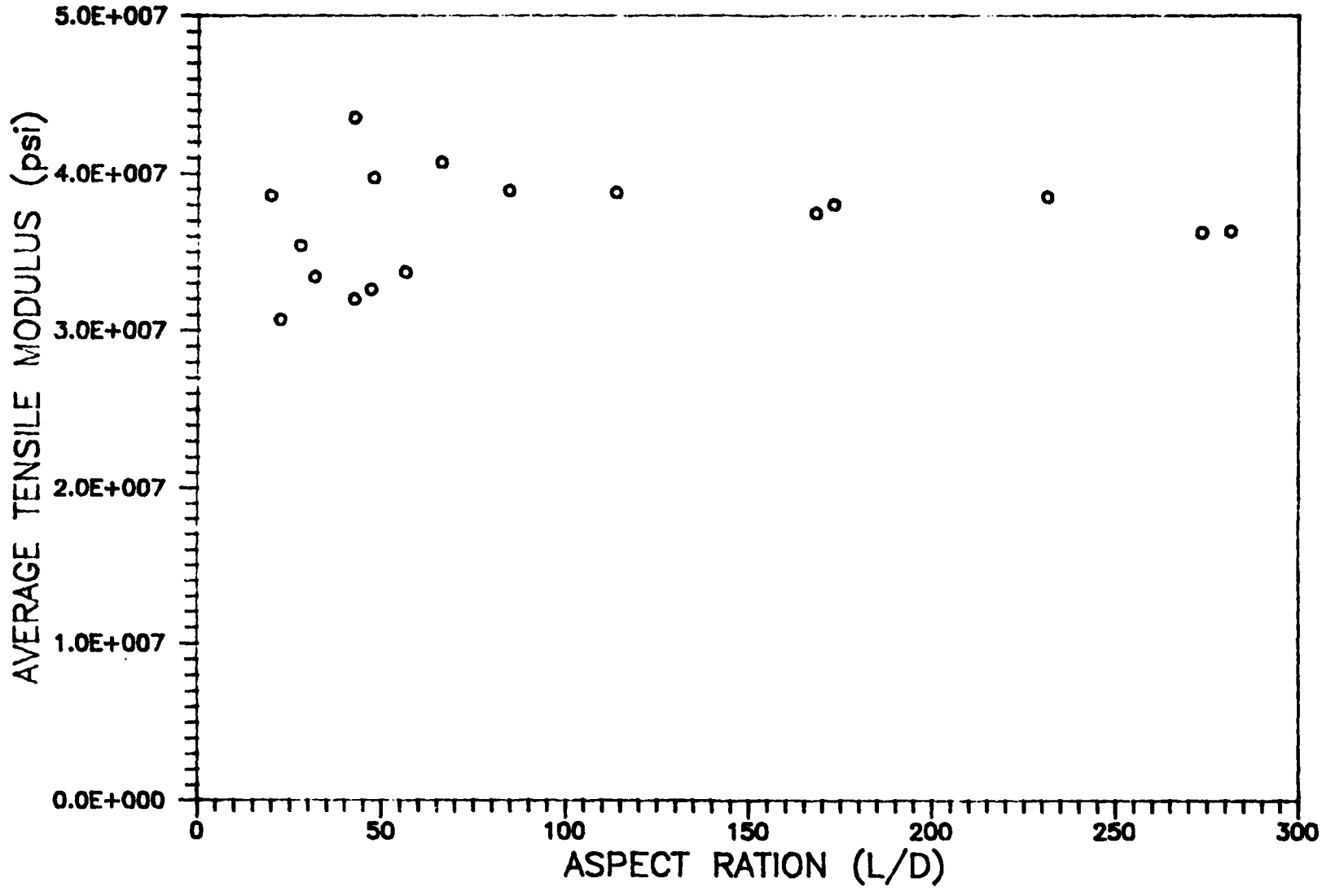

Figure 9. CORRECTED AVERAGE TENSILE MODULUS for PBO 8A

glue. Heretofor, "machine compliance" is defined as the conglomeration of the above factors. Substituting $\sigma_t = P/A$, where P is load, into Eq (5), where the machine compliance was only proportional to the load and dependent on the cross-sectional area.

$$1/E = 1/E_o + (\Delta l_m/P)(A/l_t) \tag{6}$$

Plotting the inverse of the apparent modulus versus the inverse of the aspect ratio did not change the corrected modulus or machine compliance. Since the modulus of elasticity is a material property, it should be constant regardless of any changes in sample geometry. As seen from Eq (6), the machine compliance, the term premultiplying the inverse of the aspect ratio, was also independent of variation in sample geometry.

Another approach to determine the machine compliance was to model the fiber-glue system as three elastic springs connected in series, shown in Figure 10. The premise of the analysis was the glue beads anchoring the fiber to the anvil and true machine compliance would act as springs in addition to the spring stiffness of the fiber. In order to determine the latter, the former must be determined and can be done through the following derivation. The displacement of a uniaxially loaded bar can be defined as

$$\delta = PL/AE \tag{7a}$$

where

δ = displacement (units of length)
P = uniaxial load (units of force)
L = length (units of length)
A = cross-sectional area (units of length^2)
E = modulus of elasticity (units of force/length^2)

Solving for P/δ yields

$$P/\delta = AE/L \tag{7b}$$

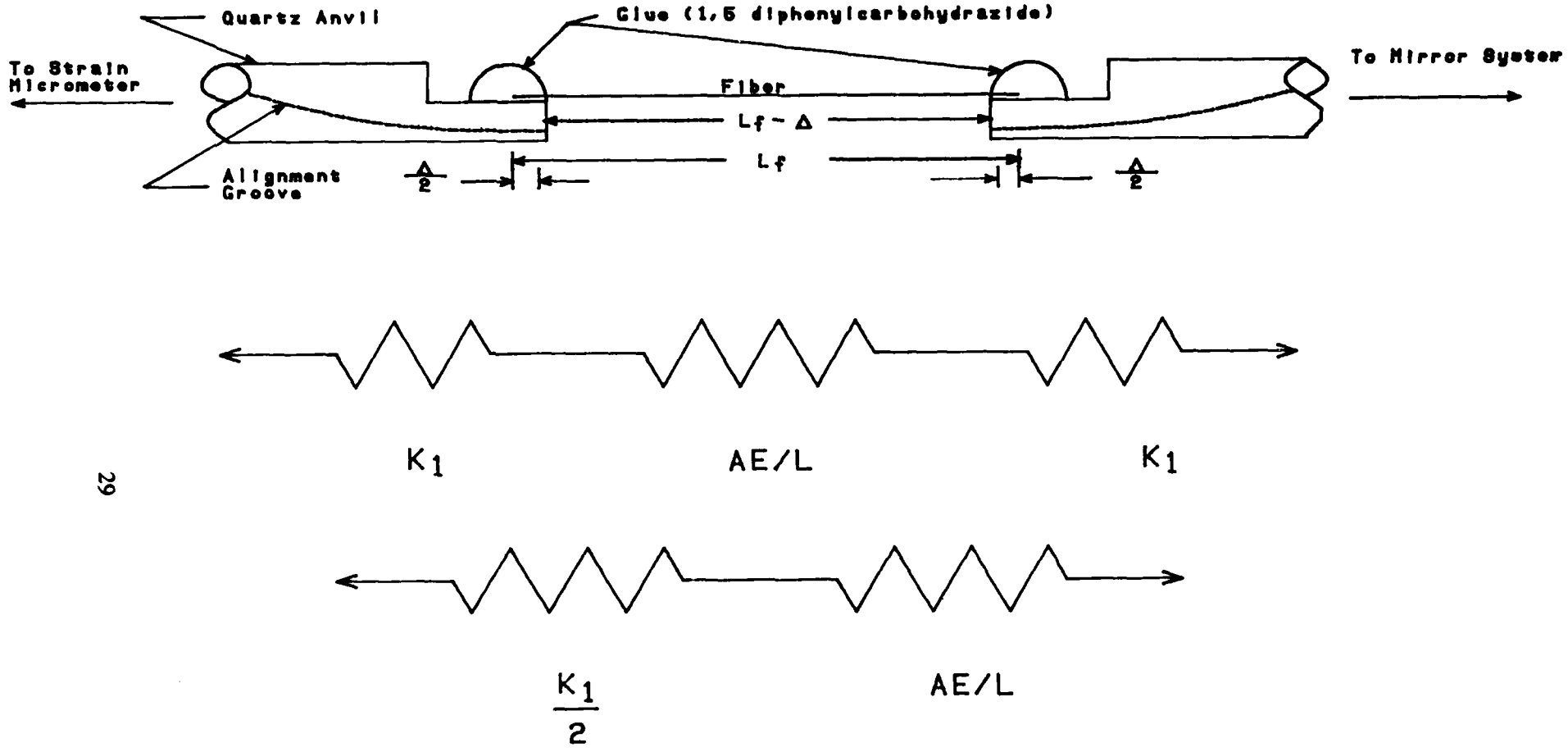

Figure 10. SPRING MODEL SYSTEM

Eq (7b) is of the form

$$F = -k_1 x \tag{7c}$$

which is the force, F, required to displace a linear, elastic spring a distance of x. The right hand side of Eq (7b) and k_1 in Eq (7c) represent the stiffness of the fiber and machine compliance; respectively. Assuming the stiffness of the system is dominated by the machine compliance for fibers of extremely short gage length, and conversely, dominated by the stiffness of the fiber for fibers of large gage length; the contribution of one individual spring connected in series within a system of springs is determined by dividing the product springs by their sum as follows;

$$1/X = 2/k_1 + L/AE \tag{7e}$$

where 1/X is the equivalent stiffness of the system which is k_1 for short or AE/L for long fibers. Solving for X and substituting the appropriate system stiffnes yields

$$k_1/2 = (k_1 AE/2L)/(k_1/2 + AE/L) = AE/L \tag{8}$$

If the modulus of elasticity and tensile stress of Eq (5) were represented in terms of load and displacement Eq (8) is obtained. The significance was that both approaches to determine the machine compliance generated the same solution.

The tensile and compressive moduli were determined by cycling the load from tension to compression or vice versa. The fiber behaved linearly as the load was cycled from compression to tension as shown if Figure 11; indicating equivalent tensile and compressive moduli. Some offset from zero did exist; however, if the fiber was loaded in tension first, the offset was in the direction of positive strain; similarly, if loaded in

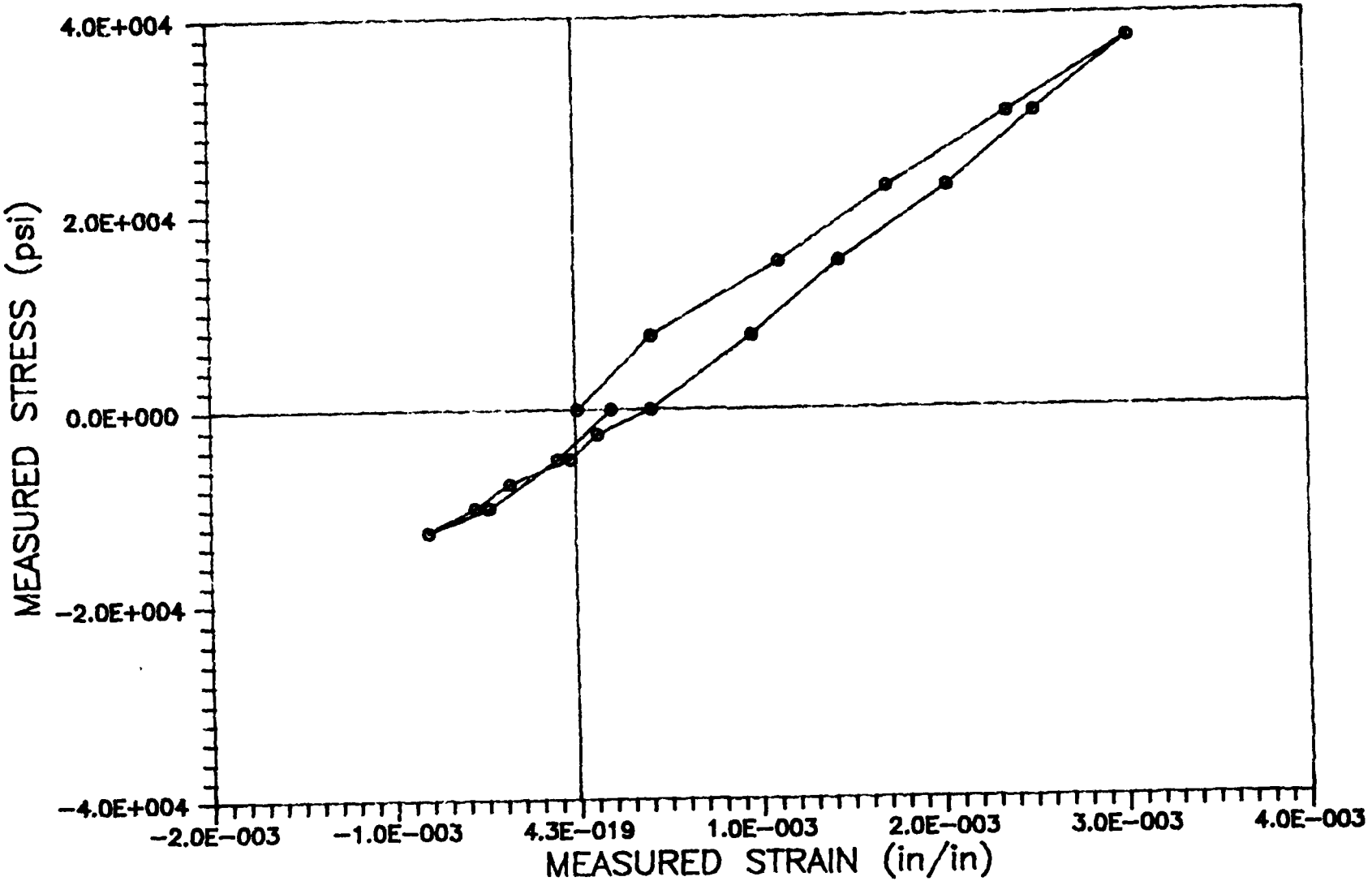

Figure 11. PBO 8A TENSION/COMPRESSION TEST

compression first the offset was in the negative strain direction. Therefore, the offset was not attributed to hysterysis or plastic deformation of the fiber. However, the possibility of the latter two phenomena in the glue or drift of the displacement zero might account forthe offset. No quantitative result was determined for the magnitude of the offset; however, due to the consistency of the behavior described above, the effects of the offset were deemed insignificant . The offset could be determined by bonding the two sample holders together then zeroing the machine. With zero load applied, rotating the large strainmicrometer, which actually was a displacement micrometer, enough to just have the extension detector images split would yield displacemental variation. The displacement micrometer could be rotated clockwise and counter-clockwise to determine the displacemental variation when the machine was in tension and compression, respectively. Due to the fragility of the machine and the unpredictability of the outcome, the above was not accomplished in fear of damaging the machine which has very few replacement parts.

The typical relationship between compressive stress and strain as a function of gage length is shown in Figure 12. Fiber #6 demonstrated an initially high modulus, but due to the large gage length of 0.5mm, it buckled causing premature failure and a subsequent low modulus. With a gage length of 0.2mm, fiber #5 had a low modulus and compressive strength. The low modulus might be attributed to the machine compliance as discussed earlier or possible errors in measuring the gage length. The low compressive strength could only be credited to fiber misalignment or a nonuniform stress distribution. Fiber #8 had a gage length of 0.45mm and the highest modulus of the three. Later measurements of compressive properties were determined with fibers whose gage length were between 0.2 - 0.5mm, inclusive.

Using Eq (3), with the tensile machine compliance curve mean corrected modulus of E_t = 35.9 Mpsi, d = 17.5μm, G = 0.174Mpsi; the minimum gage length allowable to avoid boundary effects on the stress distribution was 0.53mm. The shear modulus for PBO was unknown, but was approximated by using the shear modulus of PBT,

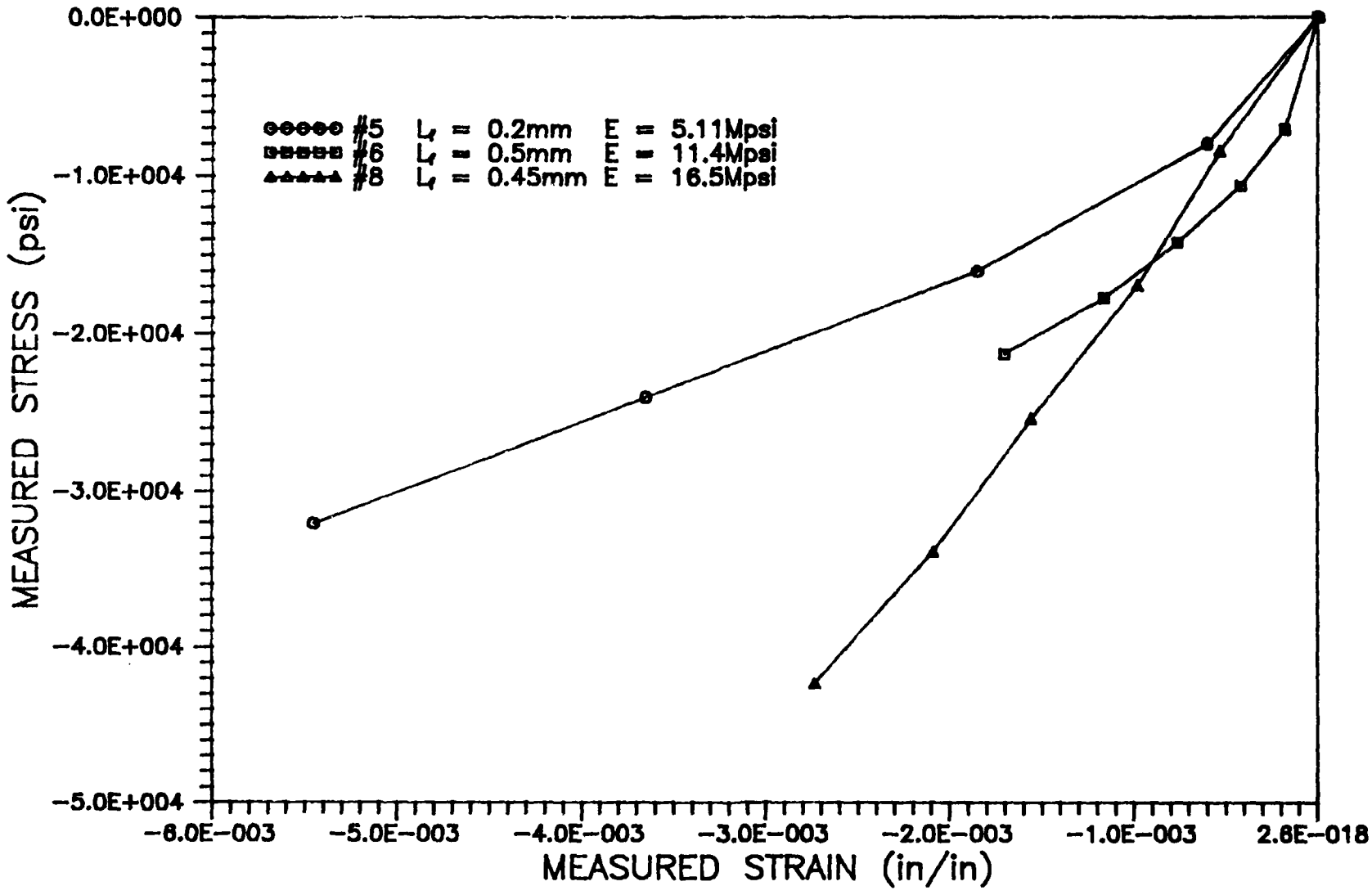

Figure 12. EFFECTS OF EULER BUCKLING and STRESS DISTRIBUTION on MODULUS of ELASTICITY

poly(p-phenylenebenobisthiazole) (21). From fiber #5 in Figure 12, the minimum aspect ratio to avoid end effects was 12. The minimum aspect ratio, from Eq (3), was approximately 30 which was on the decreasing portion of the curve meaning something was driving the modulus lower beside the non-uniform stress distribution, or the approximation for minimum gage length was not applicable for PBO.

The Euler Buckling criterion was adequate for a rough upper estimate, but the empirical and analytical data revealed a wide dichotomy in minimum gage lengths. Recall the Euler Buckling analysis yielded a maximum gage length requirement of 0.81mm. The dependence of the apparent modulus on the gage length was also present in the compression measurements as shown in Figure 13 and 14. In the compression tests, the modulus varied with the gage length just as in the tension tests. The apparent modulus range was from 10 - 20Mpsi, as listed in Table V, which was significantly lower than the tensile modulus range. From the compression compliance curve shown in Figure 15, the corrected modulus and machine compliance were 35.3Mpsi and 5.20 x 10^{-10}in'/lb. Both these values were within 3% of the corresponding tensile quantities. The extrapolated corrected modulus from Figure 15 was initially questioned due to the distance the curve had to be extended without having any data points in the that region. Assuming the machine compliance was constant in both tension and compression, the corrected compressive modulus could be obtained by using Eq (5) and the tensile machine compliance. The resulting average corrected compressive modulus was 35.6Mpsi.

The variation above and below the linear curve fit was present in both the tension and compression compliance curves. From Figure 16, the effective gage length might actually be longer than the measured gage length. The fiber was glued to each anvil, a perfect boundary didn't exist since the glue didn't instantaneously anchor the fiber. In actuality the fiber must extend into the glue some unknown amount, depending on the type of glue, fiber, and interface between them, before the glue supported the fiber. The additional length needed to support the fiber plus the distance between the two anvils was the

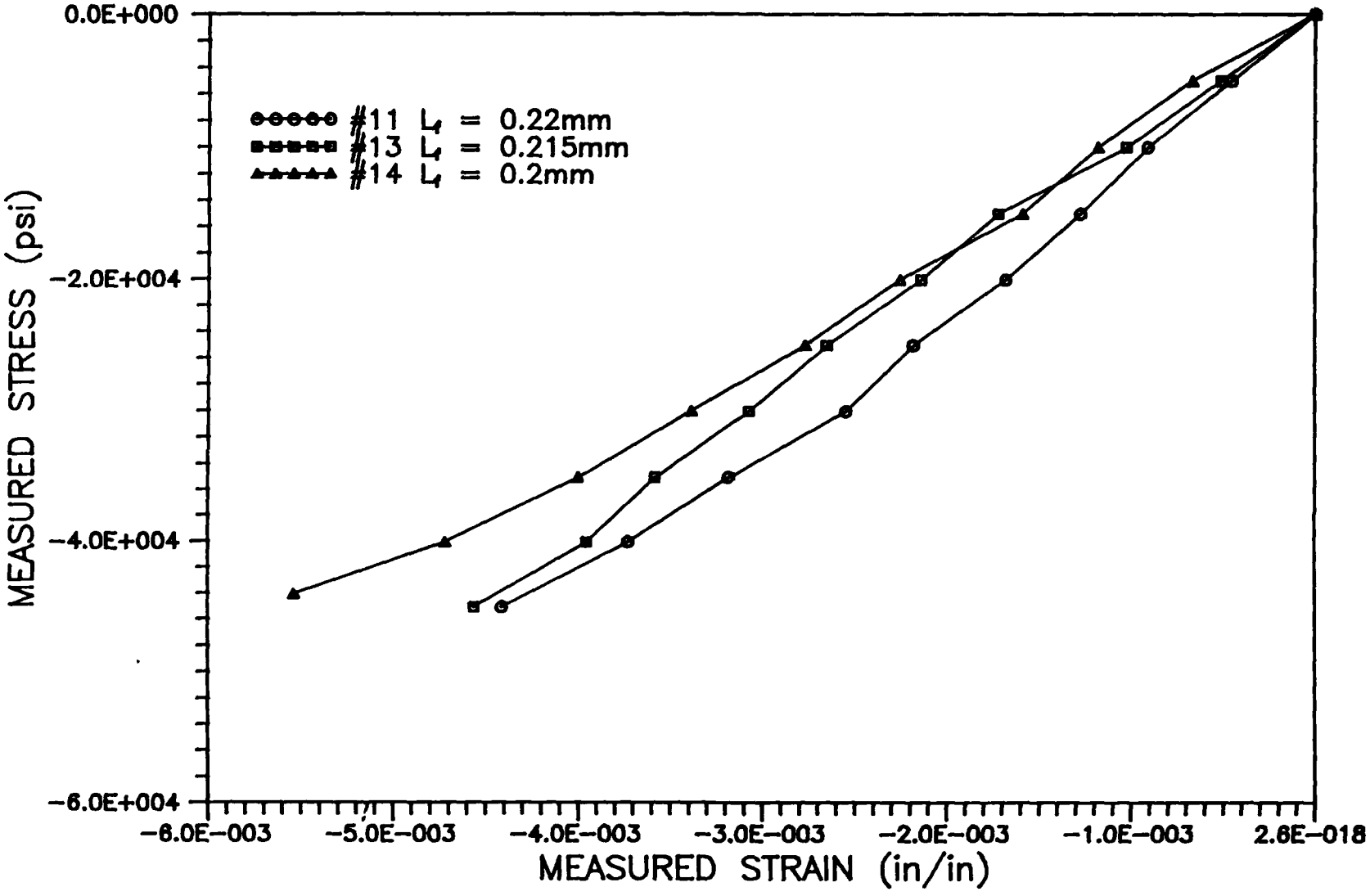

Figure 13. COMPRESSION TESTS for PBO 8A

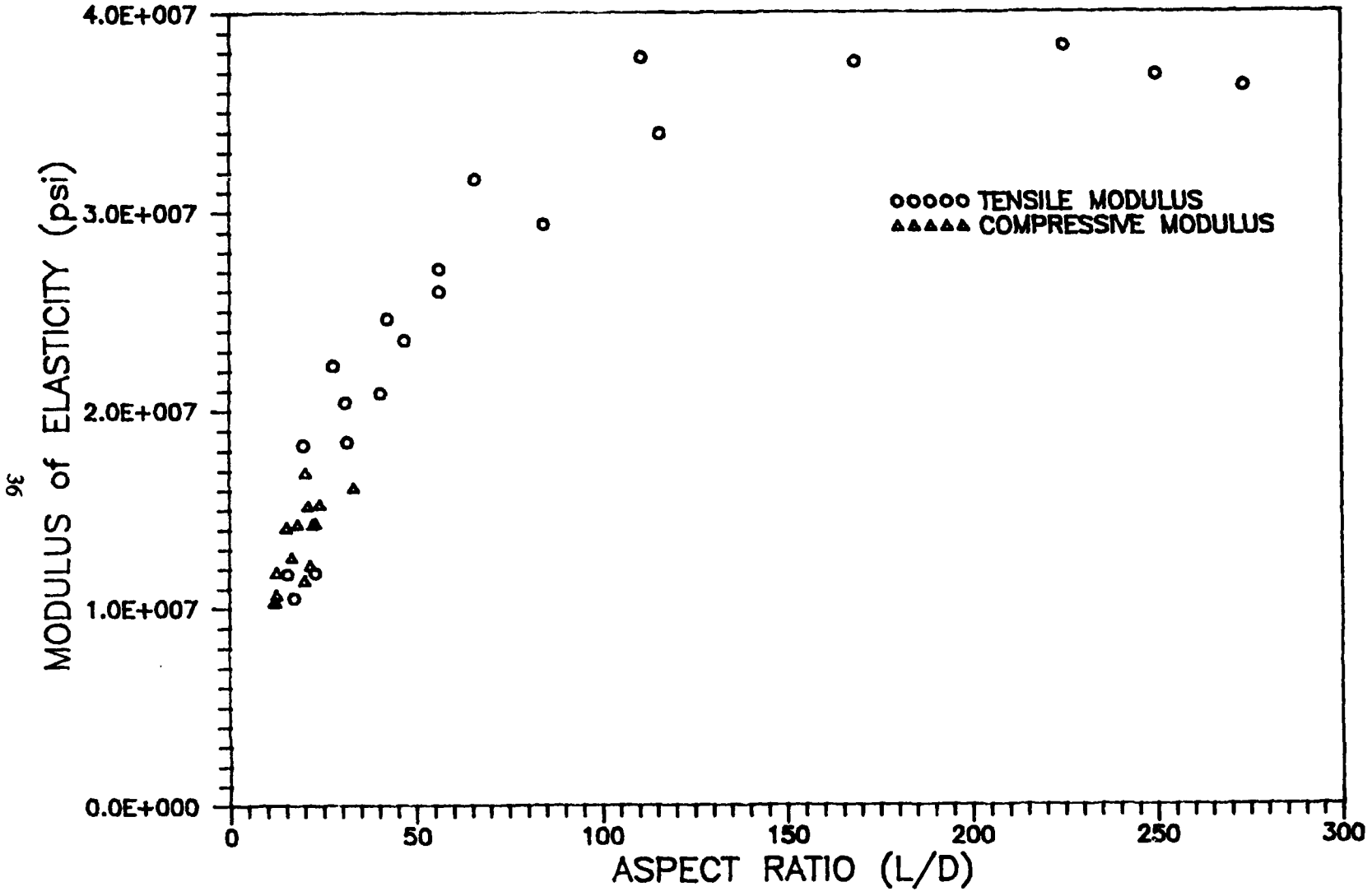

Figure 14. VARIATION of MODULUS of ELASTICITY with ASPECT RATIO for PBO 8A

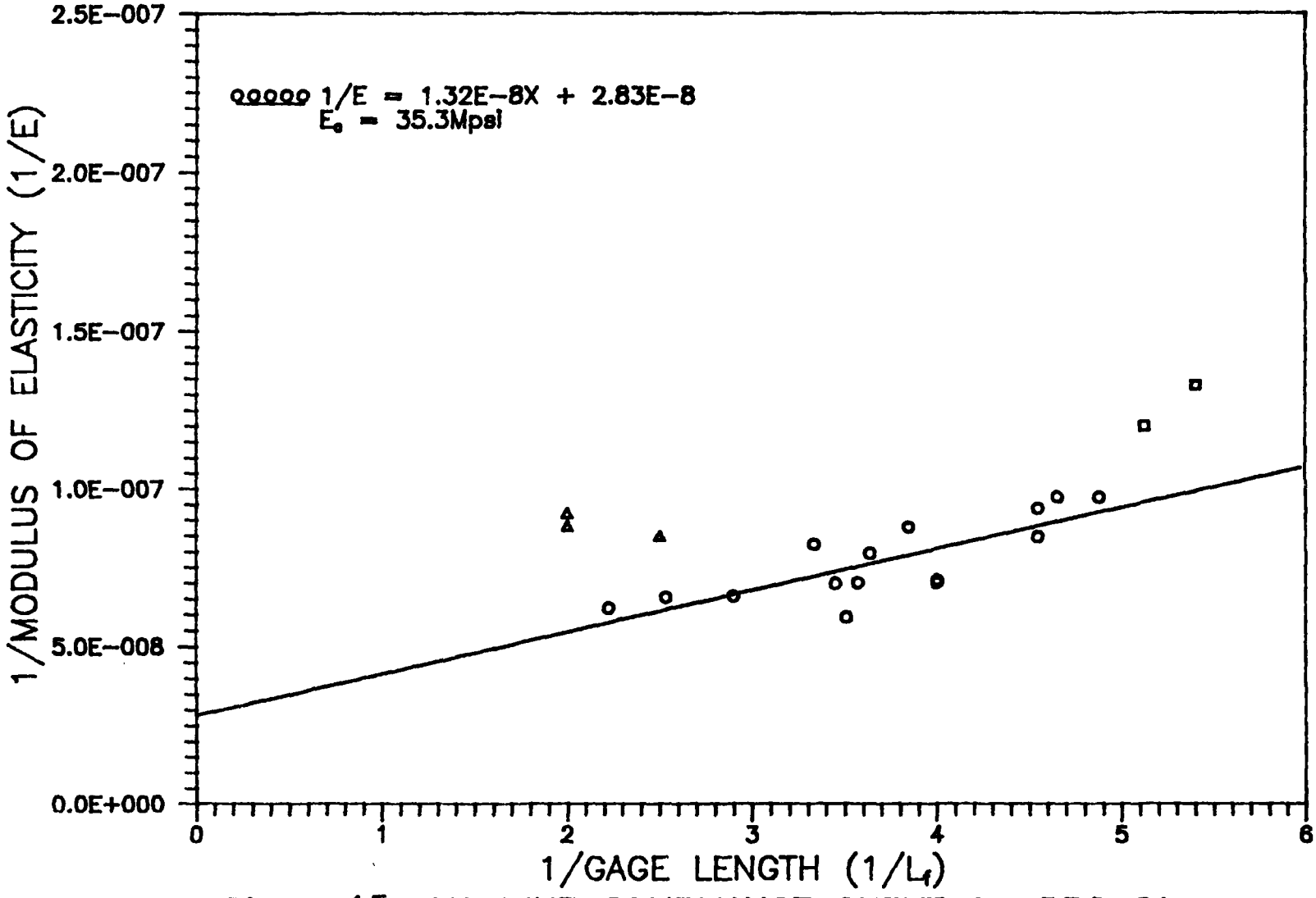

Figure 15. MACHINE COMPLIANCE CURVE for PBO 8A COMPRESSION TESTS

Table V Compressive Modulus Variation with Gage Length for PBO 8A

Fiber #	Diameter (μm)	Gage Length (mm)	Compressive Modulus (Mpsi)
9N	17.5	0.265	7.94
14N	17.5	0.195	8.32
13N	17.5	0.215	10.3
10N	17.5	0.22	10.7
11	16.5	0.5	10.9
6	14.9	0.5	11.4
20	12.9	0.26	11.4
5	17.5	0.4	11.8
11N	17.5	0.22	11.8
27	13.9	0.3	12.2
23	16.5	0.275	12.6
22	16.5	0.25	14.1
14	12.6	0.28	14.3
16	13.8	0.25	14.3
15	12.6	0.29	14.3
10	16.4	0.345	15.2
7	16.3	0.395	15.3
8	13.5	0.45	16.1
26	14.0	0.285	16.9

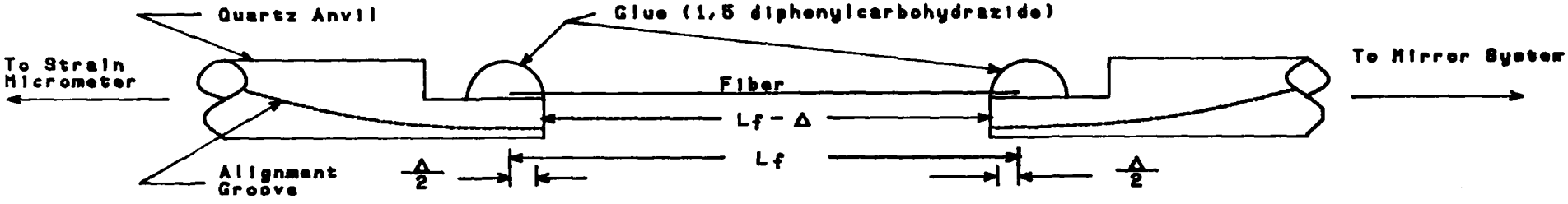

Figure 16. MISREADING the GAGE LENGTH DIAGRAM

effective gage length. The misreading of the gage length can be determined by slightly varying the derivation of Eq (5). Using the effective gage length as l_f-Δ for the 'old' l and substituting into Eq (4c) yields

$$\sigma_t = E(\Delta l_f + \Delta l_m)/(l_f - \Delta) \tag{9a}$$

where Δ is the error attributed to misreading the gage length.

$$\sigma_t/E = \Delta l_p/l_f(l_f/(l_f - \Delta) + \Delta l_m/(l_f - \Delta) \tag{9b}$$

Adding $\pm\Delta$ to l_f in the numerator of the first term of Eq (9b)

$$1/E = \Delta l_p/\sigma_t l_f[1 + \Delta/(l_f - \Delta)] + \Delta l_m/\sigma_t(1/l_f\text{-}\Delta) \tag{9c}$$

Simplifying to obtain the desired y = mx + b form

$$1/E = \Delta l_p/\sigma_t l_f + [\Delta l_f\Delta/\sigma_t l_f + \Delta_m/\sigma_t][1/(l_f - \Delta) \tag{9d}$$

where

$$1/E_o = \Delta l_p/\sigma_t l_f \tag{9e}$$

$$1/E = (1/E_O) + [\Delta/E_O + \Delta l_m/\sigma_t][1/(l_f - \Delta)] \tag{10}$$

Equation (10) was used to determine the gage length misreading including the effects of the machine compliance. A similar derivation was used to determine the effects of glue displacement combined with misreading the gage length and the machine compliance by adding the term Δl_g to the numerator of Eq (9a) and resulted in the following equation:

$$1/E = 1/E_O + [\Delta/E_O + \Delta l_m/\sigma_t + \Delta l_g/\sigma_c][1/(l_t - \Delta)] \quad (11)$$

From Eq (5), (10), and (11), as the gage length increased the effect it had on the apparent modulus decreased; in the limit of l_t going to infinity, the corrected and apparent moduli are equal. Error caused by misreading the gage length or glue displacement; if present, constructively add to lower the modulus values; thereby, increasing the slope of the compliance curve. Recall, Figure 6 and 15 showed variation above and below the linear curve forced through the data points. Misreading the gage length would only shift the curve above the linear fit not below. Glue slippage would have the same effect as the misreading error. Both errors, if present, because the slope to increase, but the corrected modulus remained constant. Misreading the gage length was not fiber dependent; the unknown additional distance into the glue on the anvil needed to support the fiber would be expected to remain relatively constant for all fibers of similar composition and dimension. Fiber slippage would depend on the bond between the fiber and the glue; therefore, it would be possible that one fiber may slip, and another may not even if the fibers were of the same type. Due to the random scatter of data on the compliance curve, the existence of errors in the PBO fibers due to misreading the gage length and/or fiber slippage was inconclusive.

The type of variation present didn't reinforce the theories of misreading the gage length or fiber slippage, both dictating an increase in slope for shorter gage lengths which was not consistently present. The square data points in Figure 15 correspond to fibers which were misaligned or had a nonuniform stress distribution, but it was impossible to distinguish which one was present. The triangular data points represent fibers that buckled resulting in the lower compressive modulus.

In the compression tests, the stress-strain relation was nonlinear in some instances. This could be due to plastic deformation or out of plane displacement of the fiber. Gradual kinkband formation would account for the nonlinearity; however, the nature of kinkband

formation is not known. In roughly 50% of the fibers tested, the load prior to failure resulted in an elastic deformation which would not indicate gradual kinkband formation. Since the deformation at failure could not be determined, the linearity or nonlinearity of the deformation was unknown. The deformation at the critical load was indeterminable since the mirror images could not be realigned. The inability to realign the images after failure produced the linear stress-strain relation from zero load to fracture. The appearance of a non-linear stress-strain relation existed for fibers with relatively large gage lengths; however, this was not attributed to plastic deformation of the fiber in these cases. In those fibers exhibiting this phenomenon, the non-linear behavior was due to gradual bowing of the fiber caused by an induced moment from fiber misalignment or possibly plastic deformation of the glue. The load was not large enough to cause buckling, but did cause the non-linear displacement. The bowing of the fibers could possibly be caused by fiber misalignment or due to the formation of kinkbands. The former was difficult to detect due to the low power of the travelling microscope. When kinkbands were formed the applied load no longer acted in line with the longitudinal axis of the fiber, but was resolved into normal and shear stresses acting perpendicular and parallel to the plane of the kinkband. These two stresses might cause the bowing which was evident in some of the polymeric fibers, thus yielding non-linear displacements.

KEVLAR 29™ AND 49™

Kevlar 29™ and 49™ were polymeric fibers tested to further examine the reliability of direct compression testing of fibers of extremely short gage length. Figure 17 showed representative tension tests with little variation in apparent modulus as the gage length exceeded 5.0mm. The offset from the origin after the fiber was unloaded was present in almost every tension test and was always in the direction of positive strain; thus reinforcing the assertion that the offset was due to machine imprecision, plastic deformation of the glue, or hysterysis in the glue. Significant variation was present in fibers of gage lengths less than 1.0mm as shown by the tension/compression measurements in Figure 18. The nonlinearity seen in the final load increments of the compressive loading in Figure 17 cannot be attributed to any one cause but might be due to fiber misalignment, nonuniform stress distribution, and/or microbuckling of the microfibril. The tension/compression tests exhibited linearity when passing through the origin as expected indicating equivalent tensile and compressive moduli. Again, the offset from the origin upon unloading was negative strain for compression and positive strain for tension. The fiber tensile modulus was no longer dependent on gage length as the gage length exceeded 1.25mm which resulted in an aspect ratio of 100 as shown if Figure 19. The modulus approaches an asymptote at approximately 13.5Mpsi which was slightly higher than the 12.0Mpsi obtained from the Instron data (21). The diameter of the fiber did not alter the average tensile modulus versus aspect ratio plot; therefore, little or no dependence on fiber diameter by the stress distribution or tensile modulus existed. A summary of the fiber tension tests are listed in Table VI; those measurements marked with an asterisk had misaligned fibers.

The machine compliance curve shown in Figure 20 yielded a corrected modulus of 14.1Mpsi and a machine compliance of 4.70×10^{-10}in'/lb. The square data points correspond to moduli values where the modulus no longer depended on the gage length; therefore, they were not included in the linear regression calculation to determine the best for the data. Using the tensile machine compliance and Eq (5), the corrected tensile moduli were plotted in Figure 21. The mean corrected tensile modulus was 14.1 with a standard

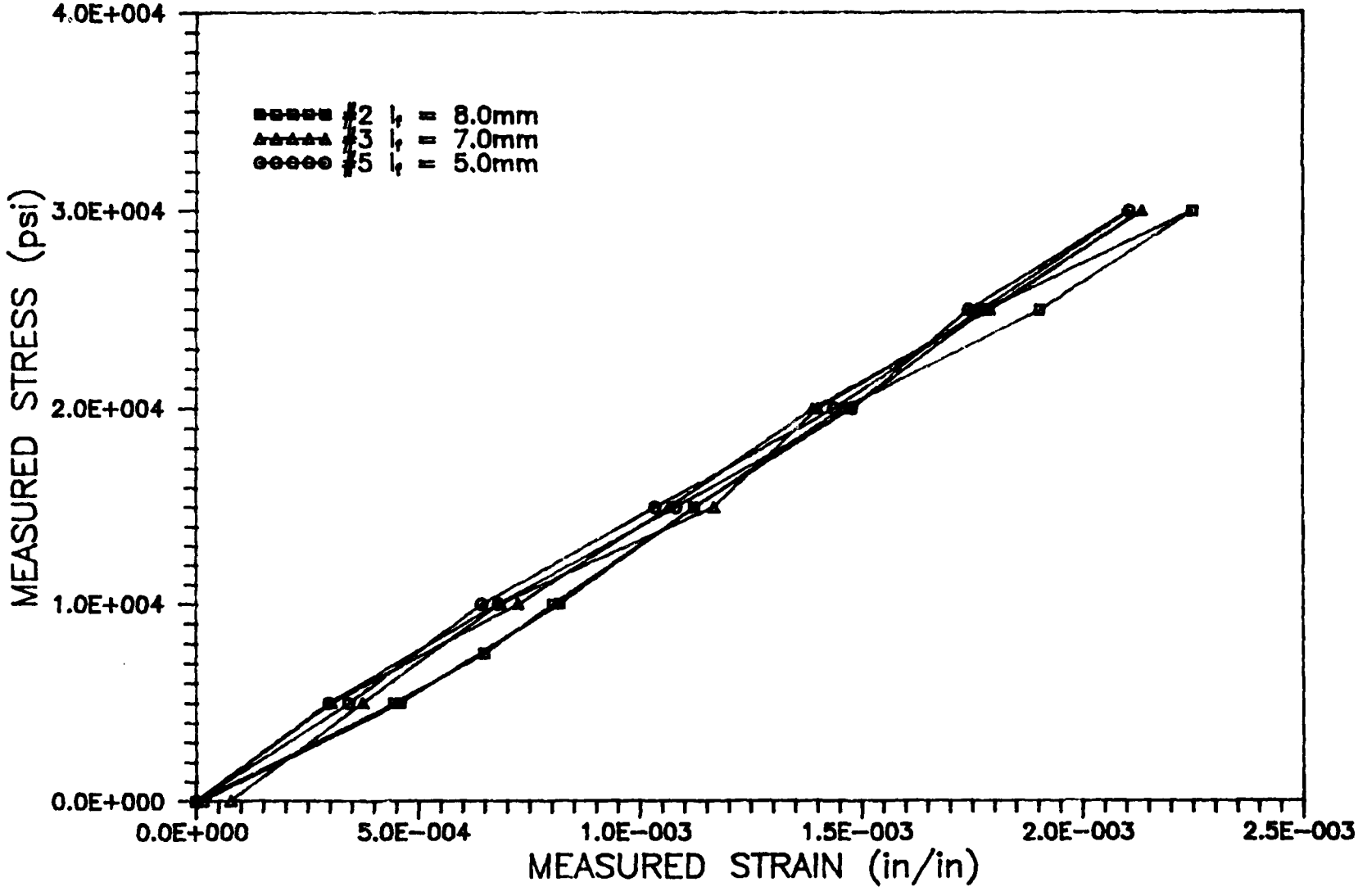

Figure 17. KEVLAR 29™ TENSION TESTS

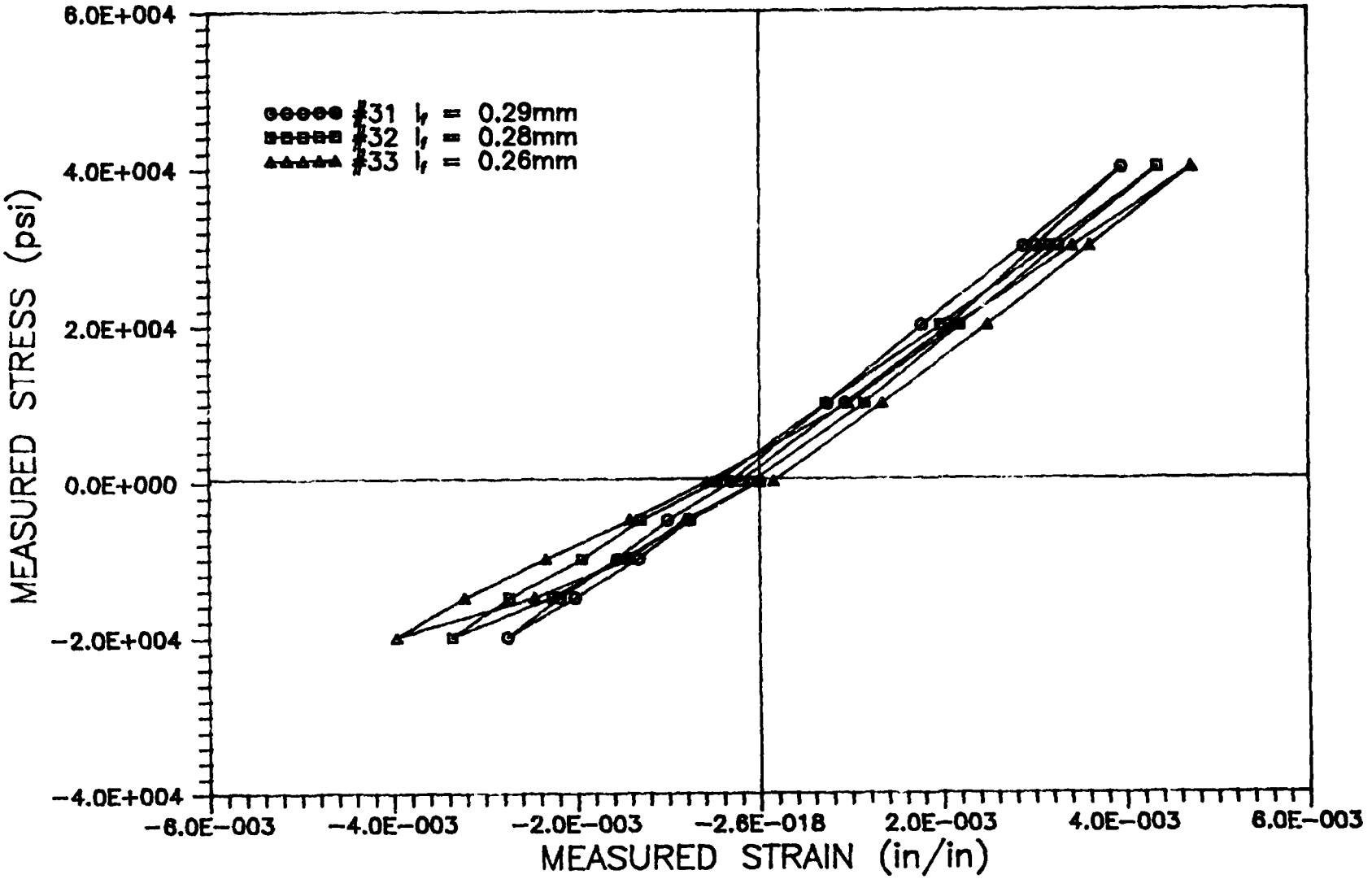

Figure 18. KEVLAR 29™ TENSION/COMPRESSION TESTS

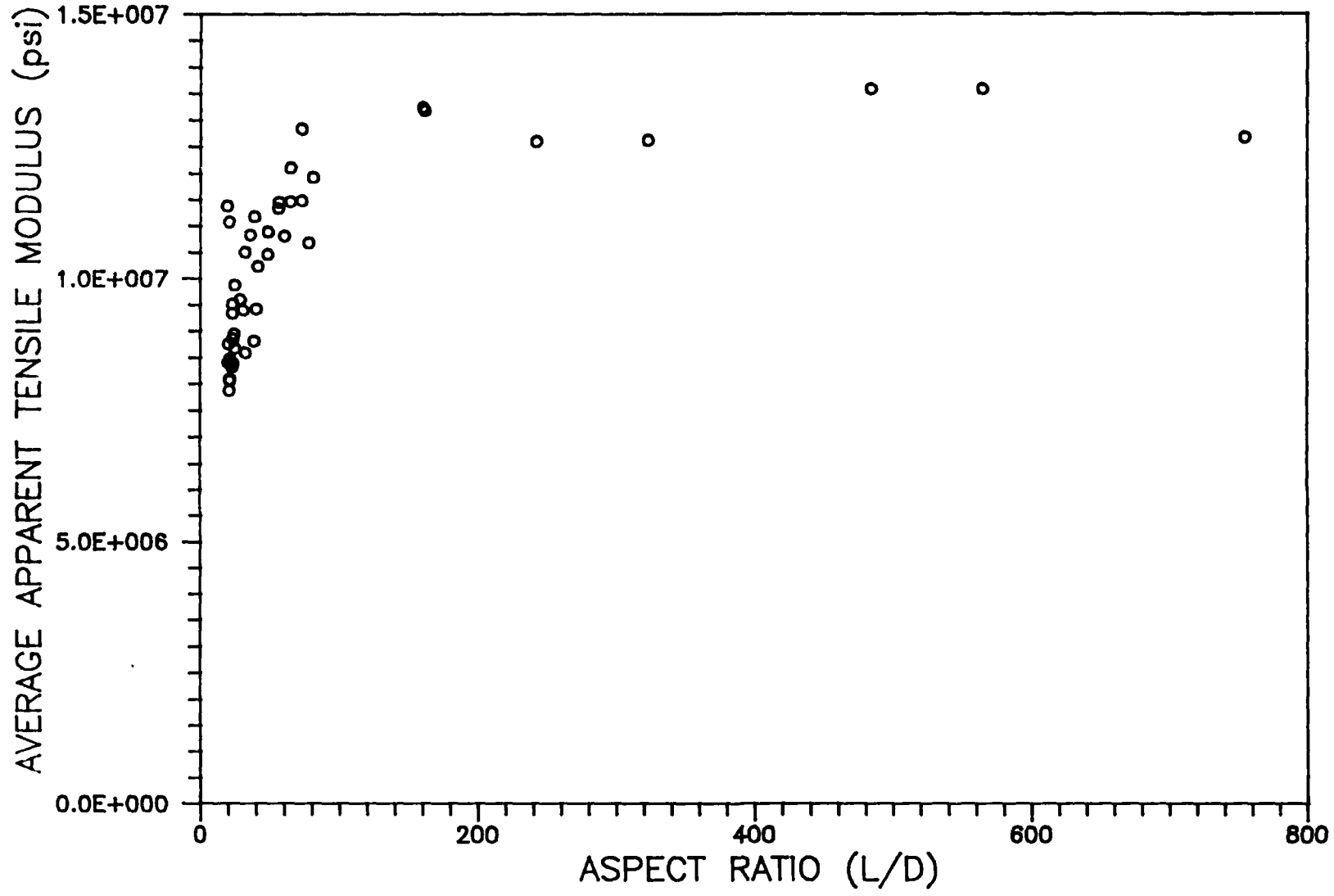

Figure 19. VARIATION of AVERAGE APPARENT TENSILE MODULUS with ASPECT RATIO for KEVLAR 29™

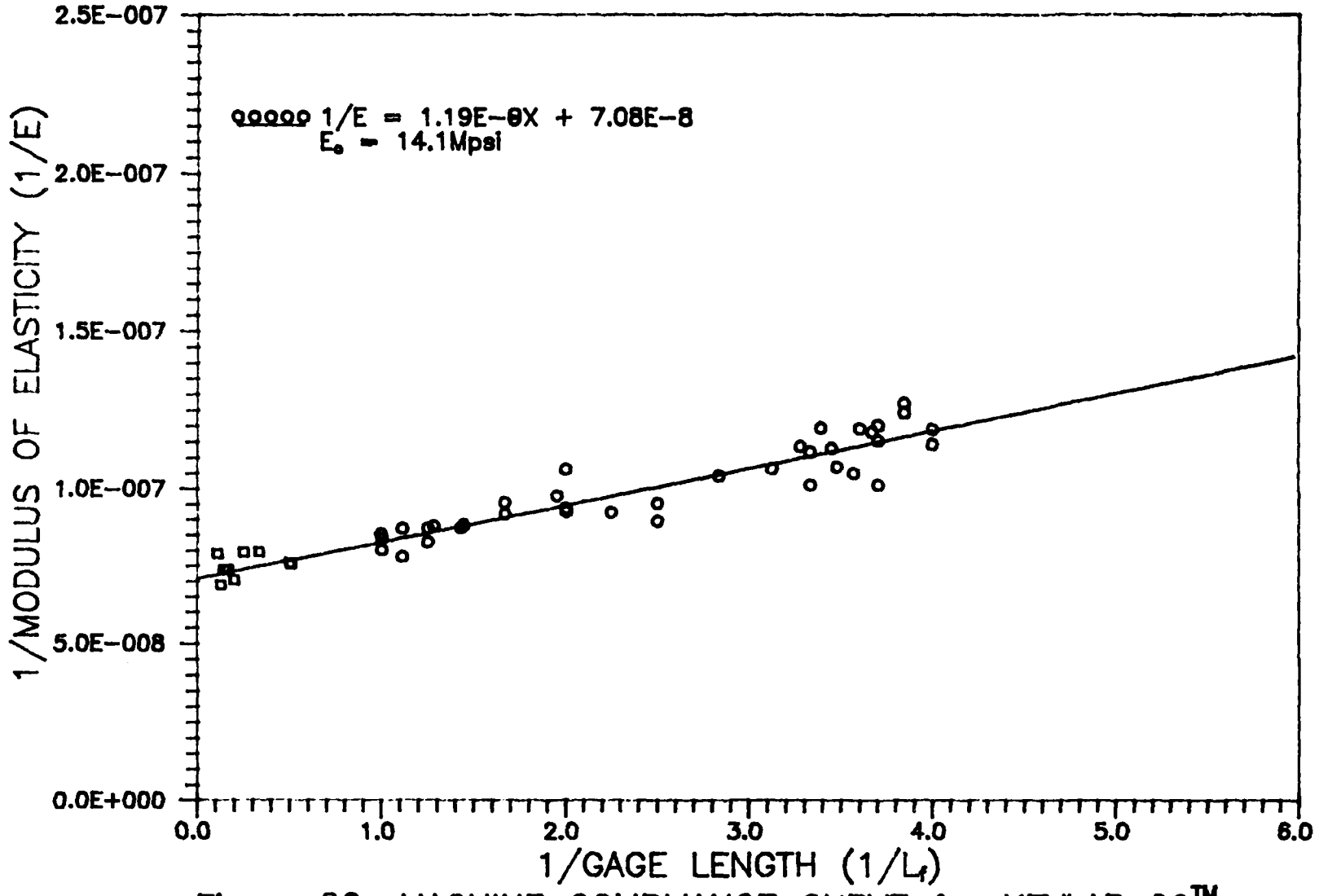

Figure 20. MACHINE COMPLIANCE CURVE for KEVLAR 29™ TENSION TESTS

Table VI Tensile Modulus Variation with Gage Length for Kevlar 29™

Fiber #	Diameter (μm)	Gage Length (mm)	Tensile Modulus (Mpsi)
33	12.4	0.26	7.87
48	13.0	0.26	8.06
46	13.0	0.27	8.32
45	13.0	0.295	8.38
32	12.4	0.2775	8.39
49	13.0	0.25	8.41
47	13.0	0.2725	8.47
39	12.4	0.27	8.66
34	12.4	0.25	8.76
44	13.0	0.305	8.81
30	12.4	0.29	8.85
29	12.4	0.3	8.94
31	12.4	0.287	9.34
38	12.4	0.32	9.39
26	12.4	0.5*	9.42
52	12.2	0.28	9.52
28	12.4	0.3525	9.60
51	12.2	0.3	9.87
53	12.2	0.27	9.88
15	12.4	0.5125	10.2
14	12.4	0.6	10.5
17	12.4	0.4	10.5
43	13.0	0.5	10.7
36	12.4	0.5	10.8
16	12.4	0.445	10.8
25	12.4	0.6	10.9
37	13.0	0.4	11.2
13	12.4	0.6925	11.3
35	12.4	0.78	11.4
24	12.4	0.7	11.45
23	12.4	0.8	11.46
22	12.4	0.9	11.49
42	13.0	1.005	11.7
21	12.4	1.0	11.9
12	12.4	0.8	12.1
10	12.4	1.0	12.5
8	12.4	3.0	12.6
6	12.4	4.0	12.6
1	12.4	9.35*	12.7
11	12.4	0.9	12.8
9	12.4	2.0	13.2
20	12.4	1.98	13.2
4	12.4	5.0	13.6
3	12.4	7.0	13.6
5	12.4	5.0	14.2
2	12.4	8.02	14.6

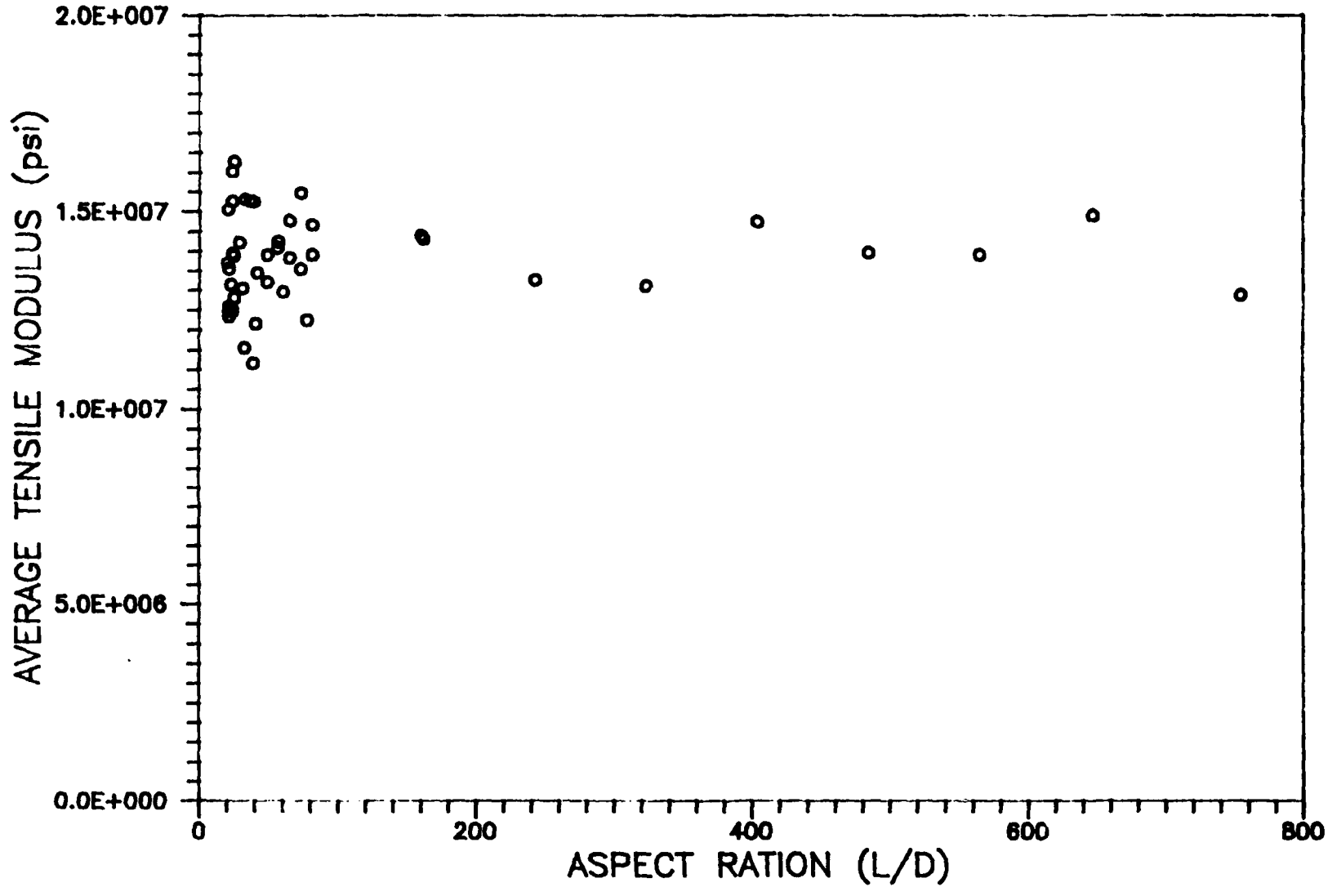

Figure 21. CORRECTED AVERAGE TENSILE MODULUS for KEVLAR 29™

deviation of 1.1Mpsi.

The shear modulus for Kevlar 29™ was unknown, therefore the minimum gage length required as determined by Eq (3) was unobtainable. Using Eq (2), the maximum gage length to avoid Euler Buckling was 0.35mm.

The compression compliance curve, data listed in Table VII, is shown in Figure 22 and yielded a corrected modulus of 11.2Mpsi and machine compliance of 5.38 x 10^{-10}in'/lb. The scatter of data as the gage length decreased illustrated a greater sensitivity to a non-uniform stress distribution and fiber misalignment than for the longer fibers. Using the tensile machine compliance and Eq (5), the corrected mean compressive modulus was 11.2Mpsi.

The dependence of the modulus on the gage length was present in both the tension and compression tests. This is further illustrated by Figure 23 where both the tensile and compressive moduli were plotted versus the aspect ratio.

To further investigate the reliability of direct compression testing using the MTM-8, Kevlar 49™ as listed in Table VIII, another polymeric fiber, was tested. Representative tension tests are shown in Figure 24, notice little dependence of the apparent modulus on gage lengths greater than 3.0mm. Conversely, fibers with gage lengths less than 1.0mm had apparent moduli with a strong dependence on the gage length as shown in Figure 25. The fiber behaved linearly when passing from tensile to compressive loading, therefore indicating equivalent moduli. The compressive failure behavior was the same as the previous two fibers; therefore, the nonlinearity near the last load increments could not be definitively attributed to fiber misalignment, nonuniform stress distribution, misreading the gage length and/or glue slippage. The moduli no longer depended on the gage length when an aspect ratio of approximately 80, corresponding to a gage length of 0.98mm, was obtained as shown in Figure 26. The asymptotic modulus from Figure 26 was approximately 16.0Mpsi compared to 18.0Mpsi obtained from Instron measurements. The repeatability of cyclical loading was demonstrated by the previous two fibers tested and was no longer questioned. The offset phenomena was again present and followed the same trends discussed earlier.

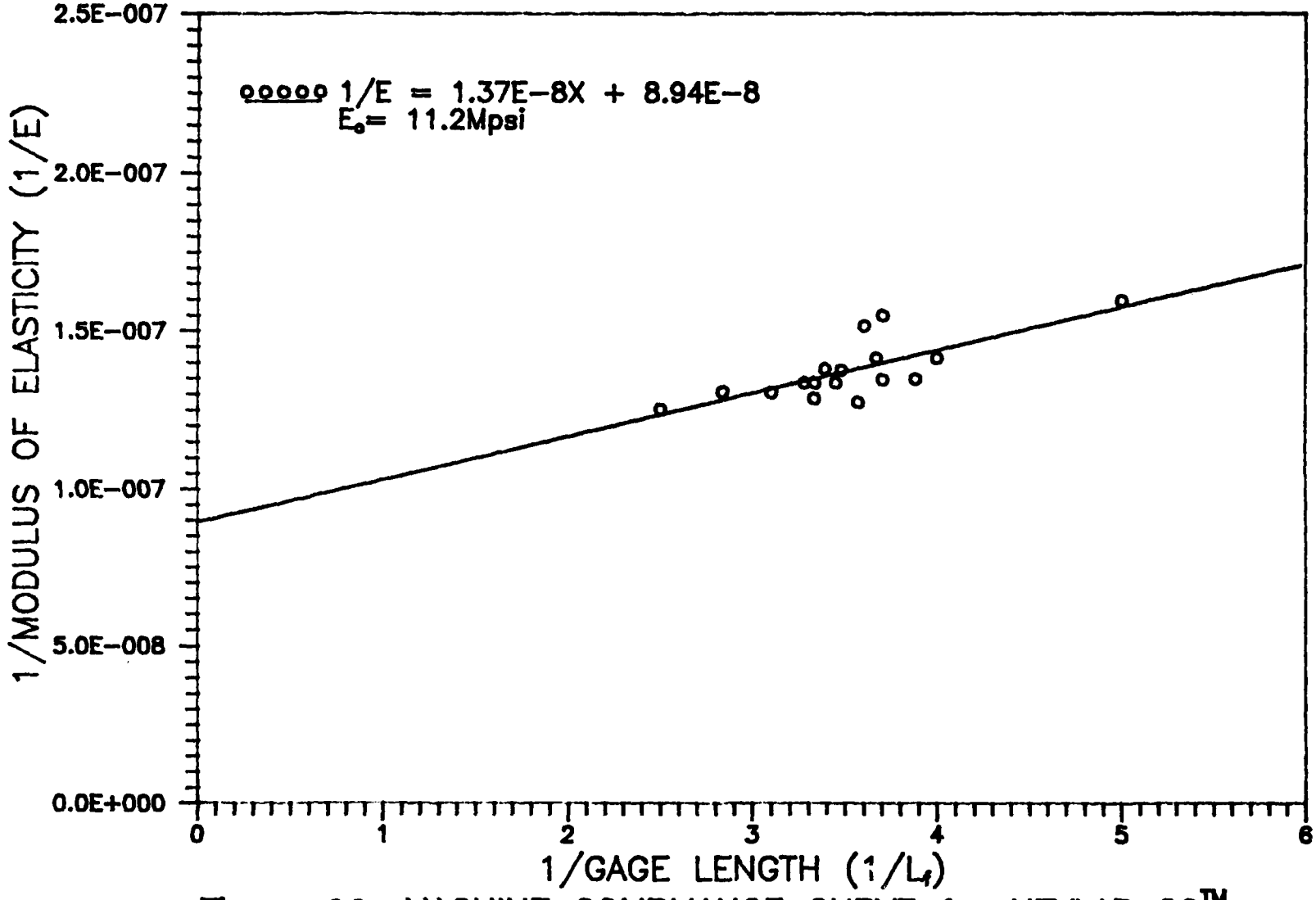

Figure 22. MACHINE COMPLIANCE CURVE for KEVLAR 29™ COMPRESSION TESTS

Table VII Compressive Modulus Variation with Gage Length for Kevlar 29™

Fiber #	Diameter (μm)	Gage Length (mm)	Tensile Modulus (Mpsi)
18	12.4	0.25	5.54
28	12.4	0.26	5.62
54	12.2	0.25	6.08
55	12.2	0.2	6.26
29	12.4	0.295	6.45
32	12.4	0.2775	6.59
31	12.4	0.2	6.73
30	12.4	0.2725	7.07
44	13.0	0.295	7.24
46	13.0	0.2875	7.27
45	13.0	0.27	7.42
39	13.0	0.305	7.49
41	13.0	0.29	7.48
51	12.2	0.3	7.78
52	12.2	0.28	7.85
27	12.4	0.27	8.23
47	13.0	0.32	9.08

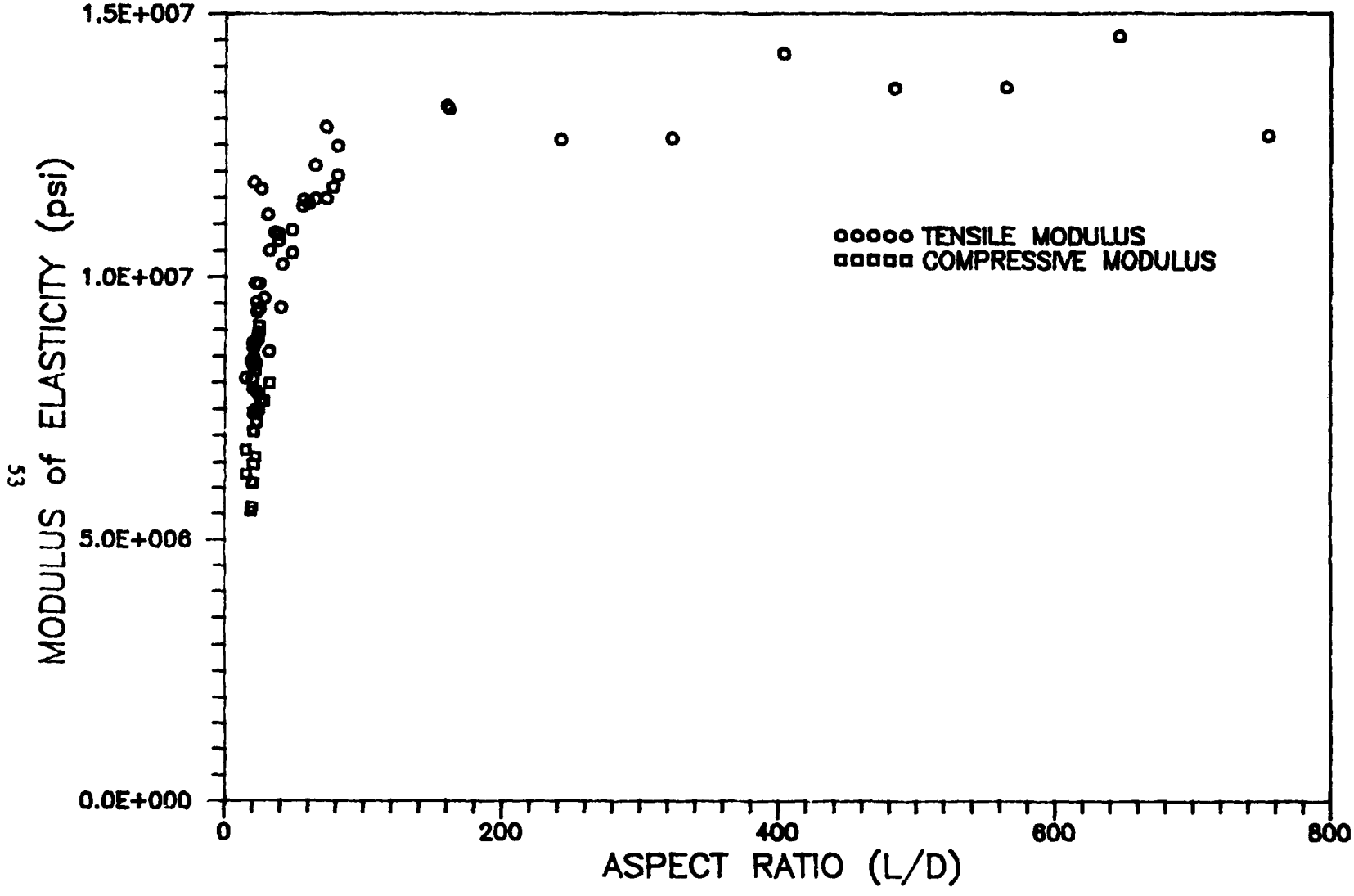

Figure 23. VARIATION of MODULUS of ELASTICITY with ASPECT RATIO for KEVLAR 29™

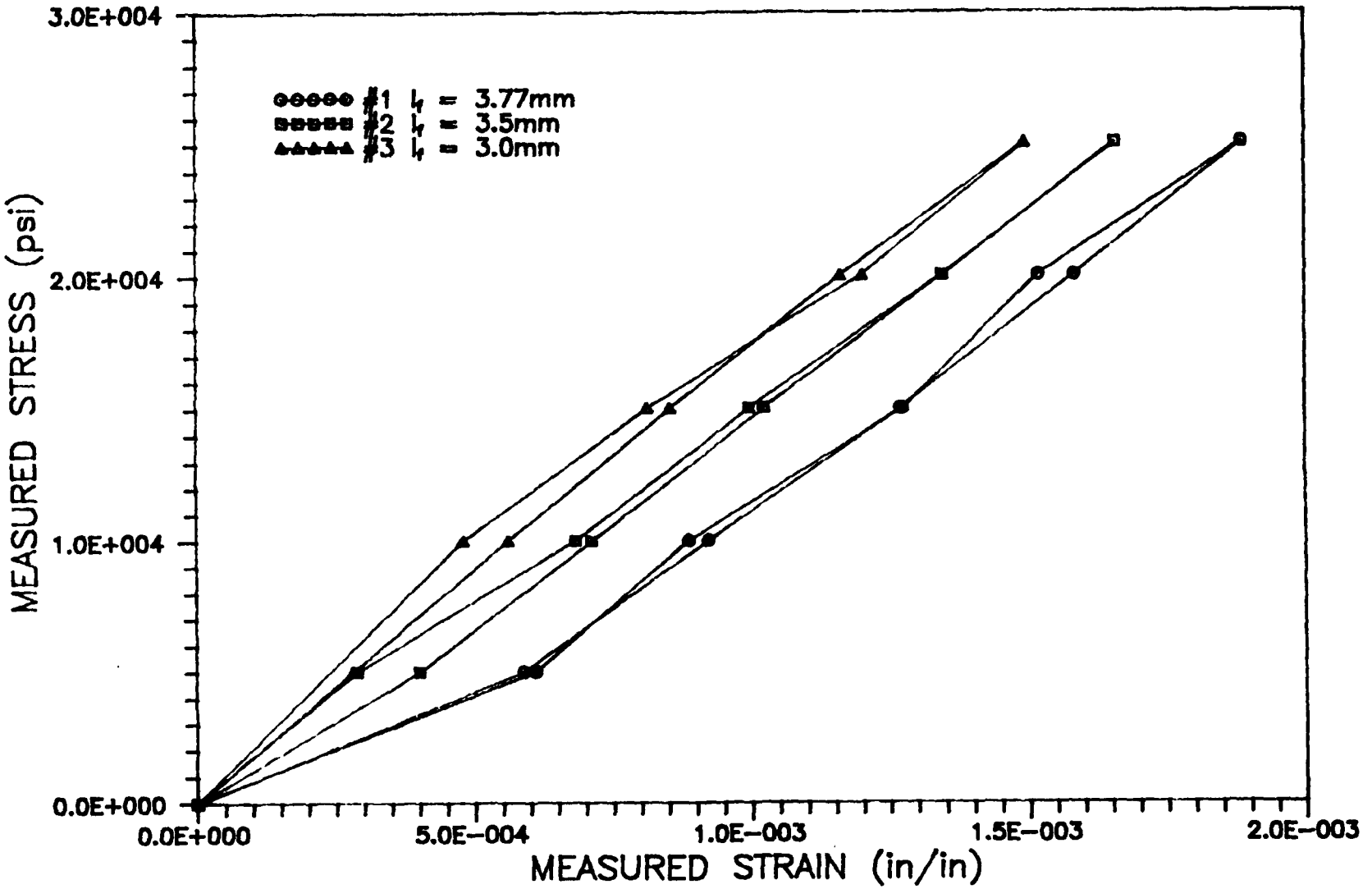

Figure 24. KEVLAR 49™ TENSION TESTS

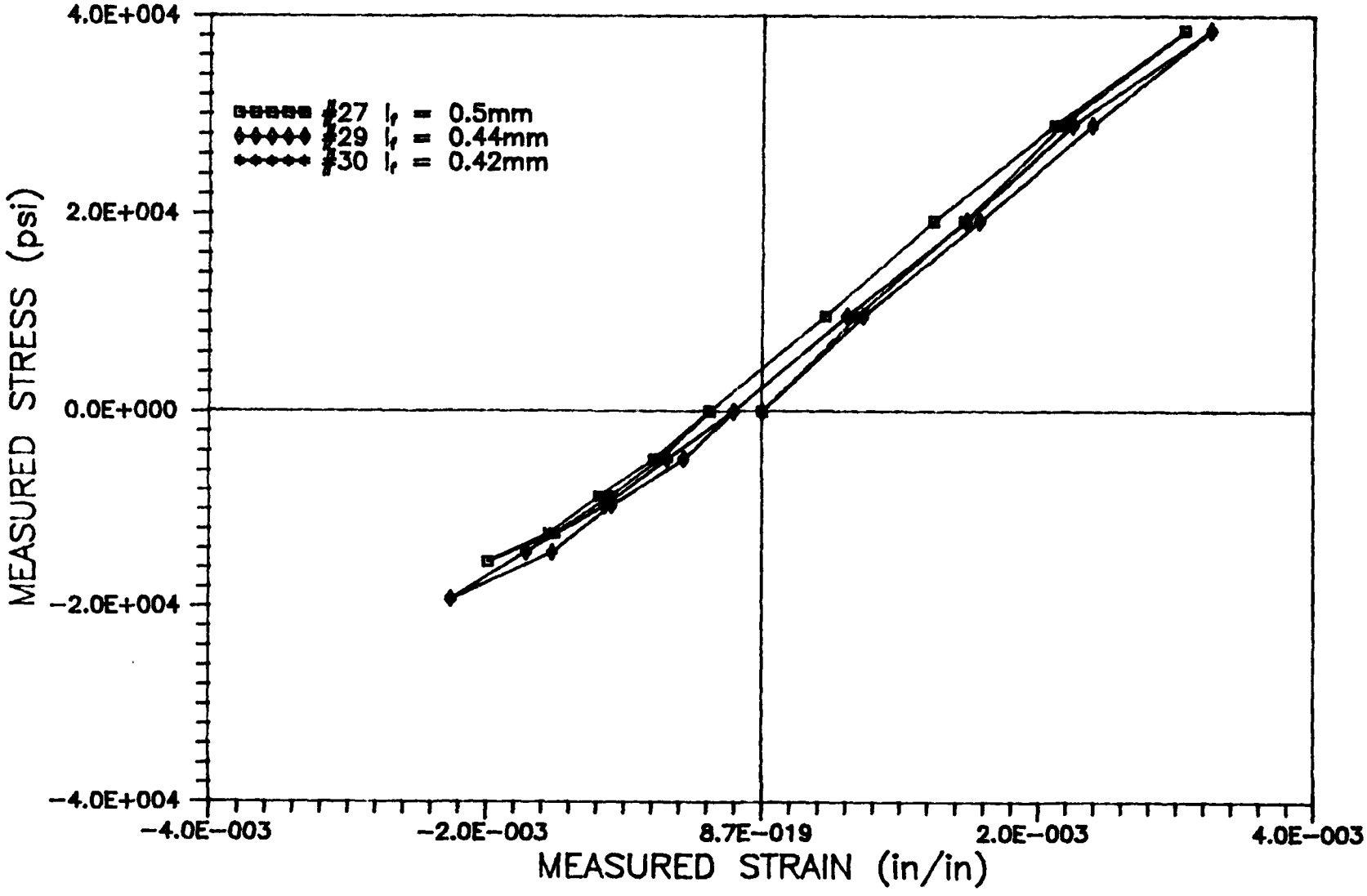

Figure 25. KEVLAR 49™ TENSION/COMPRESSION TESTS

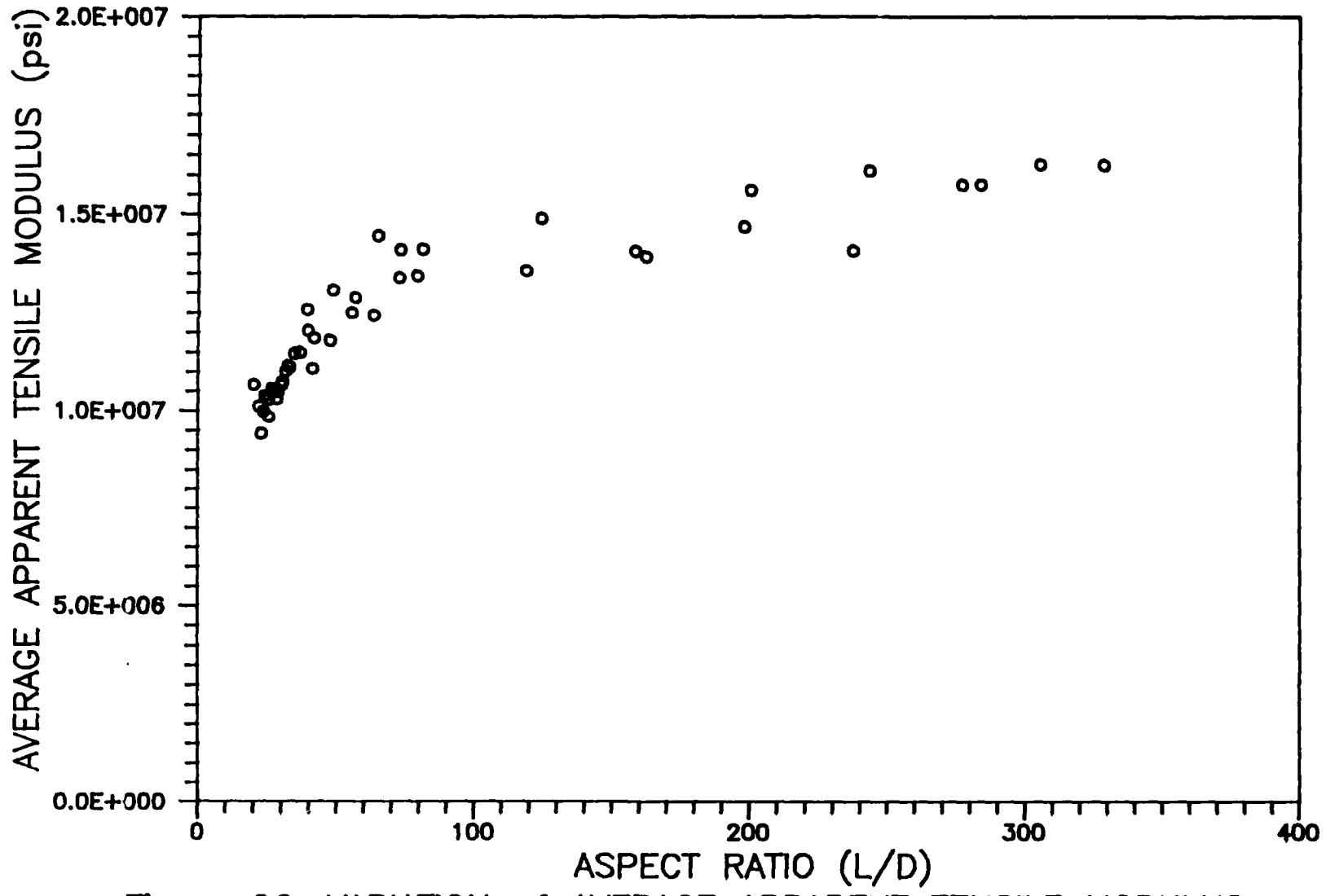

Figure 26. VARIATION of AVERAGE APPARENT TENSILE MODULUS with ASPECT RATIO for KEVLAR 49™

Table VIII Tensile Modulus Variation with Gage Length for Kevlar 49™

Fiber #	Diameter (μm)	Gage Length (mm)	Tensile Modulus (Mpsi)
61	12.0	0.25	7.07
62	12.0	0.2398	8.16
43	12.1	0.33	9.02
51	12.1	0.3125	9.09
37	12.625	0.29	9.41
49	12.1	0.31	9.85
36	12.625	0.3	9.96
38	12.625	0.28	10.11
35	12.625	0.32	10.27
33	12.625	0.36	10.29
14	12.375	0.30	10.37
48	12.1	0.33	10.48
47	12.1	0.35	10.48
34	12.625	0.34	10.56
32	12.625	0.38	10.66
15	12.375	0.25	10.66
42	12.1	0.37	10.74
31	12.625	0.4	11.0
39	12.1	0.5	11.07
46	12.1	0.4	11.1
13	12.375	0.4	11.13
30	12.625	0.42	11.16
29	12.625	0.44	11.45
28	12.625	0.465	11.48
26	12.625	0.6	11.79
45	12.1	0.505	11.85
27	12.625	0.5	12.04
24	12.625	0.8	12.42
25	12.625	0.7	12.48
10	12.375	0.7	12.87
11	12.375	0.6	13.07
23	12.625	0.9175	13.39
22	12.625	1.0	13.43
21	12.625	1.5	13.56
5	12.375	2.0	13.92
20	12.625	2.0	14.06
18	12.625	3.0	14.09
8	12.375	0.9	14.09
7	12.375	1.0	14.11
9	12.375	0.8	14.45
19	12.625	2.5	14.68
6	12.375	1.536	14.89
4	12.375	2.48	15.6
17	12.625	3.5	15.75
2	12.375	3.51	15.75
3	12.375	3.01	16.11
16	12.625	4.15	16.24

Just as in the previous two cases, the apparent tensile modulus did not depend on the fiber diameter which was determined by having no significant change between the plots of tensile modulus versus aspect ratio and tensile modulus versus gage length. The machine compliance curve is shown in Figure 27 and resulted in a corrected tensile modulus of 16.5Mpsi and machine compliance of 4.70×10^{-10}in'/lb. Again, the scatter of moduli at extremely short gage lengths could not be described by errors in misreading the gage length or glue slippage, but was attributed to increased sensitivity of the apparent moduli to the machine compliance and/or fiber misalignment. Using the tensile machine compliance and Eq (5), the corrected tensile modulus for the fibers in Figure 26 are shown in Figure 28 and had a mean of 16.5Mpsi with a standard deviation of 0.898Mpsi. The corrected moduli are in agreement with the asymptotic moduli from Figure 26 which indicated that the apparent moduli were accurately corrected for machine compliance.

The minimum gage length required to avoid a non-uniform stress distribution calculated using Eq (3) was 0.19mm. Using Eq (2), the maximum gage length allowed in order to prohibit Euler Buckling was 0.4mm.

The compression measurements for Kevlar 49™, listed in Table IX, exhibited some degree of scatter for extremely short gage lengths. The corrected compressive modulus was 15.3Mpsi with a machine compliance of 6.08×10^{-10}in'/lb as seen in Figure 29. Again, using the tensile machine compliance and Eq (5) the mean corrected compressive modulus was 16.9Mpsi.

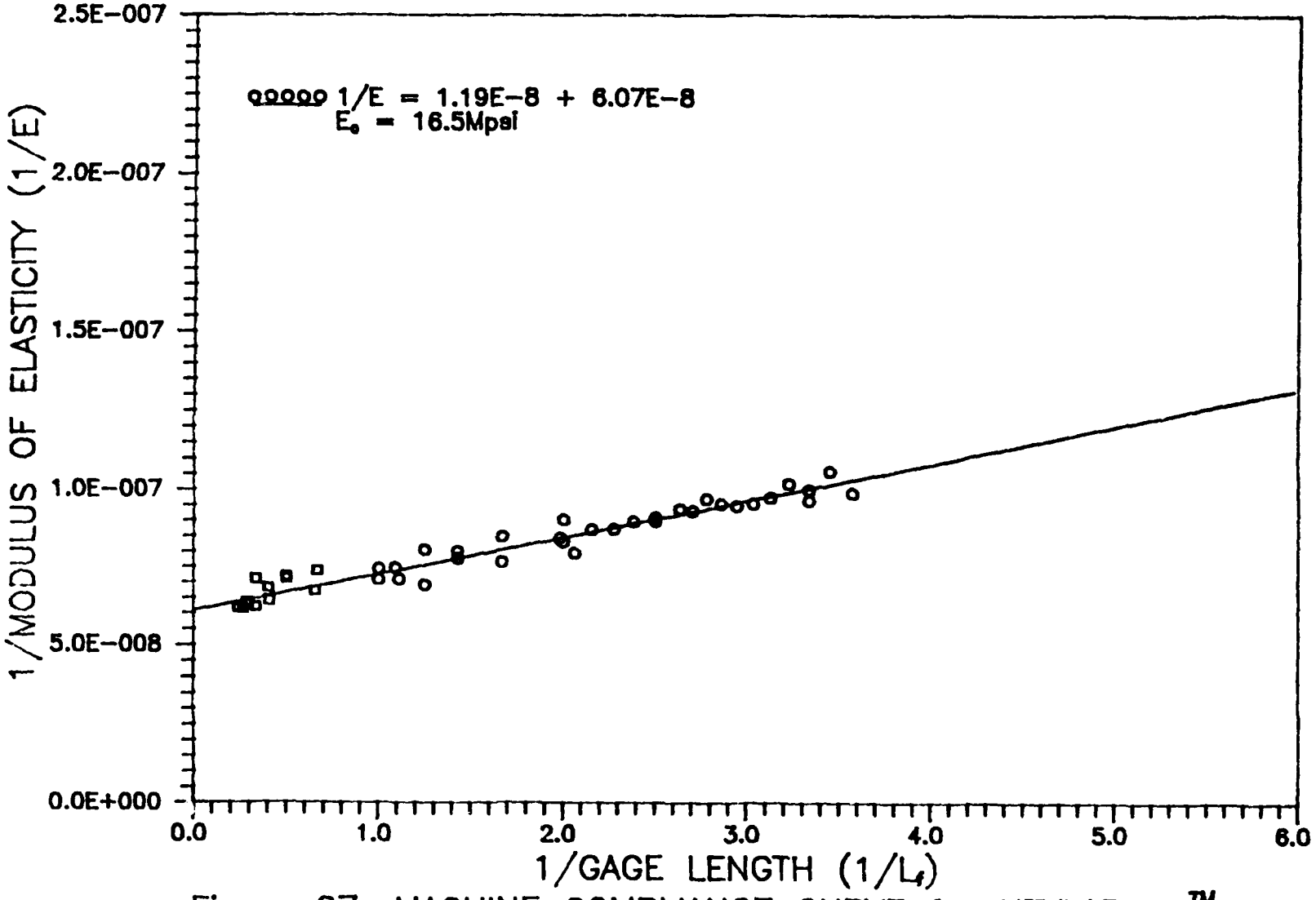

Figure 27. MACHINE COMPLIANCE CURVE for KEVLAR 49™ TENSION TESTS

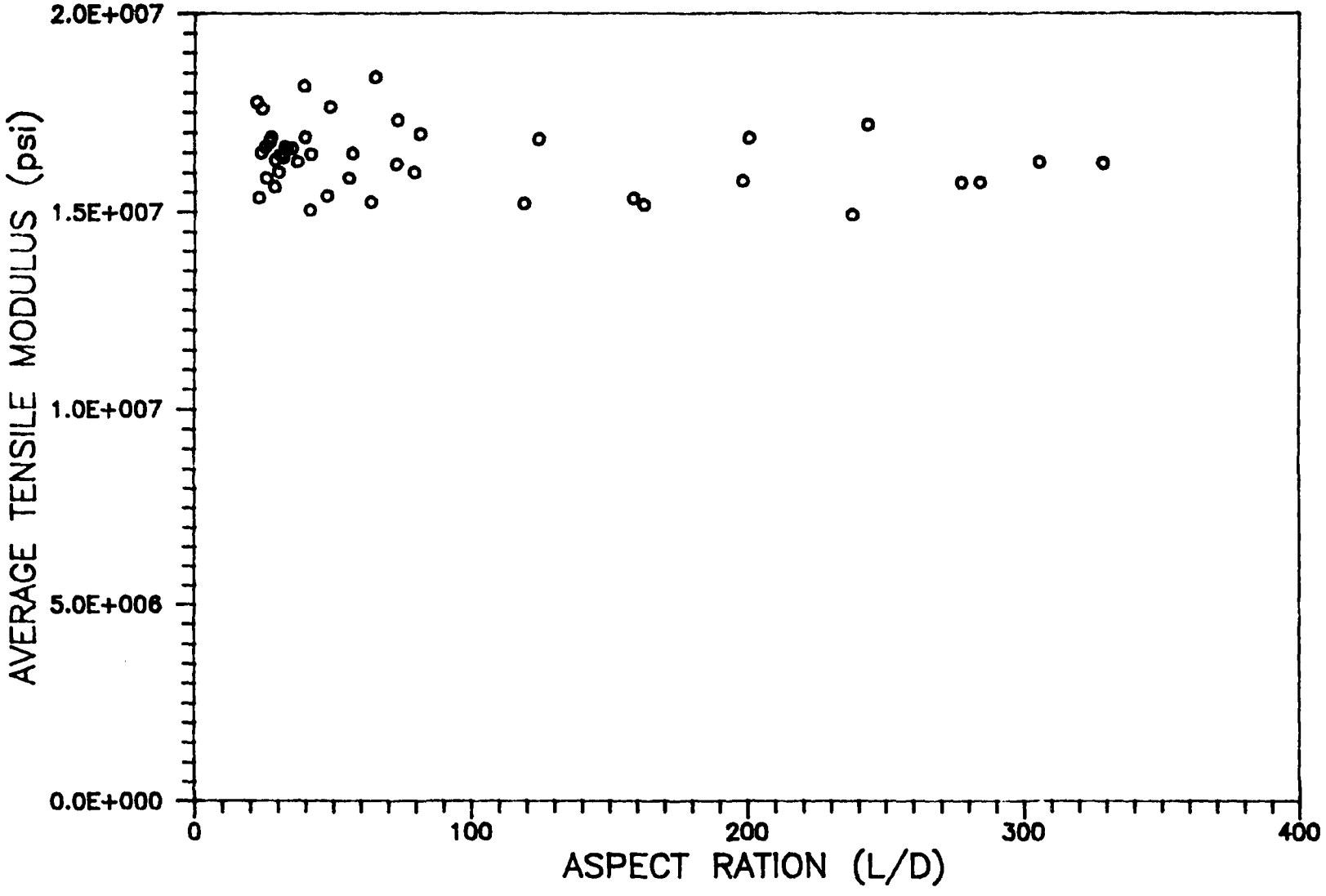

Figure 28. CORRECTED AVERAGE TENSILE MODULUS for KEVLAR 49™

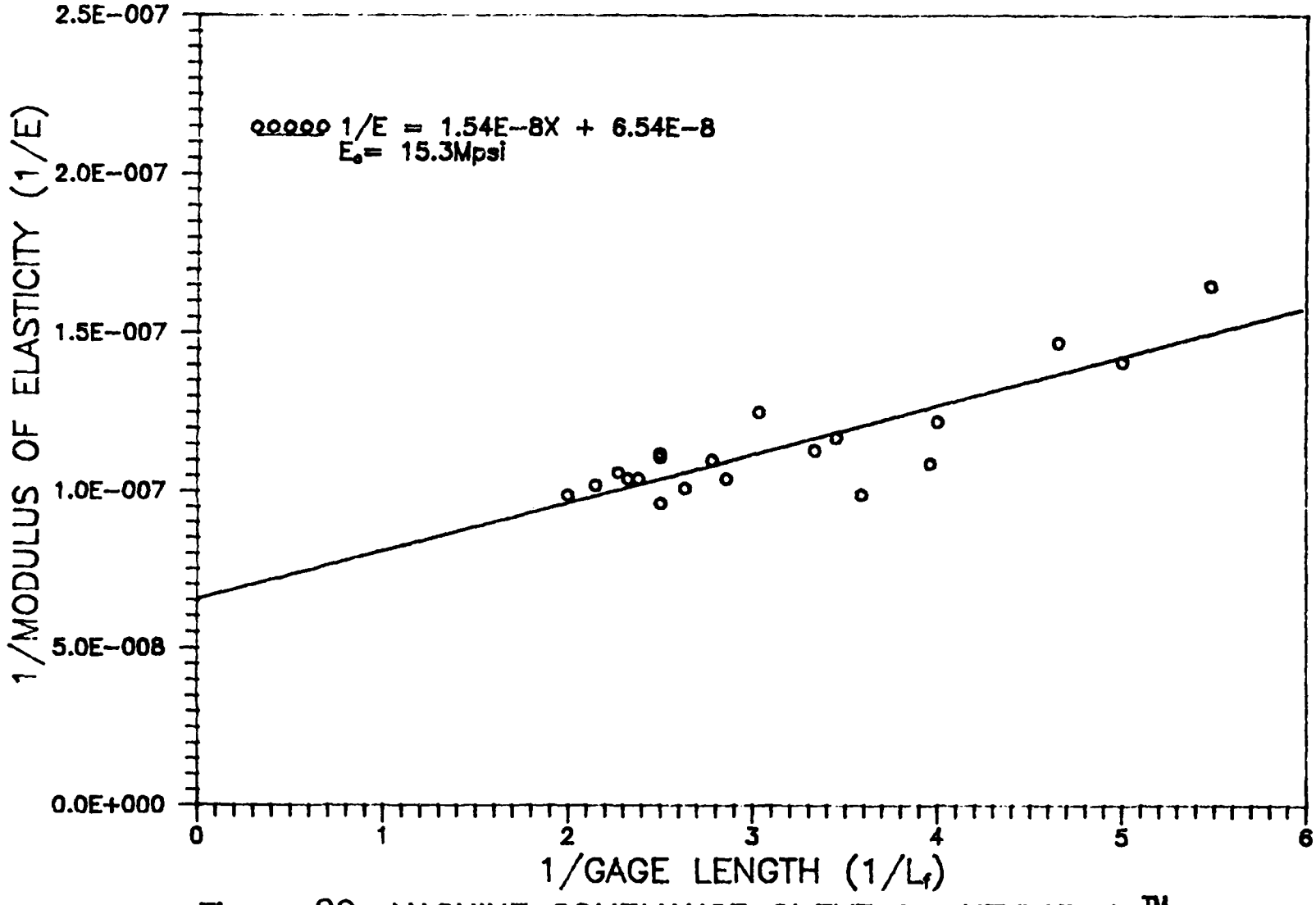

Figure 29. MACHINE COMPLIANCE CURVE for KEVLAR 49™ COMPRESSION TESTS

Table IX Variation of Compressive Modulus with Gage Length for Kevlar 49™

Fiber #	Diameter (μm)	Gage Length (mm)	Compressive Modulus (Mpsi)
30	12.625	0.42	4.51
28	12.625	0.465	4.77
40	12.625	0.43	5.33
29	12.625	0.44	5.79
47	12.1	0.35	6.11
33	12.625	0.36	6.34
38	12.625	0.28	6.39
50	12.1	0.2525	6.82
41	12.1	0.4	6.82
32	12.625	0.38	7.11
48	12.1	0.33	8.17
37	12.625	0.29	8.26
31	12.625	0.4	8.36
60	12.3	0.215	8.84
15	12.375	0.25	8.99
36	12.625	0.3	9.20

Carbon

To determine if direct compression testing was effected by the material characteristics of the fiber, an isotropic vapor grown carbon fiber, courtesy of Applied Sciences Federated, was tested. Since this was a carbon fiber, the stiffness was expected to be larger than the previous two fibers; therefore, the fiber would not be as susceptible to environmental or vibration induced disturbances. The carbon fiber was an experimental fiber with unknown material properties; this study was the first attempt at characterizing this fiber.

Representative tension tests are illustrated in Figure 30 and results listed in Table X, all carbon fibers tested had a diameter of 28.6μm. The slight differences in apparent moduli of those fibers illustrated in Figure 30 were well within an experimental error of 5%; therefore, the modulus did not depend on the gage length. As Figure 31 showed, the apparent modulus was very dependent on the gage length when the gage length was less than 1.0mm. As the gage length decreased, the apparent modulus did also. Since the gage length dependence was present in the carbon fiber, this phenomenon was not restricted to anisotropic, polymeric fibers as once thought. The linearity of the complete stress-strain curves shown in Figure 31 indicated equivalent moduli just as in the previously tested fibers. Due to the high stiffness of the carbon fiber, tensile and compressivestrengths could not be determined without reconfiguring the machine. During the compressive loading, no nonlinear behavior was present. The carbon fiber had the smallest offset from the origin upon unloading of all the fibers tested. The repeatability of cyclic loading was not in question since it was proven in the first three fibers tested. From Figure 32, the modulus lost dependence on the gage length at an aspect ratio of 100 which corresponded to a gage length of 2.86mm for a fiber diameter of 28.6μm. The asymptotic modulus from Figure 32 was approximately 37.0Mpsi.

The carbon fiber had what is called an onion skin structure. An onion is composed of many concentric layers of material with a finite gap between each layer; the carbon fiber was analogous, and as the diameter of the fiber increased so did the gaps between

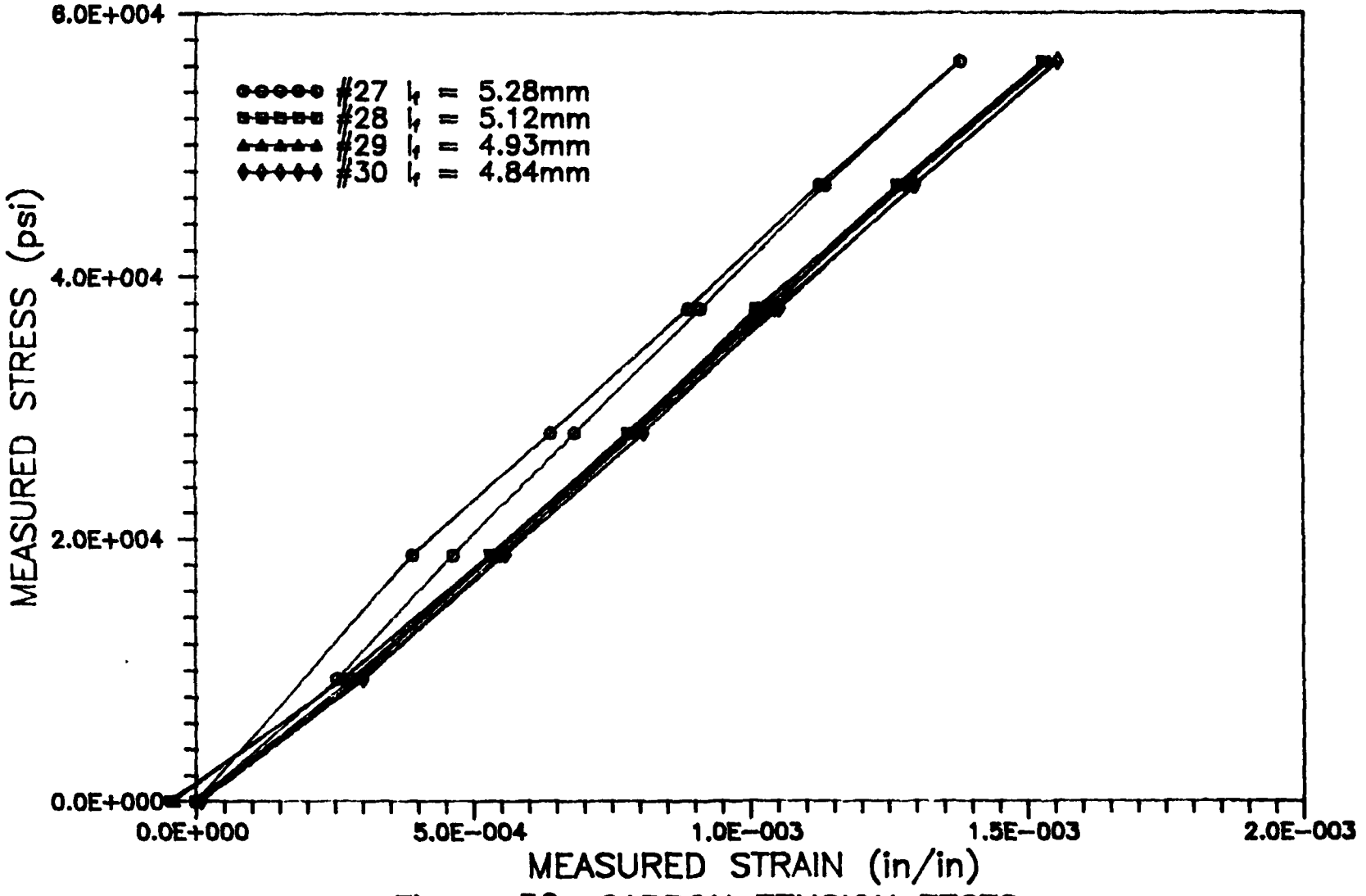

Figure 30. CARBON TENSION TESTS

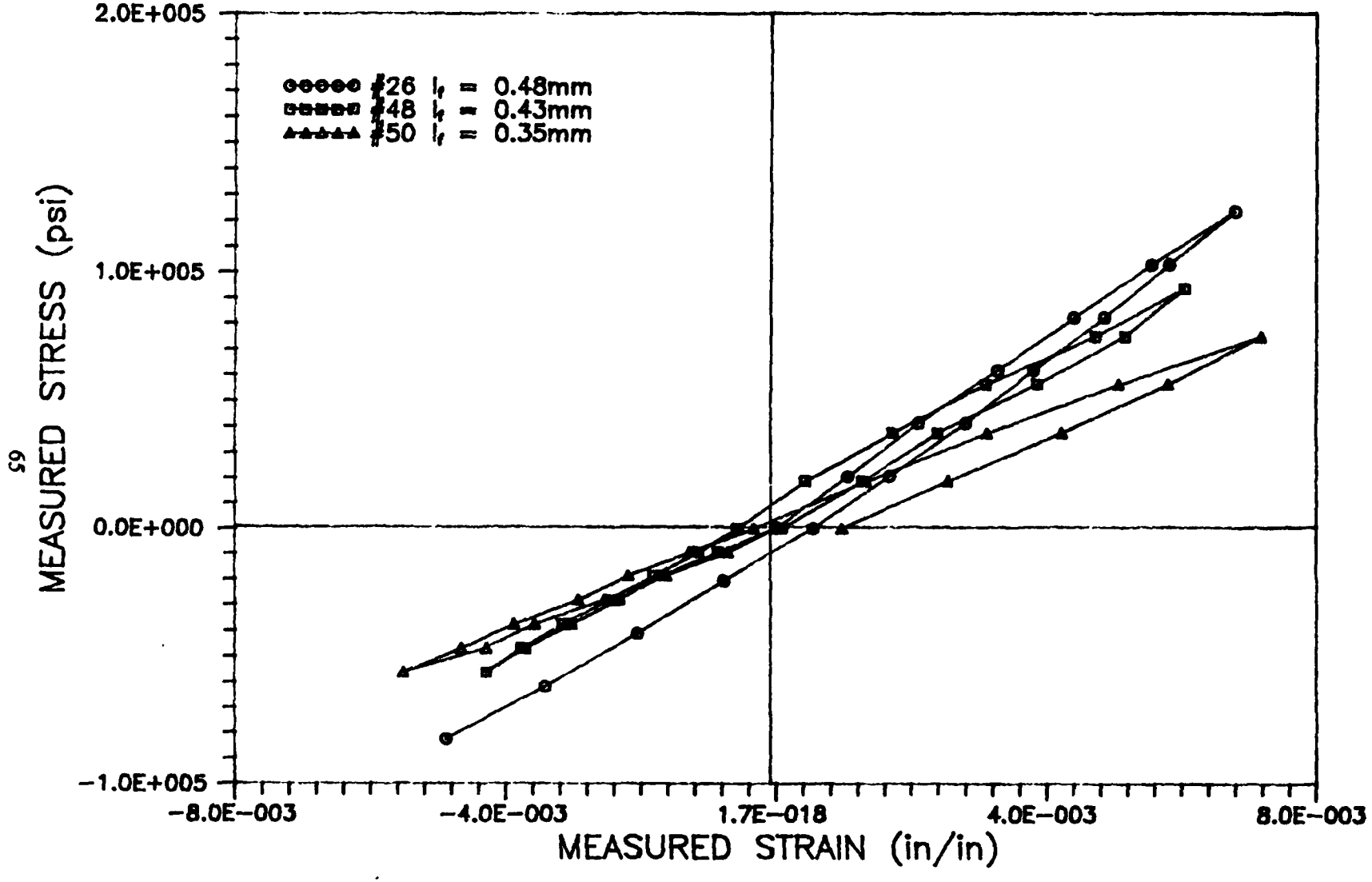

Figure 31. CARBON TENSION/COMPRESSION TESTS

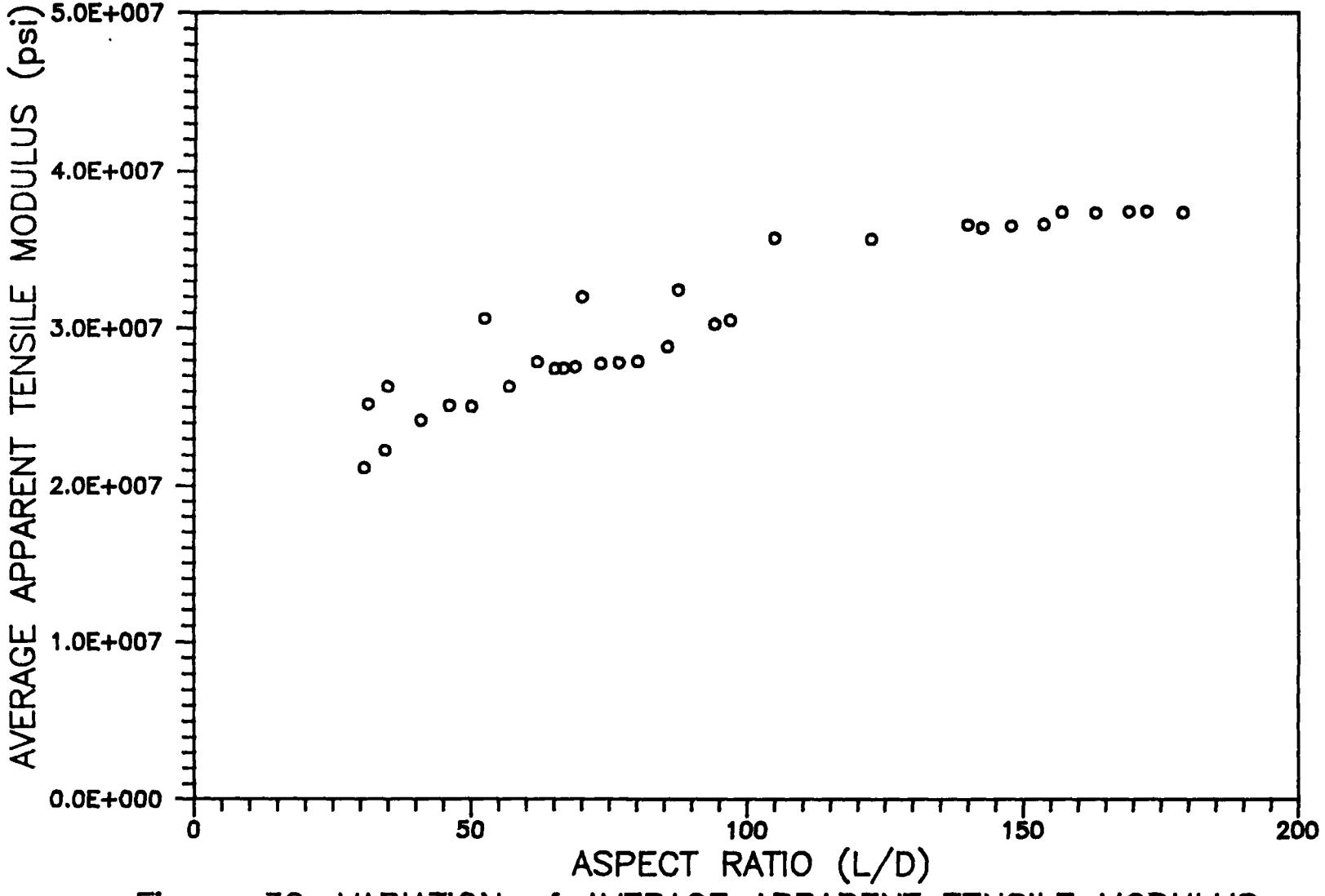

Figure 32. VARIATION of AVERAGE APPARENT TENSILE MODULUS with ASPECT RATIO for CARBON

Table X Tensile Modulus Variation with Gage Length for Carbon

Fiber #	Gage Length (mm)	Tensile Modulus (Mpsi)
51	0.26	6.63
4	0.20	7.44
52	0.255	7.53
50	0.345	10.02
2	0.355	10.66
47	0.42	12.41
9	0.72	13.17
48	0.43	13.19
8	0.75	13.53
7	1.055	15.82
46	0.5	16.46
26	0.4775	18.01
45	0.62	18.32
44	0.7125	19.81
1	0.525	20.42
25	0.5925	21.17
24	0.665	22.28
23	0.79	24.18
21	0.9675	25.04
22	0.89	25.12
43	0.9	25.21
20	1.095	26.31
42	1.0	26.31
18	1.255	27.44
17	1.285	27.48
16	1.325	27.57
15	1.42	27.76
14	1.479	27.83
19	1.195	27.88
13	1.545	27.89
12	1.65	28.81
11	1.815	30.24
10	1.87	30.48
41	1.5	30.61
40	2.0	31.98
39	2.5	32.44
37	3.5	35.69
38	3.0	35.72
35	4.075	36.41
34	4.225	36.53
36	4.0	36.61
33	4.395	36.62
31	4.665	37.36
28	5.12	37.37
32	4.49	37.4
30	4.84	37.43
29	4.932	37.47

layers (20). The gaps between layers don't support any load; therefore, the moduli would be lower for the fibers of larger diameter regardless of the gage length.

The machine compliance curve shown in Figure 33 yielded a corrected tensile modulus of 36.4Mpsi and a machine compliance of 4.48 x 10^{-10}in'/lb. The carbon fiber didn't vary from the linear relation as the gage lengths become significantly small; therefore, determining if any error due to misreading the gage length and/or glue slippage was present could not be determined. The square data points represent moduli which don't depend on the gage length; they aren't included in the linear curve. Using the tensile machine compliance and Eq (5), the apparent moduli of Figure 32 were corrected and are shown in Figure 34. The mean corrected tensile modulus was 36.4Mpsi with a standard deviation of 1.0Mpsi.

The carbon fiber was assumed isotropic since no evidence was available to contradict this assertion (20). By St. Venant's Principle, the minimum gage length required to avoid end effects was 0.286mm for a 28.6μm diameter fiber. From the Euler Buckling analysis using Eq (2), the maximum gage length allowable to preclude buckling was 0.97mm.

The machine compliance from the compression tests, data listed in Table XI, is illustrated in Figure 35 and yielded a corrected compressive modulus of 35.0Mpsi and a machine compliance of 6.10 x 10^{-10}in'/lb. The scatter in moduli was much smaller for the carbon fiber than the other three fibers which might be due to the larger diameter and greater stiffness or less sensitivity to machine compliance and/or fiber misalignment. Finally, using the tensile machine compliance and Eq (5), the mean corrected moduli was 28.5Mpsi. Since this fiber had not been previously characterized, the difference between the corrected tensile and compressive moduli might be real. However, the gage lengths for the compression test were in some cases twice as large as the those used for the preceding fibers; therefore, the carbon fibers tested in compression might have bowed due to eccentric loading or fiber misalignment.

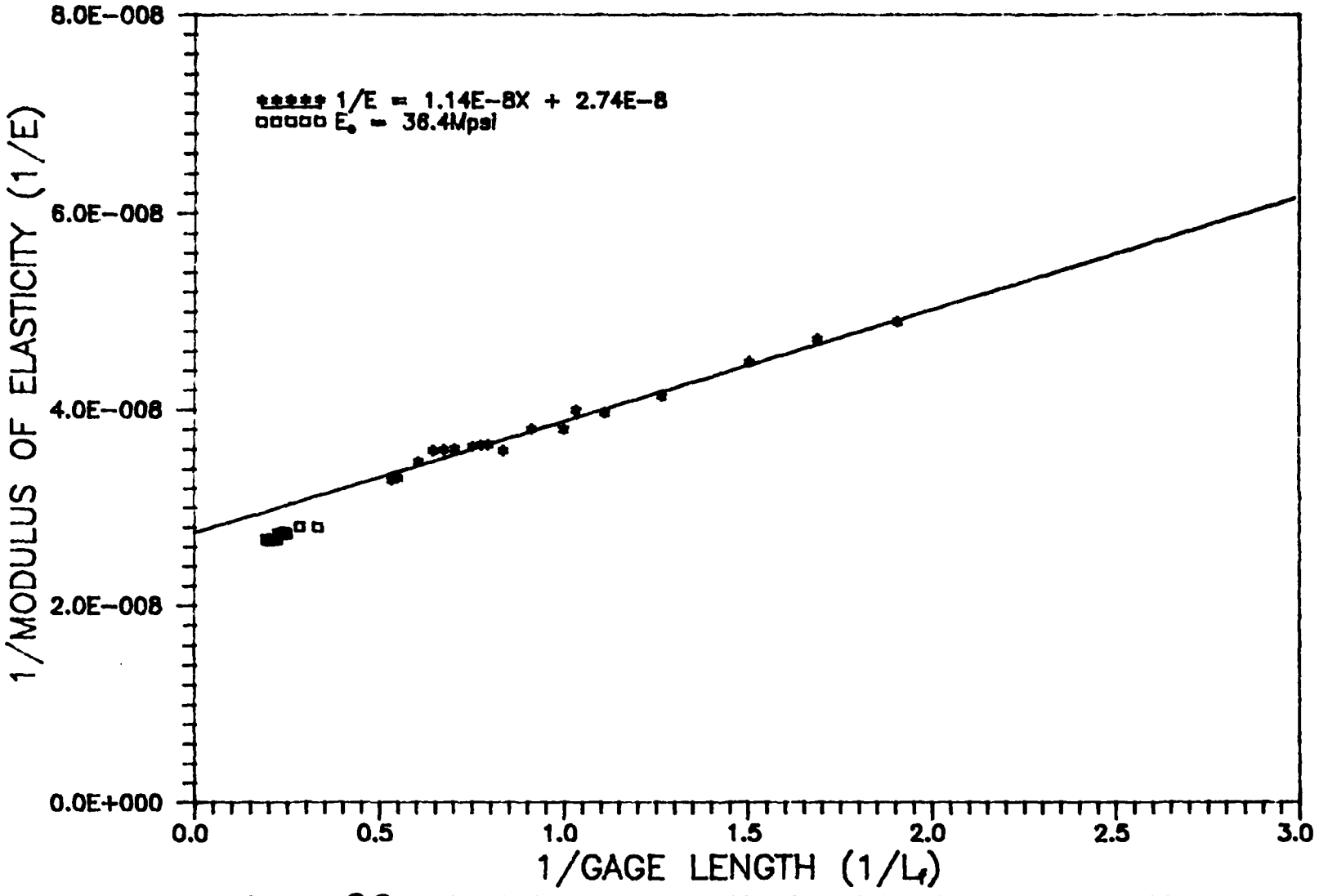

Figure 33. MACHINE COMPLIANCE CURVE for CARBON TENSION TESTS

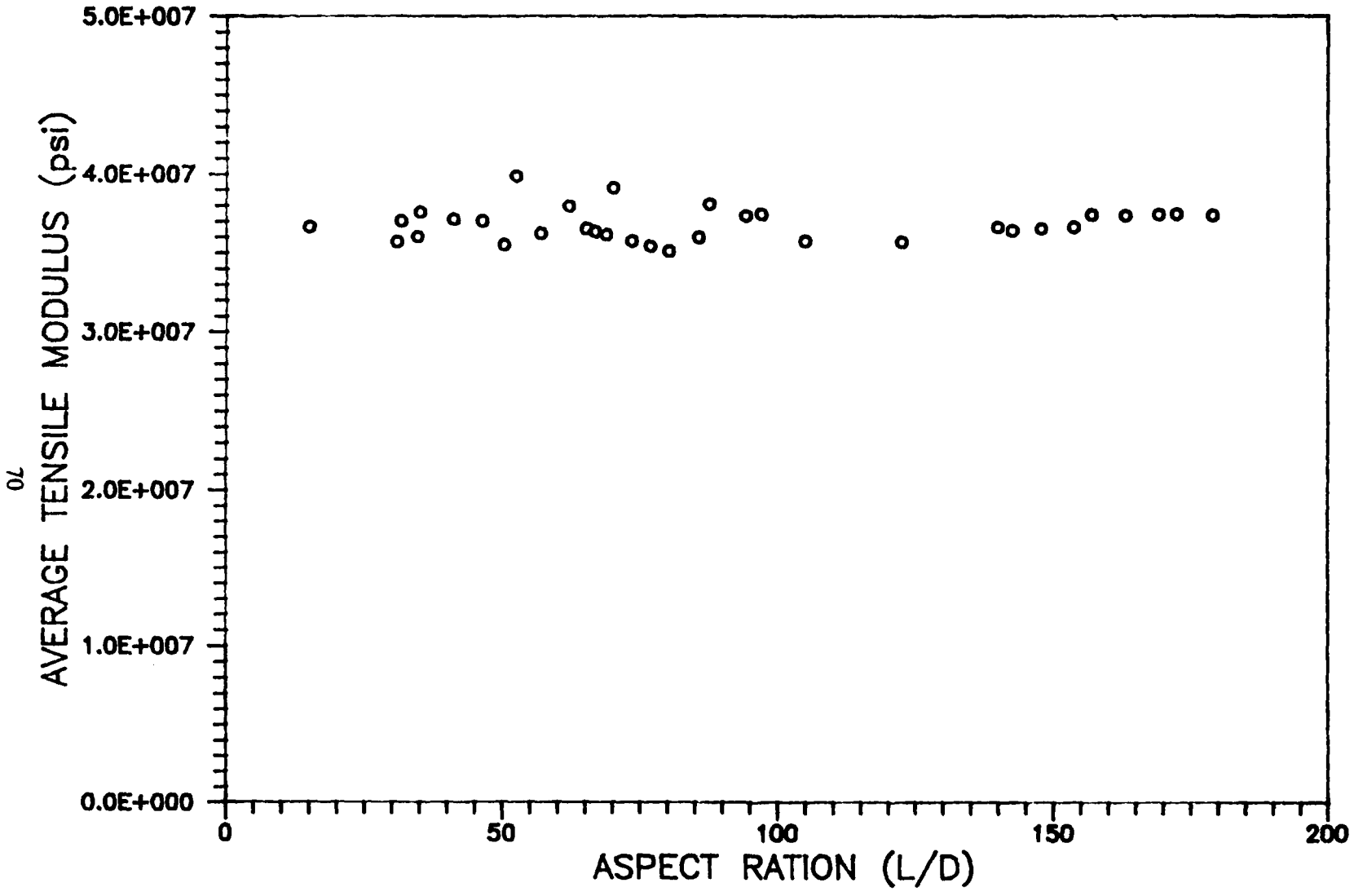

Figure 34. CORRECTED AVERAGE TENSILE MODULUS for CARBON

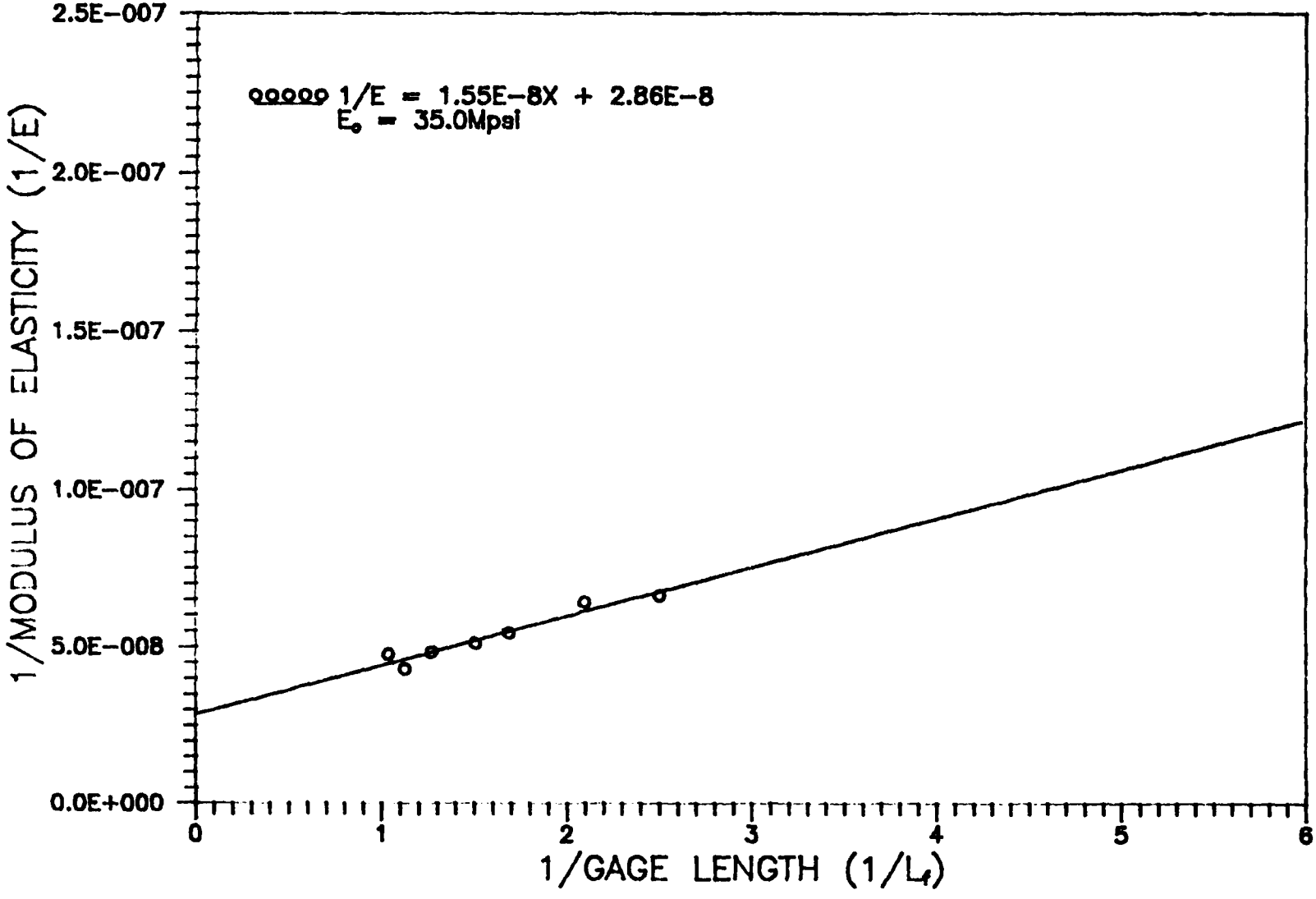

Figure 35. MACHINE COMPLIANCE CURVE for CARBON COMPRESSION TESTS

Table XI Variation of Compressive Modulus with Gage Length for Carbon

Fiber #	Diameter (μm)	Gage Length (mm)	Compressive Modulus (Mpsi)
49	28.6	0.4	15.12
26	28.6	0.4785	15.61
25	28.6	0.6	18.37
24	28.6	0.667	19.58
23	28.6	0.7875	20.67
21	28.6	0.97	21.0
22	28.6	0.893	23.28

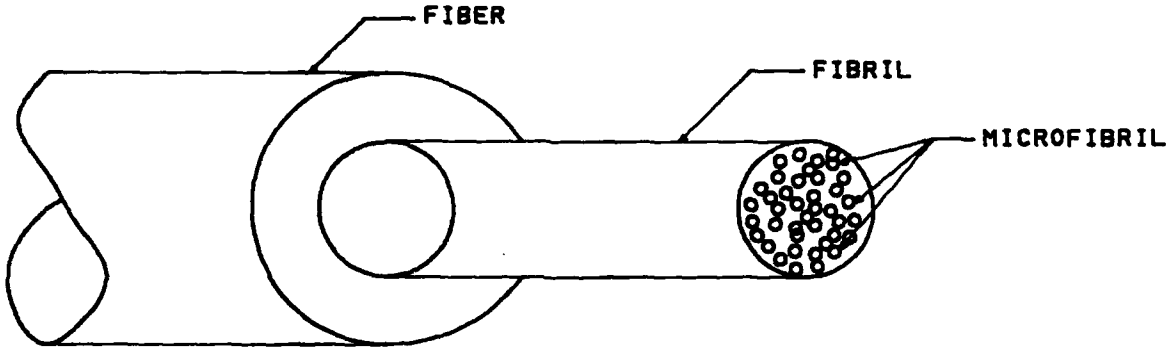

Figure 36. FIBER MICROSTRUCTURE

DISCUSSION

The PBO 8A, Kevlar 29™, Kevlar 49™, and Carbon fibers all qualitatively behaved similarly through the various tests. The three polymeric fibers were expected to perform similarly since they all were anisotropic; however, the isotropic carbon fiber acted just as the polymer fibers with respect to the moduli depending on the gage length and being effected possible glue deformation. The latter of the two phenomena was evident by the strain offset at zero load. The anisotropy of the polymer fibers did not seem to play a significant role in any of the tests.

The compliance curves for each fiber in tension and compression did result in slightly varying value for the machine compliance. In tension, the mean machine compliance was 4.74×10^{-10}in'/lb with a standard deviation of 2.50×10^{-11}in'/lb; but in compression, they were 5.69×10^{-10}in'/lb and 4.60×10^{-10}in'/lb, respectively. The true machine compliance should be constant but the overall "machine compliance" did vary in magnitude in tension and compression possibly due to glue deformation.

In trying to account for the variation of modula for the polymeric fibers of extremely small gage lengths, misreading the gage length and fiber slippage have been examined. From the earlier discussion each would only decrease, with no evidence to expect an increase, the measured moduli. Recall the data points below the linear curve in each of the polymeric fibers' compliance curves. As a result, the increase in moduli at shorter gage lengths for the polymeric fibers was inexplicable by these two theories. Error in modulus due to misreading the gage length and/or fiber slippage wasn't determined since none of the fibers definitively behaved in a manner which was predicted by either theory.

As discussed earlier, the fiber is composed of fibril, and the fibril is composed of microfibril as shown in Figure 36. The inter-element composition is inherent to polymeric fibers. Due to the orientation of the fibril and microfibril in the fiber, the fiber may experience micro-buckling of the microfibril followed by the fibril when compressively

loaded (13:34). The micro-buckling is caused by instability of the microfibril. The three dimensionality of the fiber on the microscopic level is evident and could be the cause ofthe extraordinarily low compressive strength. From a continuum mechanics approach, if the fiber could be drawn with the fibril and microfibril aligned longitudinally, the compressive strength might increase due to a more one dimensional problem with the load axes in line with the fiber axes. In addition, the secondary forces bonding the fibril and microfibril to one another may allow an even more complex stress field to exist. However, on a micro-mechanics level, work has been done to disrupt the longitudinal alignment in order to increase compressive properties (10; 12; 21:2).

A wide range of failure between the microfibril and/or fibril may occur depending on the type of loading present (5:1). The load may be transferred to the intersecting components which can either promote or hinder the load carrying capability of the fiber. If the (micro)fibril was near its critical buckling load and additional load was transferred from an adjoining (micro)fibril, the former could fail prematurely. If this was an isolated incident, the entire fiber may(not) fail; but if it initiated a gross instability, catastrophic failure might occur rapidly. Similarly, if the (micro)fibril was near its critical buckling load and could transfer the load to a neighboring sub-critical (micro)fibril, the ensuing catastrophic failure might be precluded. As mentioned earlier, buckling could be avoided if an aspect ratio of 10 was maintained; however, this was not possible with the specimens tested. The smallest gage length used could not be less than 0.18mm due to capillary action of the glue on the fiber resulting in a glue coated fiber. If the glue coated fiber was used the material properties measured would be a combination of the glue and fiber. The only way to insure buckling did not occur was to examine the fiber after each load increment through the traveling microscope. This technique may seem crude, but proved to work. If misalignment of the fiber was present, it might not have been evident until the fiber was loaded.

The reduced compressive strength in highly ordered polymeric fibers is due to great anisotropy and inhomogeneity. Morphology of these fibers isn't analogous to any metal systems, therefore, determination of the failure mechanisms is of interest. For a more in depth discussion of the morphology of the PBO fibers see Appendix B.

The nonuniform stress distribution, if present, resulted from the anisotropy of the fiber and fiber misalignment causing a three dimensional problem which was difficult to avoid due to the imprecision of the machine. However, the magnitude of the effect of the nonuniform stress distribution on the compressive properties of polymeric fibers has yet to be determined. During the application of the load, the right anvil moved toward the left via a system of levers and torque arms. This system was not ideal, therefore the right anvil had been noticed to move vertically and laterally during load application. The unwanted movement of the right anvil was seldom and occurred arbitrarily. No quantitative results were obtained which determined the effects of fiber or anvil misalignment; however, the existence of either was manifested by a nonlinear stress-strain curve. The effects of the anisotropy of the fiber were evident in the average tensile modulus versus aspect ratio curves where decreasing gage length resulted in decreasing modulus due to the end effects becoming more prevalent. The empirical data dictated a larger minimum gage length for all of the fibers tested, for this reason the applicability of Eq (3) as derived by Horgan for anisotropic fibers, is questioned. The empirical data followed the same trends as those reported by Arridge and Folkes for ultra high modulus polyethylene fibers; however, Eq (3) underestimated the minimum gage length for every fiber tested. (4:497;13:500) The most reliable method of determining the minimum gage length required was to increase the aspect ratio until consistent tensile moduli were obtained. By setting the gage length by the empirical data, compressive testing could not be accomplished due to Euler Buckling with the relatively large gage length.

A possible explanation for variation of modulus at small gage length was misalignment of the fiber in the sample holders resulting in combined loading and a three

dimensional stress field. The combined loading would also effect the stress distribution across the fiber cross-section resulting in lower moduli. The anisotropic, polymeric fibers would have a more pronounced response to combined loading since the transverse stiffnesses are many orders of magnitude less than the longitudinal stiffnesses. Misalignment can only be avoided by perfecting the testing technique.

Table XII shows a comparison of the compressive properties obtained using the MTM-8 versus those obtained using the elastica loop, bending beam, recoil, and composite tests. As stated earlier the Elastica Loop, Bending Beam, and Recoil tests all overestimate the compressive strength, thus it was not surprising that the direct compression technique yielded a lower compressive strength. However, for PBO the recoil test data of 30ksi was lower than the 43.1 obtained in this study. The failure strain of 0.38% was higher than the 2% obtained by the bending beam test, but failure in the bending beam test is subjectively determined and is not characterized as the inability to support the load as it is in the direct compression technique.

The composite data for Kevlar 29™ and 49™ indicated that the compressive strength was not dependent on the compressive modulus since both yielded the same compressive strength of 58ksi when they had varying moduli. However, the compressive strengths of 30.0 and 42.1ksi for Kevlar 29™ and 49™; respectively, obtained from this study did depend on the modulus.

Table XII. Comparison of Compressive Properties from Various Tests

Fiber	Loop	Bending Beam	Recoil	Composite	MTM-8
PBO 8A					
σ_{cr}	98.6(16)	60.0(16)	30.0(3)	50.0(8)	43.1 ±5.0
%ε	-	0.2(14)	-	-	0.38 ±0.12
E_c	-	-	-	-	35.0
Kevlar 29™					
σ_{cr}	-	-	50.7(3)	58.0(3)	30.0
%ε	-	-	-	-	0.40
E_c	-	-	-	12.0(8)	12.2
Kevlar 49™					
σ_{cr}	107.0(3)	108.0(16)	53.0(3)	58.0(3)	42.1 ±5.2
%ε	-	0.57(14)	-	-	0.57 ±0.28
E_c	-	-	-	18.0(8)	16.9
Carbon					
σ_{cr}	-	-	-	-	-
%ε	-	-	-	-	-
E_c	-	-	-	-	28.5

CONCLUSION

The ability of the MTM-8 to determine the compressive properties of high performance composite fibers was explored. The full stress-strain curves exhibited linear behavior when crossing the origin indicating equivalent tensile and compressive moduli. To account for the machine compliance, fibers of varying gage length were tested in both tension then compression to obtain tensile and compressive moduli. By plotting the inverse of the modulus versus inverse of the gage length the machine compliance and corrected modulus were obtained. The mean machine compliance was 4.74 x 10^{-10}in'/lb with a standard deviation of 2.50 x 10^{-11}in'/lb in tension and 5.69 x 10^{-10}in'/lb and 4.60 x 10^{-11}in'/lb in compression; respectively. The corrected moduli for PBO, Kevlar 29™, Kevlar 29™, and were 35.0, 12.2, 16.9, and 28.5Mpsi; respectively. Due to the consistency and reliability of the tension test data, the corrected compressive moduli were calculated using the tensile machine compliance. The compressive strengths, following the same order, were 43.1, 30.0, 42.1ksi; the compressive strength for carbon was not determined. The possible errors investigated were misreading the gage length, fiber slippage, glue deformation, non-uniform stress distribution, and fiber misalignment. A quantitative determination of misreading the gage length and fiber slippage was inconclusive. The glue deformation and nonuniform stress distribution, the existence of one or both was supported by the varying machine compliance during the tension and compression testing, could not be separated from the machine compliance. Analytically quantifying the minimum gage length required to avoid end effects consistently underestimated the length needed. Empirical quantification was obtained by plotting the average tensile moduli versus the aspect ratio, from this curve a minimum gage length, determined when the variation of moduli was marginal, was determined. The minimum gage length needed to avoid end effects was large enough to allow Euler Buckling if the fiber had been tested in compression at this long gage length. Fiber misalignment was the largest error factor. Misaligning the fiber in the sample holders

would cause a three dimensional stress field which not only increased the complexity of the analysis, but also reduced the tensile and compressive properties. Misalignment of the fibers in tension testing did not have as large an effect as in compression. At the smaller gage lengths, variation of both the tensile and compressive moduli was present in the compliance curves even for fibers that were believed to be aligned properly. The variation might still be due to misalignment because the misalignment might not be visible with the 100x travelling microscope. If the fiber was misaligned by less than 2.5μm, the misalignment would go undetected. The fiber diameters ranged from 12.2 - 35.3μm, therefore the eccentricity of the load caused by the misalignment would have had a substantial effect on the stress field given the small dimension of the fiber. The effects of error caused by misalignment could be lessened by increasing the number of tests for a given fiber until consistent results are obtained. The larger the test sample, the less likely small degrees of misalignment would effect the extrapolated values of moduli and the statistical mean of the compressive strength.

The MTM-8 is very labor intensive. To obtain consistent and reliable moduli from the compliance curves and compressive strength from the compression tests, one hundred or more fibers needed to be tested. Towards the latter stages of testing when efficiency of the technique was highest, each test took approximately twenty minutes. Thus, for each fiber, thirty-three hours or more would be needed to obtain reliable and consistent results. The MTM-8 would be more appropriately used to first determine if the fiber behaves linearly when transitioning from tensile to compressive loading. If the linear relation exists, the compressive modulus is equal to the tensile and a less time consuming and reliable techniques are available to determine the tensile modulus. Determining the compressive strength would involve testing enough fibers to obtain consistent results within a defined tolerance. When the fibers were mounted in the sample holders without misalignment, the values of compressive strength are very consistent yielding errors of less than 5% with respect to one another.

The MTM-8 adequately characterizes fiber compressive behavior more so than the elastica loop, bending beam, and recoil tests. The possibilities of error are user controlled in the former but not so in the latter three tests. Given adequate time to become proficient in the testing technique, the accuracy of the results using the MTM-8 are incontestable.

FUTURE WORK

The reliability of direct compression testing of high performance composite fibers could be greatly increased if fiber alignment in the sample holders could be guaranteed. In addition, the nonuniform stress distribution and/or glue deformation in fibers with extremely short gage length needed accurately defined. Euler Buckling could be avoided if aspect ratios less than 10 were used when possible.

To further explore the use of the Tecam Micro-Tensile Testing machine for direct compression testing of composite fibers, the following modifications should be considered. The single most needed improvement to the MTM-8 is to increase the magnification power of the travelling microscope. If the power could be increased to say 200x, the possibility of misaligning the fiber is greatly reduced; therefore, decreasing the number of tests needed to obtain reliable results. In addition, if a video camera to the travelling microscope would allow constant monitoring of the fiber while under load, thus kinkband formation and propagation would be visible. This capability would allow compressive failure mechanisms to be studied, thereby gaining a better understanding of compressive failure behavior. With knowledge of kinkband formation, non-linearities in the stress-strain curve could be sighted, thus giving a more accurate characterization; and ultimately leading toward the improvement of polymer fiber compressive strength.

REFERENCES

1. Adams, W.W., T. Grieshop, T. Helminiak, M. Hunsaker, J.F. O'Brien, M. Altieri, S.J. Bai, M. Brandt, A.V. Fratini, W-F. Hwang, T. Haddock, S.J. Krause, and P.G. Lenhert, "Processing, Properties, Structure, and Morphology of PBO and ABPBO Polymer Fibers", AFWAL-TR-86-4011, 1986.

2. Allen, Steven R., "Mechanical and Morphological Correlations in Poly(p-phenylenebenzobisthiazole) Fibers", AFWAL-TR-83-4045, July 1983.

3. Allen, Steven R., "Tensile Recoil Measurement of Compressive Strength for Polymeric High Performance Fibers", Journal of Materials Science 22(1987) 853-859.

4. Arridge, R.G.C., and M. J. Folkes, "Effect of Sample Geometry on the Measurement of Mechanical Properties of Anisotropic Materials", Polymer, Vol 17 June, (1976).

5. Askeland, Donald, R. The Science and Engineering of Materials. PWS Engineering, Boston, MA 1984.

6. Brush, D. O. and Bo O. Almroth. Buckling of Bars, Plates, and Shells. McGraw-Hill Book Company; New York, NY 1975.

7. Chai, Herzl, "Postbuckling Analysis of Laminated Media", Visiting Scientist, AFWAL/MLBP, 1988.

8. Chauh, C. C. and J. Im. Personal Interview. Dow Chemical Company, 1 Nov 1988.

9. Chen, K. J., and R. J. Diefendorf, "Residual Stress in High Modulus Carbon Fibers", Progress in Science and Engineering of Composites; T. Hayashi, K. Kawata, and S. Umekawa, Ed., ICCM-IV, Tokyo, 1982.

10. Chuah, H. H., T. T. Tsai, K. H. Wei, C. S. Wang, and F. E. Arnold, "Crosslinked Benzobisthiazole Rigid-Rod Copolymers Via Labile Methyl Groups", American Chemical Society Meeting, 9 - 14 April, 1989.

11. Cohen, Yachin, "Structure Formation in Solution of Rigid Polymers Undergoing a Phase Transition", AFWAL-TR-87-4030, 1987.

12. Dang, T. D., L. S. Tan, K. H. Wei, H. H. Chuah and F. E. Arnold, "Pseudo-Ladder Structures Via Dihydroxy Pendant Benzobisthiazole Rigid-Rod Polymers", American Chemical Society Meeting, 9 - 14 April, 1989.

13. DeTeresa, S.J., "The Axial Compressive Strength of High Performance Polymer Fibers", AFWAL-TR-85-4013, 1985

14. Horgan, C. O., Journal of Elasticity 1972,2,169,335: International Journal of Solids Structures 1974,10,837.

15. Keller, Capt Russel L. Examination of High Performance Polymer Fibers Under Compressive Deformation. MS Thesis, AFIT/GAE/AA/86D-5. School of Engineering, Air Force Institute of Technology (AU), Wright-Patterson AFB OH, December 1986.

16. Kumar, Satish. Structure and Properties of High Performance Polymeric and Carbon Fibers - An Overview. University of Dayton Research Institute, AFWAL Materials Laboratory, Polymer Branch, Wright-Patterson AFB OH, 1988

17. Lenhert, Galen, Visiting Scientist. Personal Interview. AFWAL/Materials Laboratory, Wright-Patterson AFB OH, 5 OCT 1988.

18. Lindsey, Kenneth, Personal Interview. AFWAL Materials Laboratory/Mechanics Branch, Wright-Patterson AFB OH, 1 APR through 1 OCT 1988.

19. Techne (Princeton) Limited. Micro-Tensile Testing Machine. Instruction Book. 1963.

20. Wang, C-S., Research Chemist, University of Dayton Research Institute. Personal Interview. AFWAL Materials Laboratory/Polymer Branch, Wright-Patterson AFB OH, 1 Mar through 28 Nov 1988.

21. Wang, C. S., J. Burkett, S. Bhattacharya, H. H. Chuah, and F. E. Arnold, "Disruptive Packing Order Via Bulky Benzobisthiazole Rigid-Rod Polymers", American Chemical Society Meeting, 9 - 14 April, 1989.

APPENDIX A: TEST PROCEDURES

All of the testing undertaken in this effort was completed using the Tecam MTM-8 Micro-Tensile Machine. The MTM-8, pictured in Figure 37, is the only machine available today capable of direct compression testing of composite fibers.

Due to the limited use of the MTM-8 no standard testing procedure has been developed, thus the testing procedure used became very dynamic as the technique was optimized. All of the fibers were viewed with an optical microscope at 200x prior to testing in order to determine the average diameter, and to examine the fiber for existing kinkbands or gross defects. Damaging the fiber prior to mounting was quite possible due to the frailty of the fibers and having to move the fiber from spool, to microscope, to MTM-8. In addition, the fibers were placed in a glass petri dish to prevent wind currents from bending the fiber and causing kinkbands.

The displacements are recorded from a micrometer which employs two mirrors and a light source for a null balance.

The fiber mounting procedure is quite involved and takes many hours to perfect. During the initial stages of testing only one fiber could be successfully mounted in approximately 1 hours, and the reliability of this mount was questionable. As experience was gained, the mounting time was reduced to fifteen minutes with a high degree of reliability. The fibers were mounted on the quartz anvils as shown in Figures 16 and 38. The first method used was to hold the fiber by attaching a piece of tape to the fiber then picking up the fiber by the taped portion with tweezers. The fiber was then mounted on the left anvil, since it is much less sensitive to jarring than the right, by holding the micro-soldering iron under the anvil to melt the glue while holding the fiber on the anvil. This method was very inadequate since a very steady hand was needed to hold the fiber and soldering iron at the same time without out putting any undo strain on the fiber. Once the left side was mounted the fiber was separated from the tape by a scissors which usually damaged the fiber

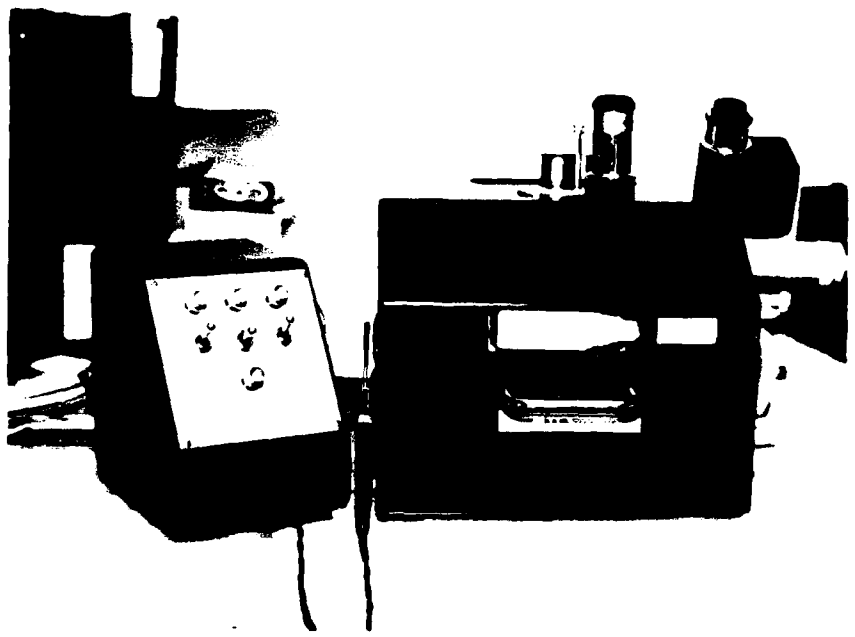

Figure 37. Picture of Tecam Micro-Tensile Testing Machine

Figure 38. PICTURE of FIBER ANIVLS

considerably since the fiber was bent as it was sheared between the two blades. Again resulting in very questionable results.

A new technique was developed to hold the fiber while mounting which limited the chances of damaging the fiber. The fiber was balanced atop the tweezers then laid on the two anvils simultaneously followed by melting the glue. Confidence in testing an undamaged fiber was high, however since the fiber was not firmly held while transferring from the petri dish to the anvils; the fiber had a tendency to blow away or be thrown of the tweezers by static electricity. To limit the air currents around the machine, the machine was partially enclosed by a plexiglass hood, moved into an isolated room where the air circulation was minimal, and a dust mask was worn by the operator to limit exhaling on the fiber. The static electricity problem was overcome by using a anti-static gun.

Having the fiber securely glued to the anvils, the one dimensionality of the fiber must be ensured. The traveling microscope had cross hairs on the lens; therefore, the cross hairs were positioned on one end of the fiber then traversed the length of the fiber. Any deviation from the cross hair horizontal line was corrected. The cross hairs were stencilled on the objective lens and this lens could be rotated for focussing; therefore, the cross hairs could also rotate. Transverse translation of the cross hairs had to be checked before each test. Furthermore, the vertical direction was also aligned by using the travelling microscope. If one anvil was out of focus with respect to the other then a correction was needed. In addition, a hand held jeweler's magnifying glass of 10x was used to determine vertical alignment. The correction process was indeed difficult. The left anvil can move both horizontally and vertically. Making corrections in both directions was done using the movement controls on the left anvil. Depending on which anvil was out of alignment, the glue was remelted, and the left anvil was moved until alignment was achieved or the glue solidified. If the glue solidified before the repositioning was complete, the process become iterative. The process was the same for both the horizontal and vertical corrections.

The realignment process was very difficult to accomplish without damaging the fiber. In order to reduce the number of repositioning iterations, grooves were cut in the quartz anvils so the fiber could simply be dropped into the grooves and glued. The alignment was not always perfect, but the repositioning task was much easier, and the mounting time was decreased from approximately ninety minutes to fifteen. Fiber damage during mounting would go undetected until the test was completed and raw data reduction was accomplished; therefore, a significant amount of time would be wasted. If the fiber needed to be repositioned more than ten times then the fiber was usually damaged, and the time used to mount a new fiber was far less than the time spent to do the test, reduce the data, and find out the results are erroneous.

To remove the fiber from the anvils after a test was completed, the glue was remelted, by holding a micro-soldering iron just below the anvil, on the right anvil then the left anvil was moved away from the right with the large strain micrometer. This procedure reduced the chance of sharp movements of the right anvil. The right anvil and left mirror both were supported by two fine copper wires which were broken once when the right anvil was jarred resulting in eight hours of repair time (18).

APPENDIX B: PBO MORPHOLOGY

Fiber extrusion from a PBO dope is depicted in Figure 39. The dope was forced through the spinnery by a piston which supplied a constant pressure and entered a water bath. The fiber was very difficult to work once it entered the bath; therefore, the substructure was set. In the bath the fiber rolled on the take-up wheel, which along with the extrusion rate determines the spin draw rate, and then was rolled on a spool. The fibers on the spool were classified "as spun"; whereas, the fibers in question were annealed at 600°C. The dope was de-airiated prior to entering the resovoir to force out unwanted gases. The de-ariation was similar to the extrusion by having the dope forced through many small holes at the bottom of a resovoir. Alignment of polymer chains might occur during one or both of these processes resulting in the fibril/microfibril substructure. Not all of the gas was extracted from the dope, therefore when the fiber was drawn, voids and porosities might exist. Furthermore, as the fiber travelled through the water bath, water diffused into the fiber. Once the fiber was dry, the water had diffused out leaving the cavity it occupied behind; thus creating additional voids. The greater the alignment, the greater the mechanical properties; therefore, the optimum spin draw rate largely determined how the substructure was aligned. Cohen and others found that the fiber was composed of highly oriented structural components internally held together by primary forces, but were only loosely bonded to each otherthrough secondary forces (11:4). Figures 30 showed the nature of the discretely connected regions. The fiber components, fibril and microfibril range in size from microns to nanometers, respectively. The fiber structure was a product of processing methods used, but no quantitative explanation exists for how the discrete components evolved.

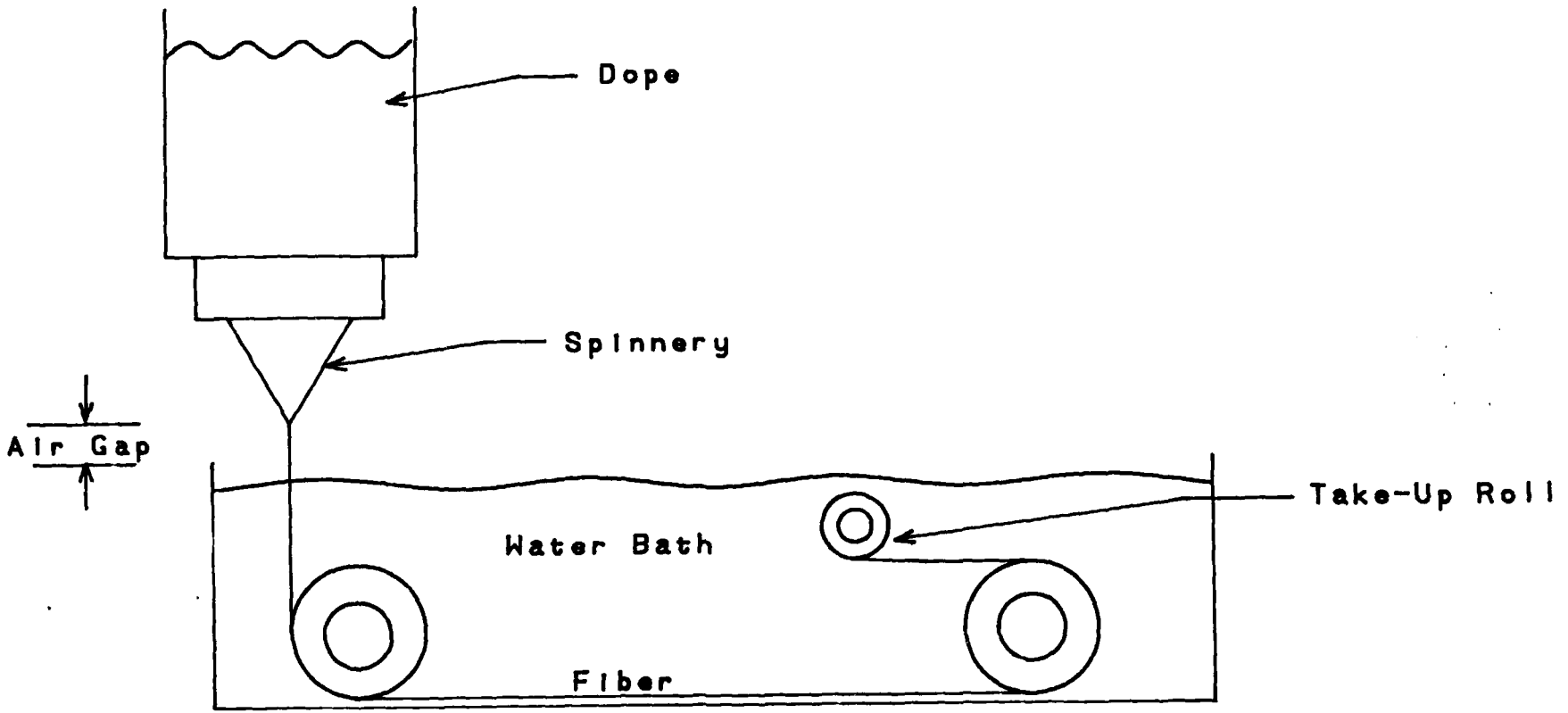

Figure 39. FIBER PROCESSING DIAGRAM

VITA

Scott A. Fawaz was born in [redacted] on [redacted] He graduated from Hutchinson High School [redacted] He attended the United States Air Force Academy, in Colorado Springs, Colorado where he graduated in 1987 with a Bachelor of Science in Engineering Mechanics. In July 1987, he started his graduate study for a Master of Science in Aeronautical Engineering at the Air Force Institute of Technology.

[redacted]

UNCLASSIFIED
SECURITY CLASSIFICATION OF THIS PAGE

REPORT DOCUMENTATION PAGE

Form Approved
OMB No. 0704-0188

1a. REPORT SECURITY CLASSIFICATION UNCLASSIFIED	1b. RESTRICTIVE MARKINGS
2a. SECURITY CLASSIFICATION AUTHORITY	3. DISTRIBUTION/AVAILABILITY OF REPORT Approved for public release; distribution unlimited
2b. DECLASSIFICATION/DOWNGRADING SCHEDULE	
4. PERFORMING ORGANIZATION REPORT NUMBER(S) AFIT/GAE/AA/88D-13	5. MONITORING ORGANIZATION REPORT NUMBER(S)
6a. NAME OF PERFORMING ORGANIZATION School of Engineering 6b. OFFICE SYMBOL (If applicable) AFIT/ENY	7a. NAME OF MONITORING ORGANIZATION
6c. ADDRESS (City, State, and ZIP Code) Air Force Institute of Technology Wright Patterson AFB, Ohio 45433	7b. ADDRESS (City, State, and ZIP Code)
8a. NAME OF FUNDING/SPONSORING ORGANIZATION Materials Laboratory 8b. OFFICE SYMBOL (If applicable) MLBP	9. PROCUREMENT INSTRUMENT IDENTIFICATION NUMBER
8c. ADDRESS (City, State, and ZIP Code) Wright Aeronautical Laboratories Wright Patterson AFB, Ohio 45433	10. SOURCE OF FUNDING NUMBERS PROGRAM ELEMENT NO. / PROJECT NO. / TASK NO / WORK UNIT ACCESSION NO.

11. TITLE (Include Security Classification)
COMPRESSIVE PROPERTIES OF HIGH PERFORMANCE POLYMERIC FIBERS

12. PERSONAL AUTHOR(S)
Scott A. Fawaz, 2Lt, USAF

13a. TYPE OF REPORT	13b. TIME COVERED	14. DATE OF REPORT (Year, Month, Day)	15. PAGE COUNT
MS Thesis	FROM _____ TO _____	1988 December	102

16. SUPPLEMENTARY NOTATION

17. COSATI CODES			18. SUBJECT TERMS (Continue on reverse if necessary and identify by block number)
FIELD	GROUP	SUB-GROUP	
11	05		Polymer Fibers, Direct Compression Testing, ~~PBO~~, ~~Kevlar~~ 29 ~~Kevlar 49~~ (TM), Thesis.

19. ABSTRACT (Continue on reverse if necessary and identify by block number)

Thesis Advisor: Dr. Anthony N. Palazotto
Department of Aeronautics and Astronautics

Abstract on reverse

Approved for public release IAW AFR 190-1
12 Jan 1989

20. DISTRIBUTION/AVAILABILITY OF ABSTRACT	21. ABSTRACT SECURITY CLASSIFICATION
☒ UNCLASSIFIED/UNLIMITED ☐ SAME AS RPT. ☐ DTIC USERS	Unclassified
22a. NAME OF RESPONSIBLE INDIVIDUAL Anthony N. Palazotto	22b. TELEPHONE (Include Area Code) 22c. OFFICE SYMBOL 513-255-2998 AFIT/ENY

DD Form 1473, JUN 86 Previous editions are obsolete. SECURITY CLASSIFICATION OF THIS PAGE
UNCLASSIFIED

UNCLASSIFIED

Block 19 Continued:

In directing the research effort for improving the compressive properties of rigid rod polymeric composite fibers, a reliable testing technique for determining compressive properties is needed. The technique developed used the Tecam Micro-Tensile Testing Machine, MTM-8 and allowed direct tension and compression testing of composite fibers of extremely short gage length. The measured data was analyzed for corrections in machine compliance and possible errors in gage length misreading, fiber slippage, glue deformation, fiber misalignment, and nonuniform stress distribution. A non polymeric fiber was tested to determine if any fiber material dependence existed. The data was compared to the compressive properties obtained from the elastica loop, bending beam, recoil, and composite tests. This was the only known research of high performance polymer fibers in direct tension and compression testing which allowed the construction of a full stress-strain curve.

In developing the technique, the gage length and load cycle had to be determined as well as mounting the fiber without damage. The gage length used had to limit the possibilities of Euler Buckling and a nonuniform stress distribution across the cross-section of the fiber.

The stress strain relationships covering both tension and compression were constructed for poly(p-phenylene benzobisoxazole), PBO, Kevlar 29 (TM), Kevlar 49 (TM), and an experimental carbon fiber. Compressive strengths were determined for the first three fibers, however, the compressive strength of the carbon fiber was out of the range of the machine. The apparent tensile and compressive moduli were gage length dependent, as the gage length decreased; the moduli decreased. The corrected tensile and compressive moduli were obtained from machine compliance curves.